VOLUME 85 NO. ST6
JUNE 1959

JOURNAL of the

Structural Division

PROCEEDINGS OF THE

AMERICAN SOCIETY OF CIVIL ENGINEERS

BASIC REQUIREMENTS FOR MANUSCRIPTS

This Journal represents an effort by the Society to deliver information to the reader with the greatest possible speed. To this end the material herein has none of the usual editing required in more formal publications.

Original papers and discussions of current papers should be submitted to the Manager of Technical Publications, ASCE. Authors should indicate the technical division to which the paper should be referred. The final date on which a discussion should reach the Society is given as a footnote with each paper. Those who are planning to submit material will expedite the review and publication procedures by complying with the following basic requirements:

1. Titles should have a length not exceeding 50 characters and spaces.

2. A 50-word summary should accompany the paper.

3. The manuscript (a ribbon copy and two copies) should be double-spaced on one side of 8½-in. by 11-in. paper. Papers that were originally prepared for oral presentation must be rewritten into the third person before being submitted.

4. The author's full name, Society membership grade, and footnote reference stating present employment should appear on the first page of the paper.

5. Mathematics are reproduced directly from the copy that is submitted. Because of this, it is necessary that capital letters be drawn, in black ink, ⅛-in. high (with all other symbols and characters in the proportions dictated by standard drafting practice) and that no line of mathematics be longer than 6½-in. Ribbon copies of typed equations may be used but they will be proportionately smaller on the printed version.

6. Tables should be typed (ribbon copies) on one side of 8½-in. by 11-in. paper with a 6½-in. by 10½-in. invisible frame. Small tables should be grouped within this frame. Specific reference and explanation should be made in the text for each table.

7. Illustrations should be drawn in black ink on one side of 8½-in. by 11-in. paper within an invisible frame that measures 6½-in. by 10½-in.; the caption should also be included within the frame. Because illustrations will be reduced to 69% of the original size, the capital letters should be ⅛-in. high. Photographs should be submitted as glossy prints in a size that is less than 6½-in. by 10½-in. Explanations and descriptions should be made within the text for each illustration.

8. Papers should average about 12,000 words in length and should be no longer than 18,000 words. As an approximation, each full page of typed text, table, or illustration is the equivalent of 300 words.

Further information concerning the preparation of technical papers is contained in the "Technical Publications Handbook" which can be obtained from the Society.

Reprints from this Journal may be made on condition that the full title of the paper, name of author, page reference (or paper number), and date of publication by the Society are given. The Society is not responsible for any statement made or opinion expressed in its publications.

This Journal is published monthly by the American Society of Civil Engineers. Publication office is at 2500 South State Street, Ann Arbor, Michigan. Editorial and General Offices are at 33 West 39 Street, New York 18, New York. $4.00 of a member's dues are applied as a subscription to this Journal. Second-class postage paid at Ann Arbor, Michigan.

Journal of the

STRUCTURAL DIVISION

Proceedings of the American Society of Civil Engineers

STRUCTURAL DIVISION
EXECUTIVE COMMITTEE
George S. Vincent, Chairman; Elmer K. Timby, Vice-Chairman;
Robert D. Dewell; Emerson J. Ruble; Charles T. G. Looney, Secretary

COMMITTEE ON PUBLICATIONS
Henry G. Schlitt, Chairman; Mace H. Bell; Gerald F. Borrmann;
Edwin S. Elcock; Kurt H. Gerstle; John E. Goldberg; Wayne C. Lewis;
Alfred L. Parme; Philip A. Upp; Halstead N. Wilcox

CONTENTS

June, 1959

Papers

	Page
Analysis of Haunched Octagonal Girder Space Frames by Edward Y. W. Tsui	1
Discussion	41

Copyright 1959 by the American Society of Civil Engineers.

Journal of the
STRUCTURAL DIVISION
Proceedings of the American Society of Civil Engineers

ANALYSIS OF HAUNCHED OCTAGONAL GIRDER SPACE FRAMES

Edward Y. W. Tsui[1] A.M. ASCE

ABSTRACT

An analytical procedure for the evaluation of stresses in haunched octagonal girder space frames is presented. The procedure is established, essentially, through generalization of the slope-deflection method. A set of tables and curves for frame constants introduced in this paper may be used to simplify, to a certain extent, actual design computations. The critical wind directions which may govern the design of members are included in this analysis.

Nomenclature

a = one-half length of a side of the octagonal girder

a_h = length of haunch at the ends of the basic girder member

A = parameter = $0.575\ (1 + u)$

A_{ij} = frame constant at i for unit deformation at j

b = width of girder

C_{mn} = frame constant at m for unit deformation at n

E = Young's modulus of elasticity

F = a force

F^x_{BA} = force at support B of member BA in the direction of X-axis

G = modulus of rigidity

h_c = depth of girder at minimum section

Note: Discussion open until November 1, 1959. To extend the closing date one month, a written request must be filed with the Executive Secretary, ASCE. Paper 2065 is part of the copyrighted Journal of the Structural Division, Proceedings of the American Society of Civil Engineers, Vol. 85, No. ST 6, June, 1959.

1. Research Engr., Missile Systems Div., Lockheed Aircraft Corp., Sunnyvale, Calif.

h_s = depth of girder at any section

H = horizontal shear

I = moment of inertia of square column sections

I_c^x, I_c^z = moment of inertia of minimum girder section about horizontal and vertical axes

I_s^x, I_s^z = moment of inertia of any girder section about horizontal and vertical axes

I_p = polar moment of inertia of the girder section

J = torsional constant

J_c = torsional constant of minimum section

J_s = torsional constant of any girder section

k = ratio of flexural rigidity to torsional rigidity

$k_c = EI_c^x/GJ_c$ = ratio at minimum section of girder

$k_s = EI_c^x/GJ_s$ = ratio at any section of girder

K = a parameter = I/z_1

K_A = a parameter = I_c^z/a

K_c = a parameter = I_c^x/a

Ln = natural logarithm

M = moment

M_{AB}^x = moment at end A of member AB about the X-axis

M_{AB}^h = moment at end A of member AB about the horizontal axis (1 AB)

$F.E.M_{AB}^x$ = fixed end moment at end A of member AB about the X-axis

p = uniformly distributed wind load per unit length of girder

P = total wind load

r = a parameter = ratio of depth of haunch at the end to the minimum depth of girder

s = variable distance along center line of girder

T = torsion

u = Poisson's ratio

V = vertical shear

w_1 = uniformly distributed vertical load per unit length of girder

w_2 = maximum value of triangular haunch load per unit length of girder

w_3 = induced vertical force per unit length of girder at distance a from the neutral axis due to moment loading

W = total vertical uniform load

X, Y, Z = rectangular coordinates

X', Y', Z' = transformed rectangular coordinates

$\Delta_x, \Delta_y, \Delta_z$ = relative translation between the ends of member in the direction of X-, Y-, Z-axis, respectively

Δx_A = absolute translation at end A of member in the direction of X-axis

α, β, γ = rotation at end of member about X-, Y-, Z- axis

ϕ = angle of attack of wind with respect to X-axis

λ = a parameter

σ = unit combined stress in column

P^x, P^y, P^z = ratio $\Delta x/a$, $\Delta y/a$, $\Delta z/a$, respectively

INTRODUCTION

Stress analyses of horizontally curved beams and space frames have been studied and discussed in the past to a limited extent.[1,9,10] However, frames which have been considered so far are limited to prismatic girder and column sections. In cases where loadings are too heavy, or where a saving in materials is required, the use of the constant section girder is undesirable, and the substitution of the haunched girder (Fig. 1) in the design is justified. Because of the peculiar response of this type of frame caused by wind or similar lateral loads, it is difficult to visualize easily the critical directions which govern the design of these members. Consequently, an attempt has been made to study the stress variations versus variations in wind direction or lateral load from which governing design criteria can then be established.

General Considerations

The frames under consideration are statically indeterminate to higher degrees for arbitrarily applied forces. However, if the loads are transmitted to the frame symmetrically or anti-symmetrically (Fig. 1), the number of redundancies is greatly reduced. Even then, difficulties in analysis arise from the effects of haunching and the "curvature" of the girder.

Since the frame is composed of two basic elements, namely, the vertical columns and horizontally curved girder, an analytic procedure can be set up by adapting the classical slope-deflection concept. For the columns, the slope-deflection equations for straight members may be used;[2] for the curved girder, similar expressions for rotations and translations at the ends of the member can be derived. These expressions will be referred to as generalized slope-deflection equations. The unknown deformations and corresponding stresses may be obtained from the equilibrium conditions of the joints for any kind of loading.

If the frame constants for the curved girder are evaluated, solutions to the problems may be obtained quickly. To do this, however, it is essential that

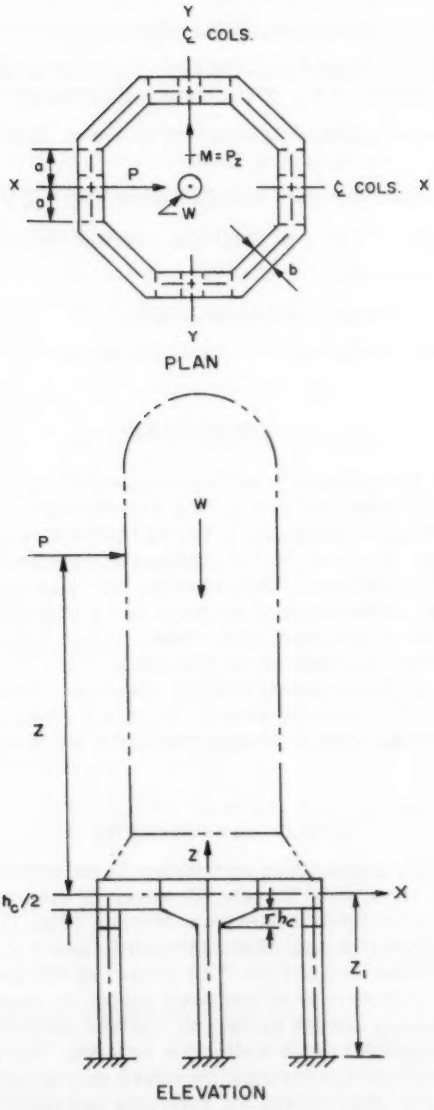

Fig. 1 Haunched Frame and Typical Loading

an appropriate expression for the torsional constant be determined.

Over a century ago, St. Venant[3] established an approximate value of J_s for the rectangular sections as follows:

$$J_s = (bh_s)^4 / 40 I_p \quad (1)$$

In terms of the dimensions of the section, Equation (1) may be transformed into

$$J_s = 3 b^3 h_s / 10 [1 + (b/h_s)^2] \quad (1a)$$

Later, St. Venant[4] developed the expression for torsional constant in series form, which may be represented in terms of hyperbolic functions as

$$J_s^* = \frac{1}{3} b^3 h_s \left(1 - \frac{192}{\pi^5}\right) \sum_{n=1,3,5\cdots}^{\infty} \frac{1}{n^5} \tanh \frac{n\pi h_s}{2b} \quad (2)$$

Andersen[5] recommended the following expression for torsion

$$J_s = b^3 h_s / 3.58 [1 + (b/h_s)^2] \quad (3)$$

Of the four expressions above, it is believed that Equation (2) is exact, while Equations (1a) and (3) give respectively higher and lower values for sections with shape factors (h_s/b) up to about 3.5. Unfortunately, the form of Equation (2) is too cumbersome for practical application. The following expression is chosen because it gives values closer to the exact expression, and is in a form which can be more easily utilized for the determination of frame constants.

$$J_s = 0.29 b^3 h_s / [1 + (b/h_s)^2] \quad (4)$$

Figure 2 compares Equations (1a) through (4).

Assumptions, Limitations, and Sign Conventions

1. Assumptions and Limitations:

   a) It is assumed that the material is homogeneous, isotropic, and linearly elastic. All strains and stresses considered are assumed to be within the elastic limit.

   b) The principle of superposition is applicable.

   c) The center of rotation of the successive section of the haunched girder is assumed to be located at the centroid of the minimum section, the locus of which lies in a horizontal plane.

   d) Torsion is uniform, i.e., longitudinal warping is negligible.

   e) If loads are transmitted from a tower, interaction between the frame and tower is disregarded.

*The same expression was derived by P. Timoshenko by means of membrane analogy.[7]

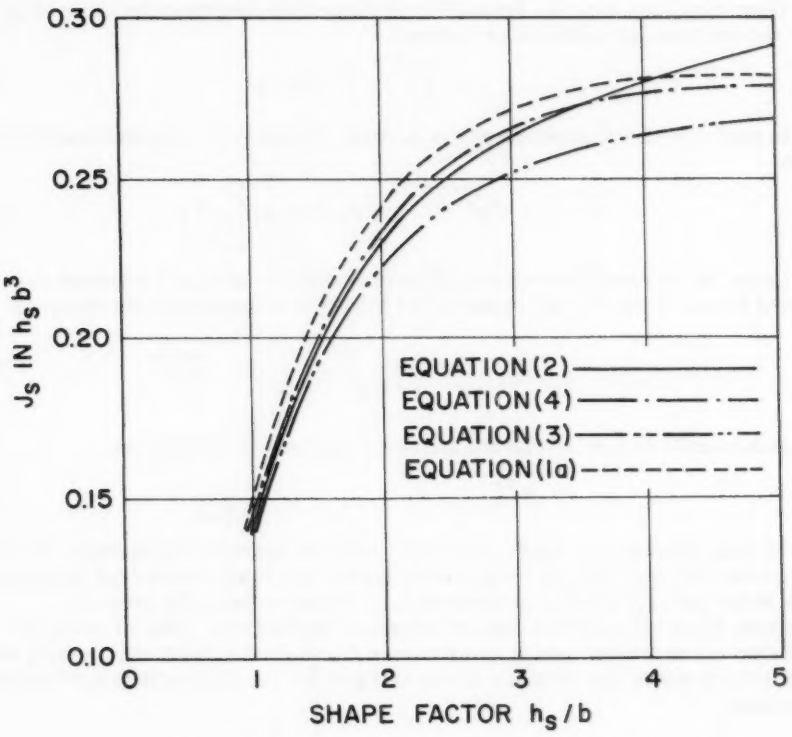

Fig. 2 Comparison of Torsional Constants

2. Sign Convention:

Leaving aside the representation of moment, torsion, and shear diagrams, which will be explained later, we will assign a right-hand-rule sign convention for both moments and rotations. Figure 3 shows these designations as well as the signs for both horizontal and vertical translations and forces. For the vertical forces ⊙ shows the force acting upward or toward the observer, and ⊗ shows the force acting downward or away from the observer.

Generalized Slope-Deflection Equations

If a horizontally "curved" member (Fig. 4) is acted upon by external loads, and if deformations have taken place, the resulting moments and forces at the ends may be expressed as functions of the external loads, deformations, and properties of the member. Since the applied loads, as well as rotations and translations of the member, may always be resolved into principal components, two uncoupled sets of equations may be established which are

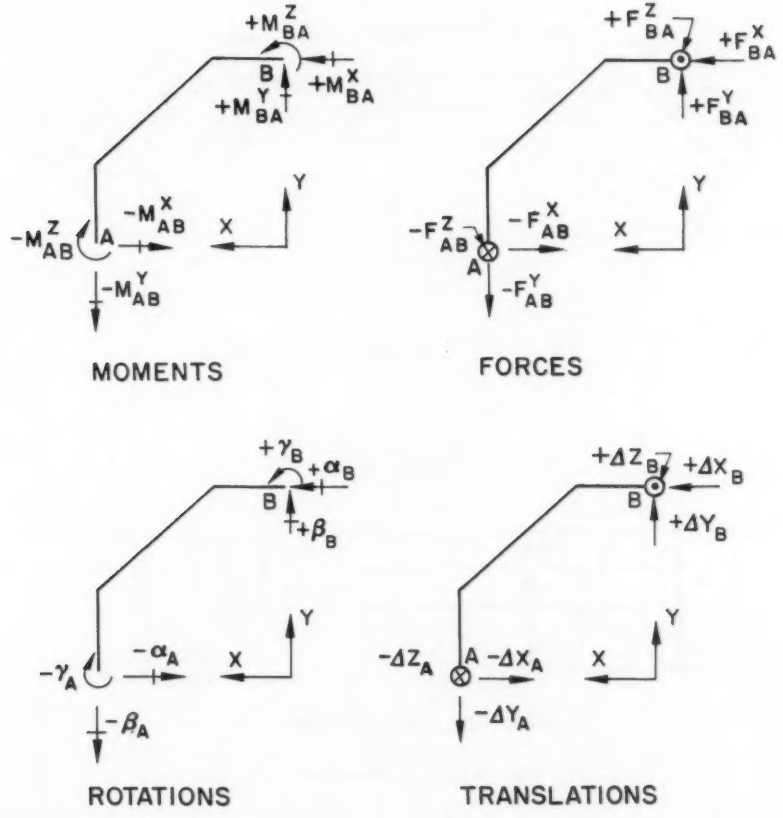

Fig. 3 Sign Convention

necessary and sufficient to prescribe all strains and stresses together.

By the method of virtual work,(6) and by following steps similar to those used for deriving the slope-deflection equations for straight members,(7) one may derive generalized slope-deflection equations for a basic horizontally "curved" member acted upon by a system of forces acting vertically,(8) as follows

$$M^{x}_{AB} = EK_c (C_{11}\alpha_A + C_{12}\alpha_B + C_{13}\beta_A + C_{14}\beta_B + C_{15}\rho^2) \pm F.E.M^{x}_{AB} \quad (5)$$

$$M^{x}_{BA} = EK_c (C_{21}\alpha_A + C_{22}\alpha_B + C_{23}\beta_A + C_{24}\beta_B + C_{25}\rho^2) \pm F.E.M^{x}_{BA} \quad (6)$$

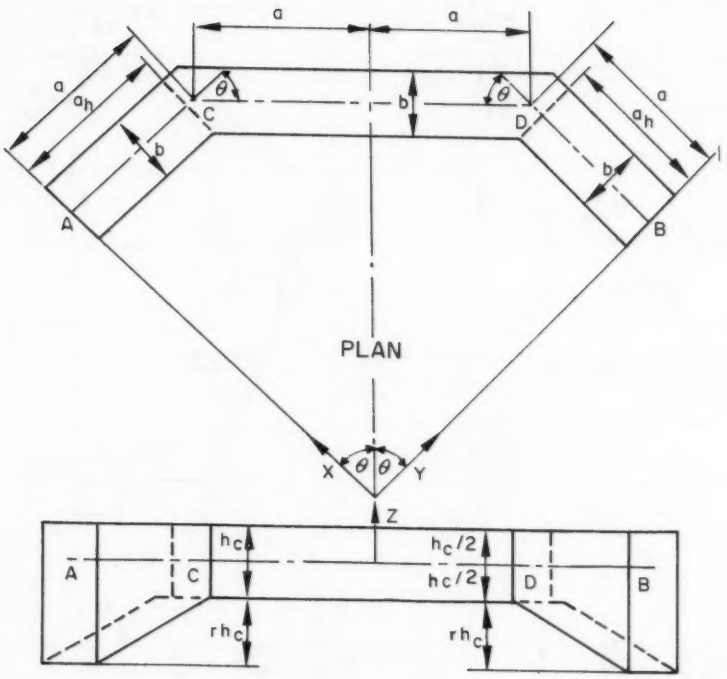

Fig. 4 Basic Member

$$M^{Y}_{AB} = EK_c \left(C_{31}\alpha_A + C_{32}\alpha_B + C_{33}\beta_A + C_{34}\beta_B + C_{35}\rho^2 \right) \pm F.E.M^{Y}_{AB} \quad (7)$$

$$M^{Y}_{BA} = EK_c \left(C_{41}\alpha_A + C_{42}\alpha_B + C_{43}\beta_A + C_{44}\beta_B + C_{45}\rho^2 \right) \pm F.E.M^{Y}_{BA} \quad (8)$$

$$F^{Z}_{AB} = -\frac{EK_c}{a} \left(C_{51}\alpha_A + C_{52}\alpha_B + C_{53}\beta_A + C_{54}\beta_B + C_{55}\rho^2 \right) \pm F.E.F^{Z}_{AB} \quad (9)$$

$$F^{Z}_{BA} = \frac{EK_c}{a} \left(C_{51}\alpha_A + C_{52}\alpha_B + C_{53}\beta_A + C_{54}\beta_B + C_{55}\rho^2 \right) \pm F.E.F^{Z}_{BA} \quad (10)$$

Table I* shows the numerical values of the frame constants for various shape factors (h_c/b) and haunch ratios (r) of the basic member. Values of

*Tables I and II are based on a Poisson's Ratio of 0.20.

TABLE I

VALUES OF BEAM CONSTANTS C_{ij} VS RATIOS r AND h_c/b

C_{ij}	$\frac{hc}{b}$	r=0.0	r=0.5	r=1.0	r=1.5	r=2.0	r=3.0	Remarks
C_{11}	0	0.79924	1.31166	1.73895	2.07797	2.34265	2.71305	$C_{11} = C_{44}$
	1	0.70765	1.11588	1.40387	1.63232	1.80529	2.04556	
	2	0.52912	0.74563	0.88540	0.99836	1.07652	1.18684	
	3	0.37304	0.48630	0.55699	0.60772	0.64634	0.70402	
C_{12}	0	0.02178	0.12207	0.21874	0.29944	0.36411	0.45535	$C_{12} = C_{21} = C_{34} = C_{43}$
	1	0.01312	0.08538	0.14107	0.19255	0.23425	0.29638	
	2	0.01280	0.04513	0.06862	0.09141	0.10744	0.13156	
	3	0.01238	0.02778	0.03828	0.04589	0.05167	0.06020	
C_{13}	0	0.29278	0.46258	0.59840	0.70371	0.78505	0.89702	$C_{13} = C_{31} = C_{24} = C_{42}$
	1	0.24142	0.37136	0.46240	0.53802	0.59727	0.68354	
	2	0.16781	0.23834	0.28854	0.33186	0.36440	0.41400	
	3	0.11327	0.15319	0.18241	0.20548	0.22447	0.25501	
C_{14}	0	0.52824	0.97103	1.35932	1.67378	1.92169	2.27140	$C_{14} = C_{41}$
	1	0.47935	0.82978	1.08257	1.28686	1.44231	1.65841	
	2	0.37415	0.54727	0.66550	0.75789	0.81958	0.90451	
	3	0.27235	0.36014	0.41287	0.44812	0.47355	0.50920	
C_{15}	0	0.34008	0.59363	0.81095	0.98487	1.12119	1.31242	$C_{15} = C_{51} = C_{45} = C_{54}$
	1	0.29850	0.49741	0.63997	0.75588	0.84483	0.97007	
	2	0.22452	0.32747	0.39519	0.45137	0.49043	0.54624	
	3	0.15987	0.21261	0.24658	0.27072	0.28914	0.31654	
C_{22}	0	0.50299	0.66469	0.77554	0.84244	0.89507	0.96416	$C_{22} = C_{33}$
	1	0.31304	0.40018	0.45643	0.50013	0.53396	0.58340	
	2	0.16586	0.20731	0.23707	0.26194	0.28155	0.31224	
	3	0.09811	0.12170	0.13972	0.15449	0.16699	0.18761	
C_{23}	0	0.23200	0.32418	0.39016	0.43817	0.47413	0.52249	$C_{23} = C_{32}$
	1	0.08473	0.11421	0.13511	0.15467	0.17094	0.19623	
	2	0.01084	0.01410	0.01715	0.02148	0.02459	0.02980	
	3	0.00277	0.00371	0.00441	0.00510	0.00581	0.00720	
C_{25}	0	0.21737	0.32589	0.40947	0.47298	0.52157	0.58798	$C_{25} = C_{52} = C_{35} = C_{53}$
	1	0.13510	0.20113	0.24749	0.28692	0.31820	0.36441	
	2	0.07400	0.10456	0.12662	0.14636	0.16112	0.18383	
	3	0.04577	0.06192	0.07373	0.08300	0.09057	0.10262	
C_{55}	0	0.23090	0.38087	0.50551	0.60386	0.68045	0.78717	
	1	0.17962	0.28934	0.36760	0.43194	0.48174	0.55276	
	2	0.12365	0.17895	0.21614	0.24759	0.26988	0.30241	
	3	0.08518	0.11371	0.13268	0.14652	0.15728	0.17363	

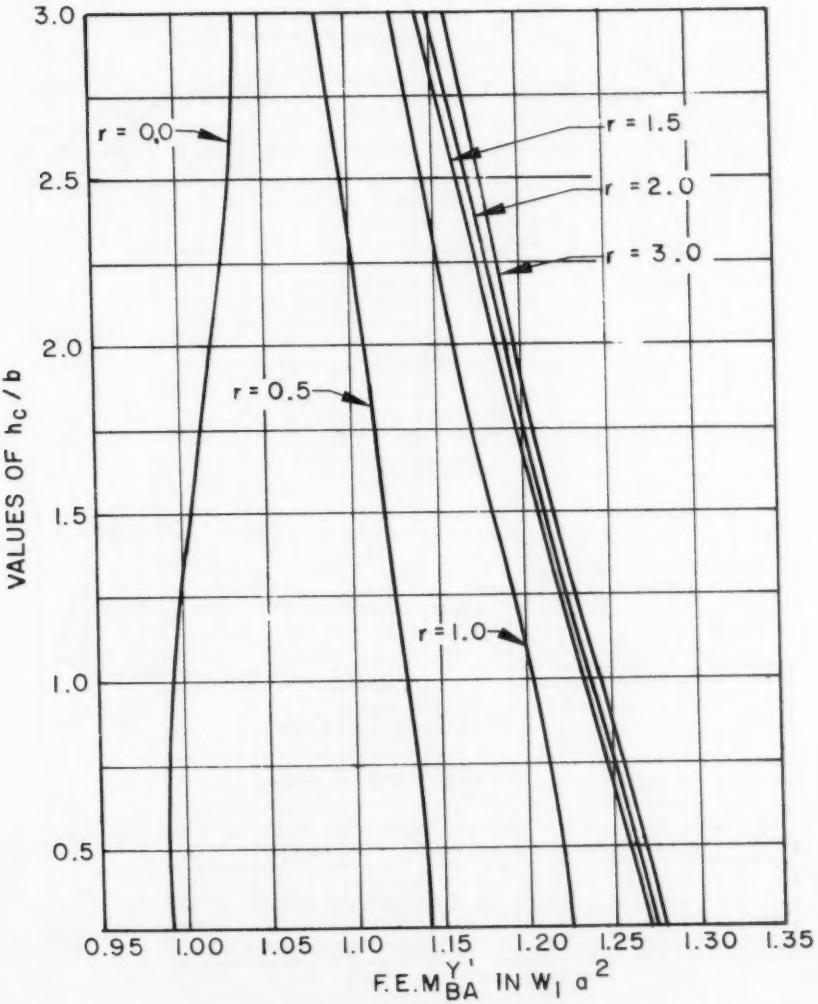

Fig. 5 Fixed End Forces - Uniform Vertical Load

fixed end forces (with respect to the transformed coordinates X', Y', Z') for various typical vertical loads are shown in Figs. 5 through 8.**

Similarly, one can establish generalized slope-deflection equations for the same basic member due to force system acting horizontally, as follows

**Figures 5 through 9 are taken from Reference (8).

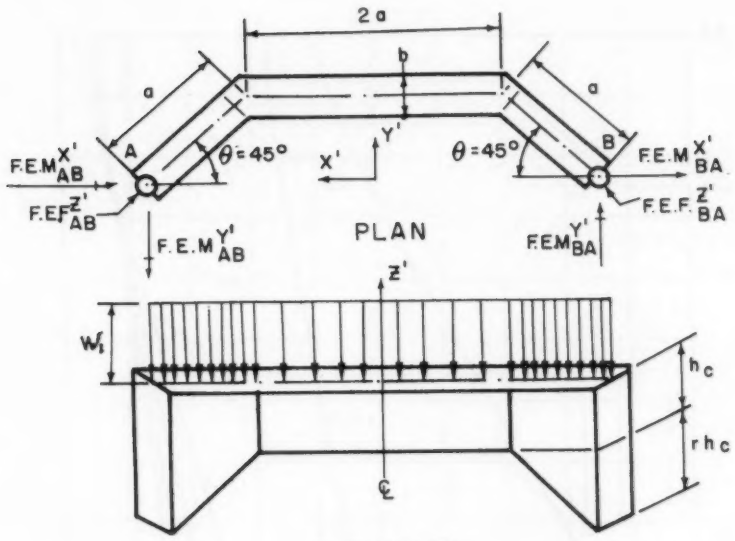

$$F.E.M^{X'}_{BA} = -1.06051\ W_1\ a^2$$

$$F.E.F^{Z}_{BA} = +2\ W_1\ a$$

$$F.E.M^{X'}_{AB} = F.E.M^{X'}_{BA}$$

$$F.E.M^{Y'}_{AB} = -F.E.M^{Y'}_{BA}$$

$$F.E.F^{Z}_{AB} = F.E.F^{Z}_{BA}$$

Fig. 5 Fixed End Forces - Uniform Vertical Load (Cont.)

$$M^{Z}_{AB} = EK_A\,(A_{11}\gamma^{*}_{A} + A_{12}\gamma^{*}_{B} + A_{13}\rho^{X} + A_{14}\rho^{Y}) \pm F.E.M^{Z}_{AB} \quad (11)$$

$$M^{Z}_{BA} = EK_A\,(A_{21}\gamma^{*}_{A} + A_{22}\gamma^{*}_{B} + A_{23}\rho^{X} + A_{24}\rho^{Y}) \pm F.E.M^{Z}_{BA} \quad (12)$$

$$F^{X}_{AB} = \frac{EK_A}{a}\,(A_{31}\gamma^{\ell}_{A} + A_{32}\gamma^{\ell}_{B} + A_{33}\rho^{X} + A_{34}\rho^{Y}) \pm F.E.F^{X}_{AB} \quad (13)$$

$$F^{X}_{BA} = \frac{-EK_A}{a}\,(A_{31}\gamma^{\ell}_{A} + A_{32}\gamma^{\ell}_{B} + A_{33}\rho^{X} + A_{34}\rho^{Y}) \pm F.E.F^{X}_{BA} \quad (14)$$

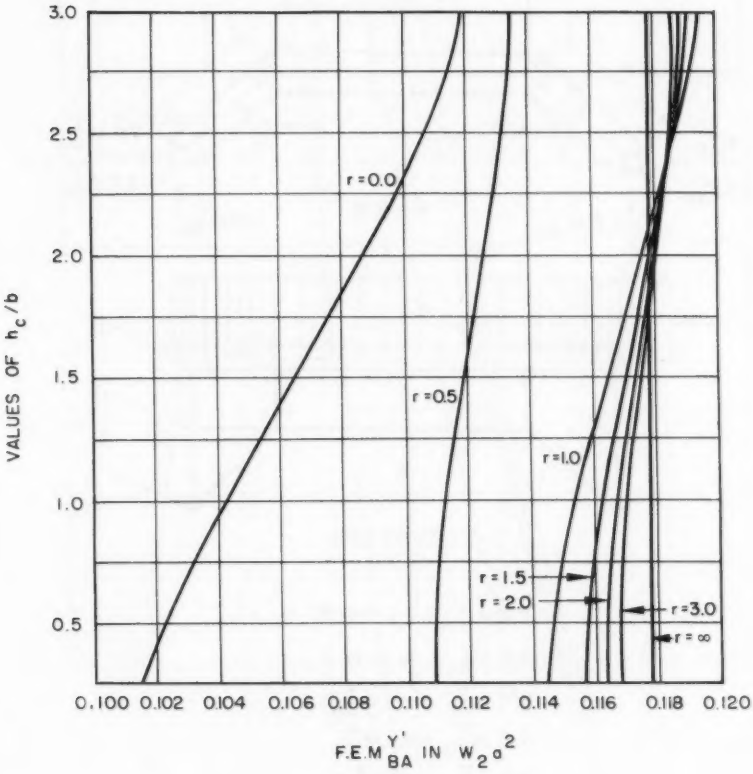

Fig. 6 Fixed End Forces - Haunch Loads

$$F^{Y}_{AB} = \frac{EK_A}{a}\left(A_{41}\gamma^{*}_{A} + A_{42}\gamma^{*}_{B} + A_{43}\beta^{X} + A_{44}\beta^{Y}\right) \pm F.E.F^{Y}_{AB} \quad (15)$$

$$F^{Y}_{BA} = -\frac{EK_A}{a}\left(A_{41}\gamma^{*}_{A} + A_{42}\gamma^{*}_{B} + A_{43}\beta^{X} + A_{44}\beta^{Y}\right) \pm F.E.F^{Y}_{BA} \quad (16)$$

Table II shows the numerical values of the frame constants for different haunch ratios (r) of the basic member. Values of fixed-end forces for the uniformly distributed wind load are plotted in Fig. 9.

Analytical Procedure

Using the ordinary slope-deflection equations for the columns and Equations (5) through (16) for the basic members of the girder, stress analyses of

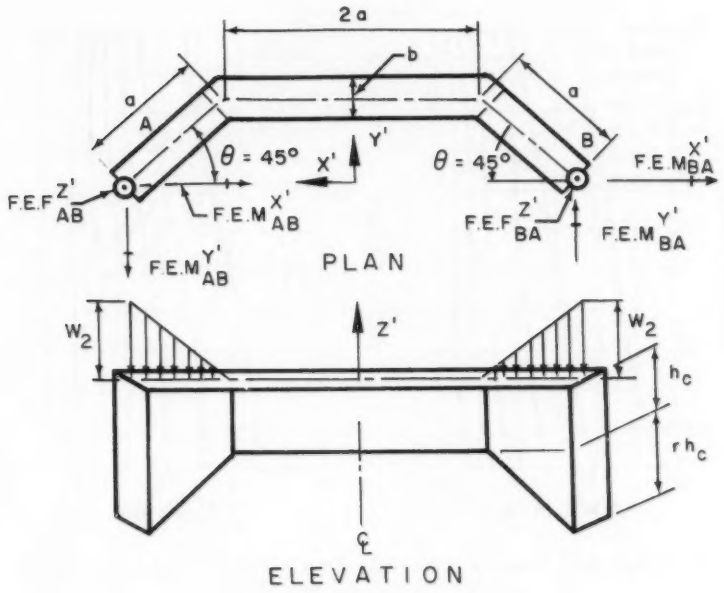

$$F.E.M^{X'}_{BA} = -0.11792\ W_2 a^2$$

$$F.E.F^{Z'}_{BA} = 0.5\ W_2 a$$

$$F.E.M^{X'}_{AB} = F.E.M^{X'}_{BA}$$

$$F.E.M^{Y'}_{AB} = -F.E.M^{Y'}_{BA}$$

$$F.E.F^{Z'}_{AB} = F.E.F^{Z'}_{BA}$$

Fig. 6 Fixed End Forces - Haunch Loads (Cont.)

frames supporting tall towers, such as that shown in Fig. 1, may be made in the following manner:

1. For uniformly distributed vertical dead and live loads (Fig. 11). The equilibrium conditions for any joint, joint A, for example, are

$$\Sigma M^{Y} = M^{Y}_{AA_1} + 2M^{Y}_{AB} = 0 \qquad (17)$$

$$\Sigma F^{X} = F^{X}_{AA_1} + 2F^{X}_{AB} = 0 \qquad (18)$$

After substituting the appropriate expressions, Equations (17) and (18) yield

$$EK\left(2\beta_A + \frac{3}{z_1}\Delta x_A\right) + EK_c\left(C_{32} + C_{33}\right)\beta_A \pm F.E.M^{Y}_{AB} = 0 \qquad (19)$$

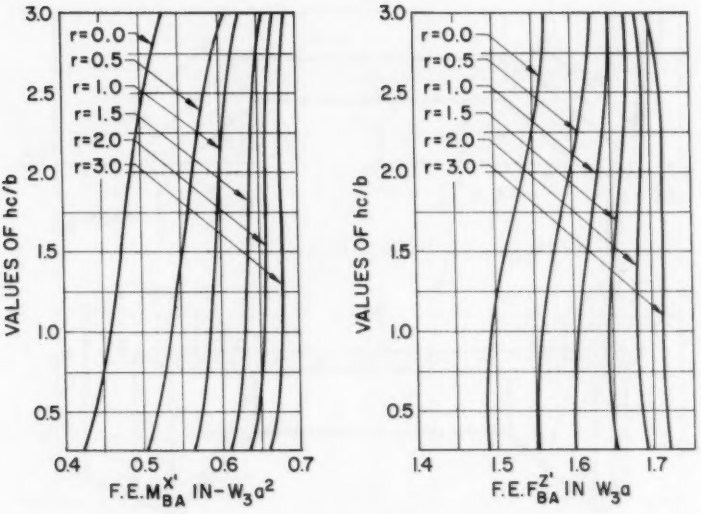

Fig. 7 Fixed End Forces - Anti-Symmetrical Triangular Loads

TABLE II

VALUES OF BEAM CONSTANTS A_{mn} VS HAUNCH RATIO r

A_{mn}	r=0.0	r=0.5	r=1.0	r=1.5	r=2.0	r=3.0	Remarks
A_{11}	2.26336	2.90189	3.66548	4.31999	4.95895	6.19199	$A_{11} = A_{22}$
A_{12}	-0.94138	-1.36324	-1.79308	-2.22491	-2.66286	-3.54670	$A_{12} = A_{21}$
A_{13}	2.07479	2.73186	3.35967	3.96418	4.55592	5.70583	$A_{13} = A_{31} = A_{24} = A_{42}$
A_{14}	-1.53152	-2.06155	-2.58452	-3.09725	-3.60784	-4.61450	$A_{14} = A_{41} = A_{23} = A_{32}$
A_{33}	2.51709	3.16811	3.79065	-4.38790	4.97242	6.10662	$A_{33} = A_{44}$
A_{34}	2.29011	2.89053	3.46975	4.02863	4.57909	5.65367	$A_{34} = A_{43}$

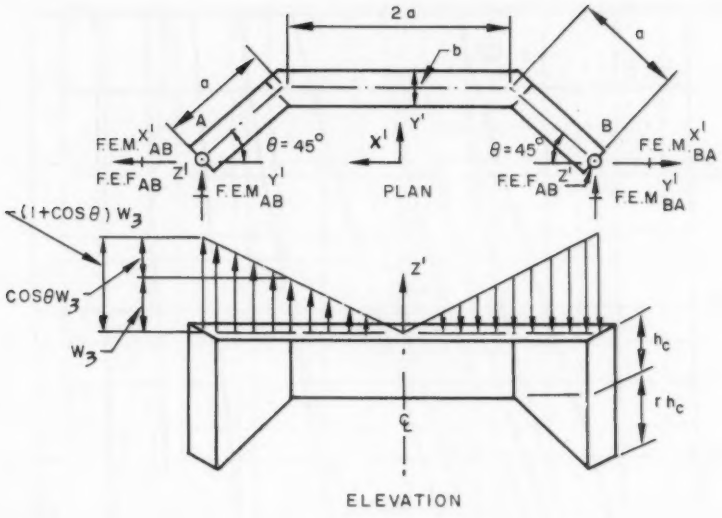

$$F.E.M^{X'}_{AB} = -F.E.M^{X'}_{BA}$$
$$F.E.M^{Y'}_{AB} = F.E.M^{Y'}_{BA}$$
$$F.E.F^{Z'}_{AB} = -F.E.F^{Z'}_{BA}$$

Fig 7 Fixed End Forces - Anti-Symmetrical Triangular Loads (Cont.)

$$K\left(3\beta_A + \frac{6}{Z_1}\Delta X_A\right) + \frac{K_A}{a^2}\left(A_{33} + A_{34}\right)\Delta X_A = 0 \qquad (20)$$

Equations (19) and (20) will give the correct solution for the unknown slope (B_A) and deflection (ΔX_A) and hence for the desired stresses. If ΔX_A, us usually a very small quantity, is omitted, the above simultaneous equations reduce to

$$E\left[2K + k_c\left(C_{32} + C_{33}\right)\right]\beta_A \pm F.E.M^{Y}_{AB} = 0 \qquad (21)$$

Equation (21) then gives the simplified solution for this loading.

2. For triangularly distributed haunch loads (Fig. 12). Since the response of the frame due to this loading is similar to that for case 1, Equations (19) and (20), or (21) alone, may be applied as long as a different fixed-end moment is used in each instance.

3. For uniformly distributed horizontal wind load (Fig. 13). The following simultaneous equations may be obtained from the equilibrium conditions for joints A or B (or A' and B')

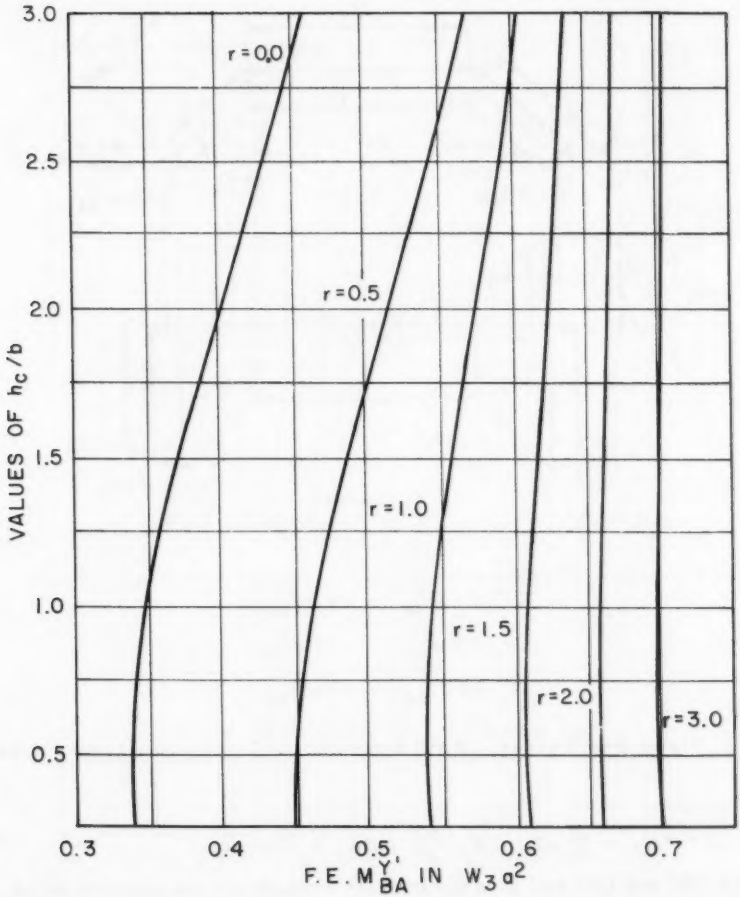

Fig. 7
Fixed End Forces - Anti-Symmetrical Triangular Loads (Cont.)

$$K\left(2\beta_A + \frac{3}{z_1}\Delta X_A\right) + K_c\left(C_{33}\beta_A + C_{34}\beta_B\right) = 0 \quad (22)$$

$$\frac{EK}{z_1}\left(3\beta_A + \frac{6}{z_1}\Delta X_A\right) + \frac{EK_A}{a}\left[A_{32}\gamma'_B + \frac{A_{33}}{a}(\Delta X_A - \Delta X_B)\right] \pm F.E.F^{x}_{AB} = 0 \quad (23)$$

$$K\left(2\beta_B + \frac{3}{z_1}\Delta X_B\right) + K_c\left(C_{43}\beta_A + C_{44}\beta_B\right) = 0 \quad (24)$$

$$\frac{EK}{k}\gamma'_B + 2\left[EK_A\left\{A_{22}\gamma'_B + \frac{A_{23}}{a}(\Delta X_A - \Delta X_B)\right\} \pm F.E.M^{z}_{BA}\right] = 0 \quad (25)$$

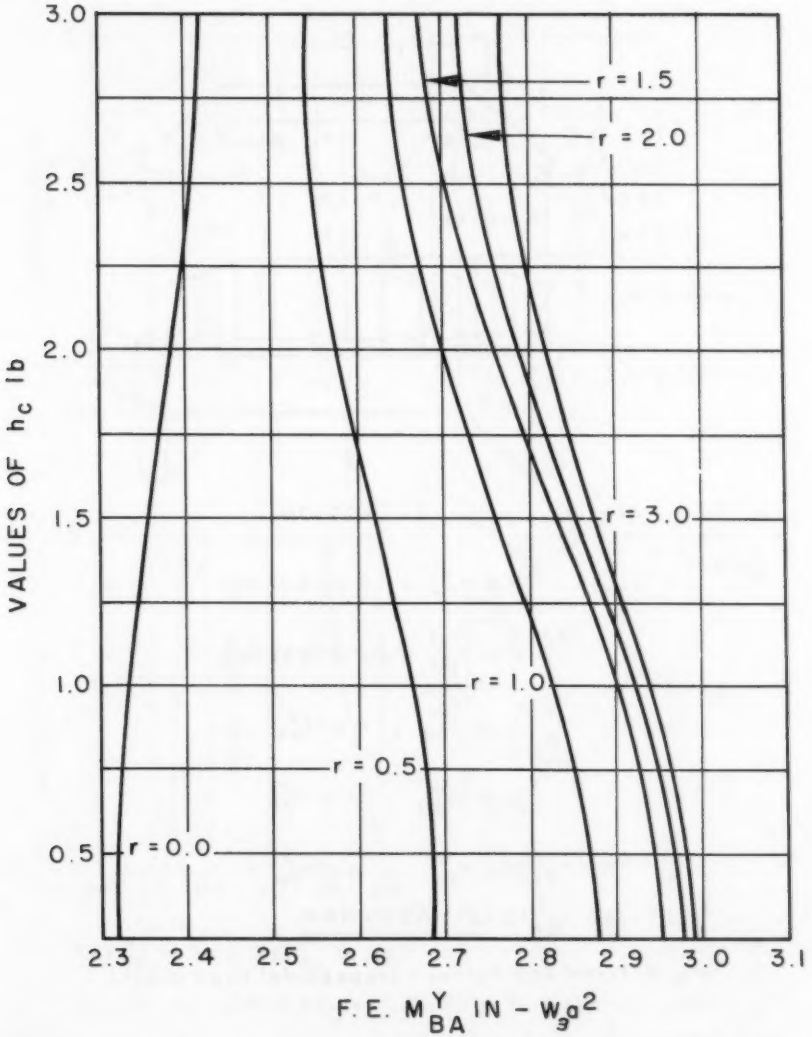

Fig. 8 Fixed End Forces - Trapezoidal Load

$$\frac{EK}{Z_1}\left(3\beta_B + \frac{6}{Z_1}\Delta X_B\right) - \frac{EK_A}{a}\left[A_{32}\gamma^{c}_{\beta} + \frac{A_{33}}{a}\left(\Delta X_A - \Delta X_B\right)\right] \pm F.E.F^{x}_{BA} = 0 \quad (26)$$

A simplified solution may be obtained from the following reduced simultaneous equations, which are established by neglecting the torsion of the column (γ_B or γ'_B) and setting $\Delta X_A = \Delta X_B$

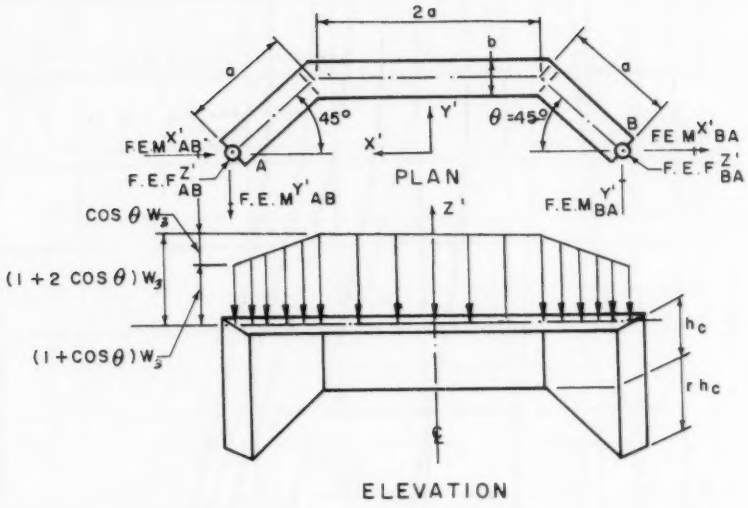

$$F.E.M_{BA}^{X'} = -2.32441\, W_3 a^2$$

$$F.E.F_{BA}^{Z'} = +4.47452\, W_3 a$$

$$F.E.M_{AB}^{X'} = F.E.M_{BA}^{X'}$$

$$F.E.M_{AB}^{Y'} = -F.E.M_{BA}^{Y'}$$

$$F.E.F_{AB}^{Z'} = F.E.F_{BA}^{Z'}$$

(d) REMARKS

Fig. 8 Fixed End Forces - Tropezoidal Load (Cont.)

$$K\left(2\beta_A + \frac{3}{z_1}\Delta X_A\right) + K_c\left(C_{33}\beta_A + C_{34}\beta_B\right) = 0 \qquad (22)$$

$$K\left(2\beta_B + \frac{3}{z_1}\Delta X_A\right) + K_c\left(C_{43}\beta_A + C_{44}\beta_B\right) = 0 \qquad (27)$$

$$\frac{EK}{z_1}\left[3(\beta_A+\beta_B) + \frac{12}{z_1}\Delta X_A\right] \pm F.E.F_{AB}^{X} \pm F.E.F_{BA}^{X} = 0 \qquad (28)$$

It should be noted that in this case the wind acts in a direction parallel to the X-axis (ϕ=0), but the same equations may be applied for any angle ϕ by the method of superposition. This will be illustrated in the numerical examples.

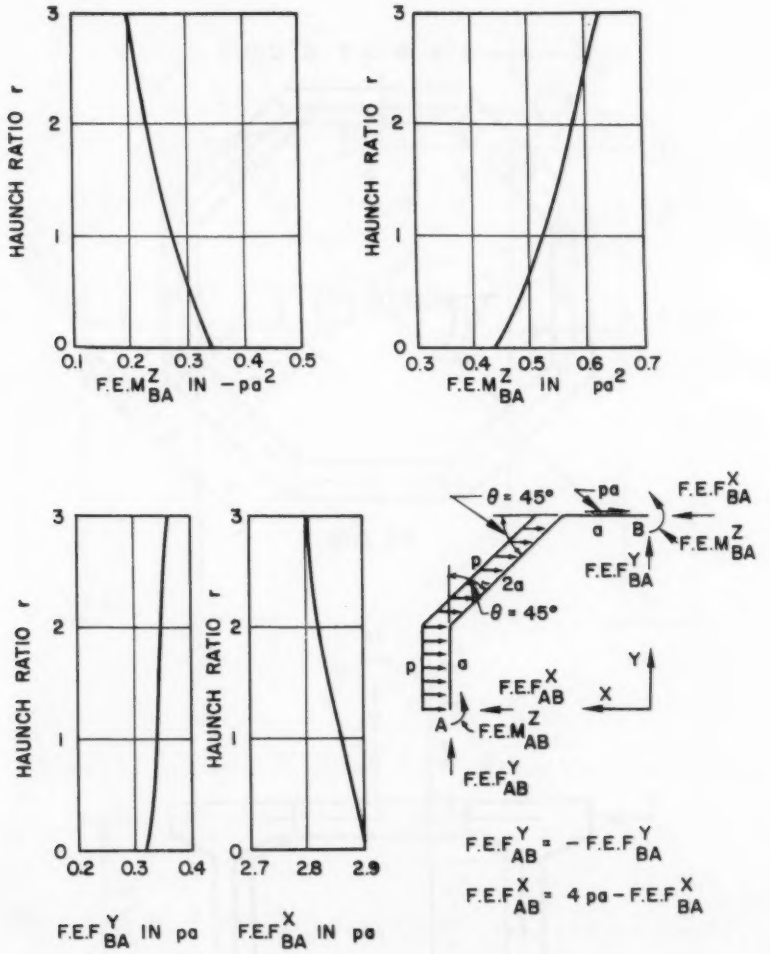

Fig. 9 Fixed End Forces - Uniform Horizontal Load

4. For anti-symmetrical moment load (Fig. 14). Referring to the projection of the deflected structure as shown in Fig. 15, the equilibrium conditions for Joints A, B, (or A', B') and the frame as a whole, the following equations can be established.

$$EK\left(2\beta_A + \frac{3}{z_1}\Delta X_A\right) + EK_c\left(c_{33}\beta_A + c_{34}\beta_B\right) \pm F.E.M^Y_{AB} = 0 \qquad (29)$$

$$K\left(3\beta_A + \frac{6}{z_1}\Delta X_A\right) + \frac{K_A}{a^2} A_{33}\left(\Delta X_A - \Delta X_B\right) = 0 \qquad (30)$$

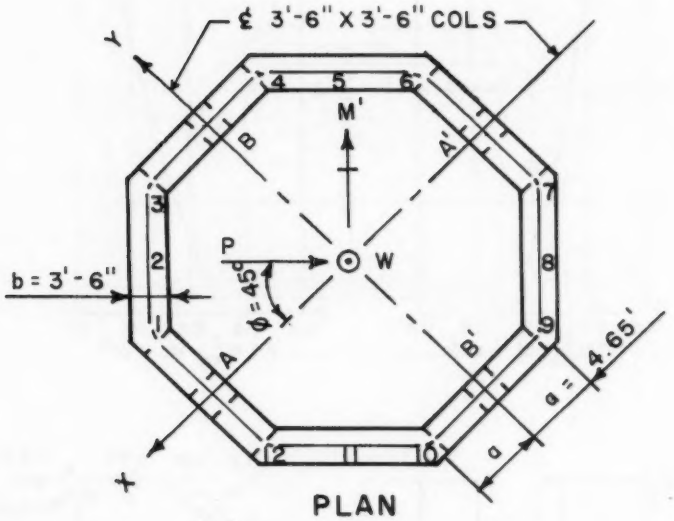

PLAN

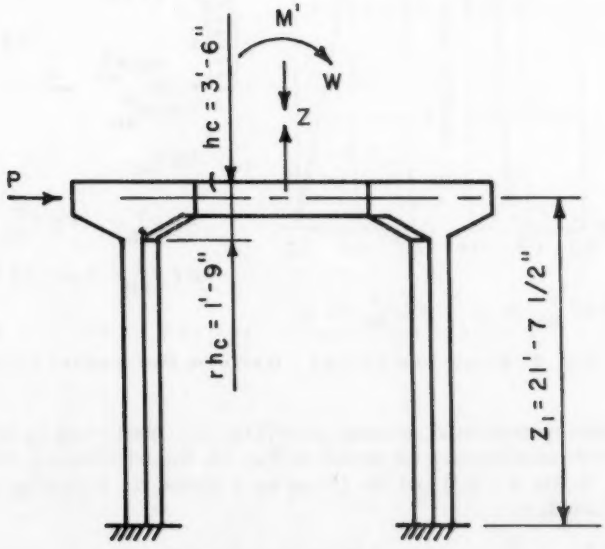

ELEVATION

Fig. 10 Dimensions and Loads for Frame I

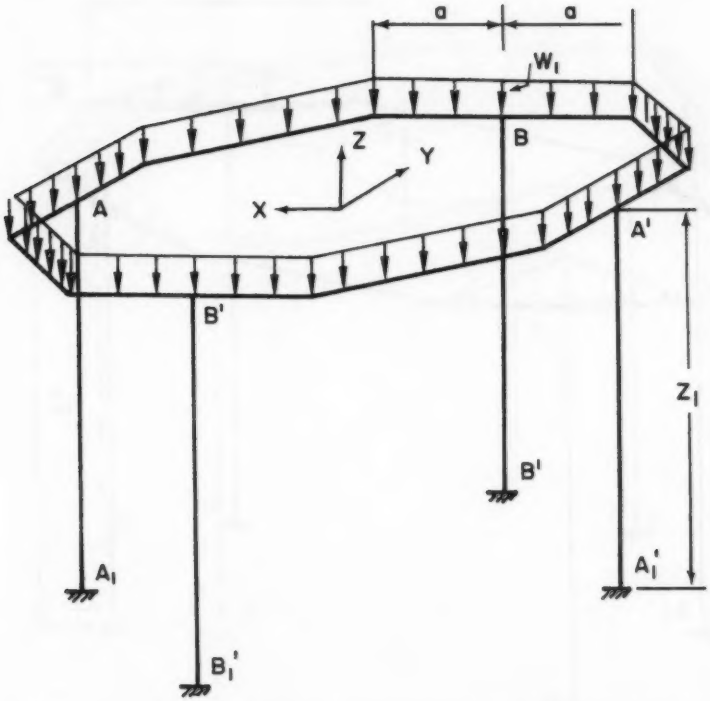

Fig. 11 Frame Subjected to Uniform Vertical Loads

$$EK\left(2\beta_B + \frac{3}{z_1}\Delta X_B\right) + EK_c(C_{43}\beta_A + C_{44}\beta_B) \pm F.E.M^{Y}_{BA} = 0 \quad (31)$$

$$\beta_A + \beta_B + \frac{2}{z_1}(\Delta X_A + \Delta X_B) = 0 \quad (32)$$

Ordinarily, the relative translation $\Delta X_A - \Delta X_B$ (or $\Delta' X_A - \Delta X'_B$) is small. If ΔX_A is made equal to ΔX_B, the number of the above simultaneous equations is reduced to three

$$EK\left(2\beta_A + \frac{3}{z_1}\Delta X_A\right) + EK_c(C_{33}\beta_A + C_{34}\beta_B) \pm F.E.M^{Y}_{AB} = 0 \quad (29)$$

$$EK\left(2\beta_B + \frac{3}{z_1}\Delta X_A\right) + EK_c(C_{43}\beta_A + C_{44}\beta_B) \pm F.E.M^{Y}_{BA} = 0 \quad (33)$$

$$\beta_A + \beta_B + \frac{4}{z_1}\Delta X_A = 0 \quad (34)$$

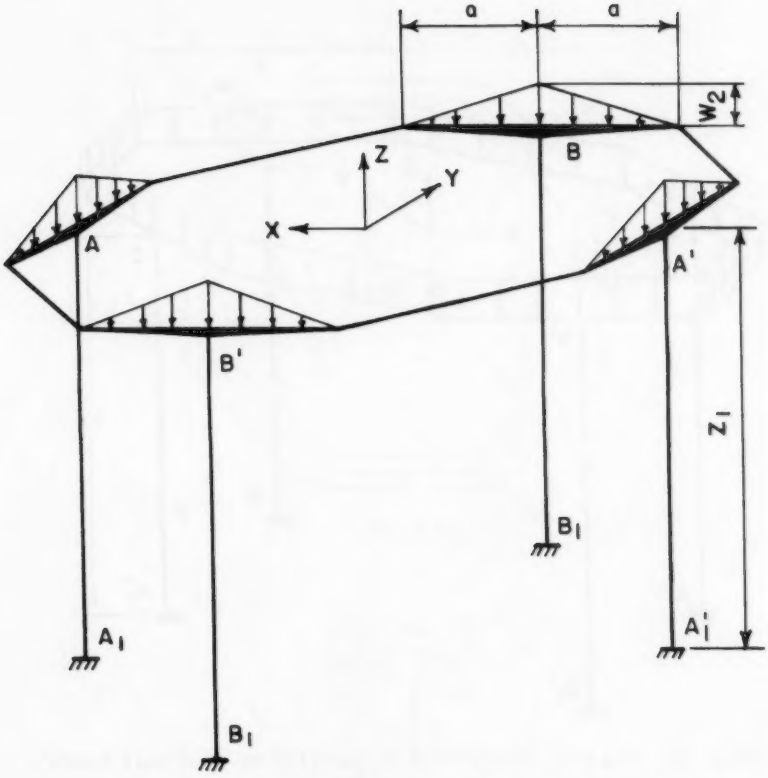

Fig. 12 Frame Subjected to Haunch Loads

Equations (29), (33), and (34) then provide the simplified solution for the unknowns and the corresponding stresses.

Numerical Illustrations*

Analysis of Frame I

Assume a reinforced concrete frame with column bases fixed, as shown in Fig. 10. Loads transmitted from a tower are:

vertical load = W = 1500 kips
lateral wind load = P = 100 kips acting at an angle $\phi = 45^{\circ}$ with respect to X-axis and assumed uniformly distributed along the girder

*All stresses for the following illustrations are evaluated from the simplified solutions.

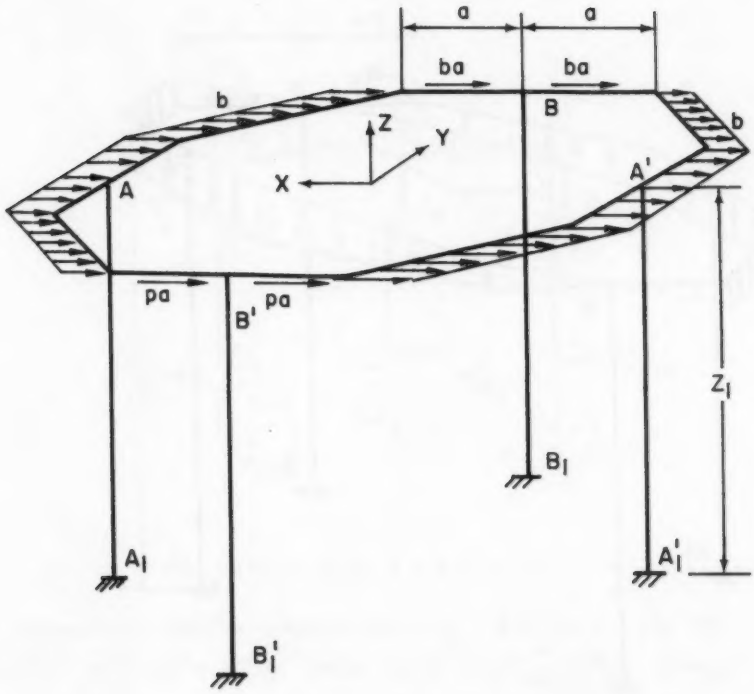

Fig. 13 Frame Subjected to Uniform Horizontal Loads

moment load due to wind = M' = Pz = 100x20 = 2000 ft-kips

Following the analytical procedure, the total stress at any point on the frame may be obtained by summing, algebraically, the stress due to the following loads acting independently:

1. Uniformly distributed vertical live and dead loads = w_1 = 1500/16x4.65 + 3.5x3.5x0.15 = 21.94 kips/ft. (Fig. 11):

For h_c/b = 1 and r = 0.5:

from Table I, C_{32} = 0.11421, C_{33} = 0.40018

from Table II, A_{33} = 3.16811, A_{34} = 2.89053

from Fig. 5, F.E.$M^{Y'}_{AB}$ = 1.13000 $w_1 a^2$

and F.E.$M^{X'}_{AB}$ = 1.06051 $w_1 a^2$

With reference to coordinates X and Y, and the given data,

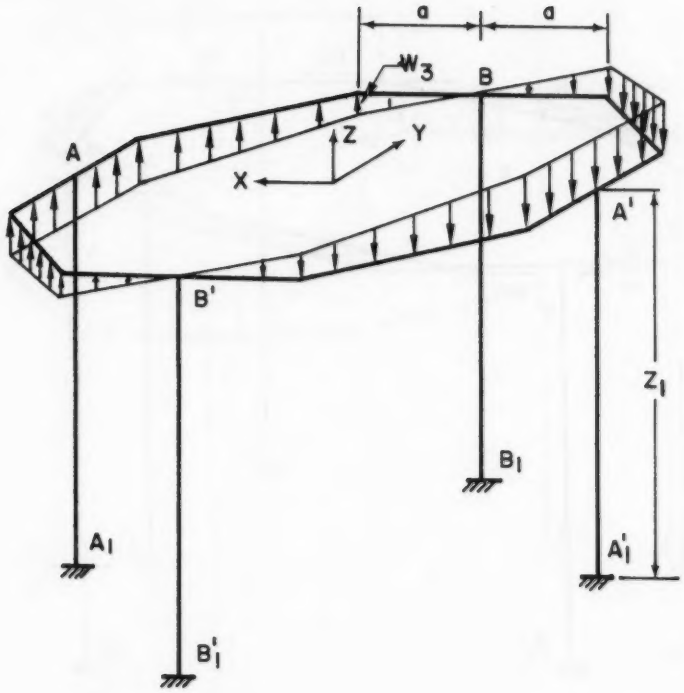

Fig. 14 Frame Subjected to Moment Load

$K = I/z_1 = 0.603$ ft^3, $K_A = K_c = I/a = 2.690$ ft^3, the numerical values of the last two terms may be evaluated as

$$F.E.M^{Y}_{AB} = -23.310 \text{ ft-kips}$$

and

$$F.E.M^{X}_{AB} = -734.808 \text{ ft-kips}$$

The solution of Equation (21) then gives $\beta_A = 9.05/E$, and the corresponding reactions are:

For column AA_1: $M^{Y}_{AA1} = 21.80$ ft-kips and $F^{X}_{AA1} = 1.58$ kips

For girder AB: $M^{Y}_{AB} = -10.90$ ft-kip and $M^{X}_{AB} = -730.11$ ft-kips

Similarly, reactions and moments at other points on the frame may be evaluated.

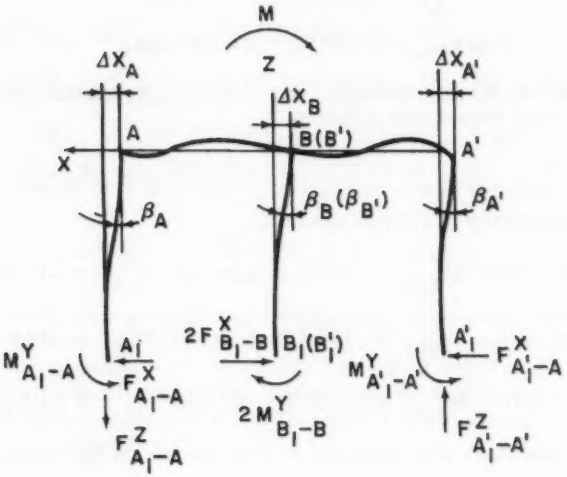

Fig. 15 Frame Deflection (on X-Z Plane) Due to Moment Load

2. Triangularly distributed haunch loads w_2 = 0.92 kip/ft. (Fig. 12).
For $h_c/b = 1$ and $r = 0.5$: From Fig. 6, $F.E.M^{Y'}_{AB} = -0.11180\ w_2a^2$

and $F.E.M.^{X'}_{AB} = -0.11792\ w_2a^2$

With reference to coordinates X and Y, the numerical values of the above expressions become:

$F.E.M^{Y}_{AB} = -0.09$ ft-kips and $F.E.M^{X}_{AB} = -3.23$ ft-kips

Equation (21) then yields $\beta_A = 0.33/E$, and the end reactions are:

For column AA_1: $M^{Y}_{AA1} = 0.08$ ft-kip and $F^{X}_{AA1} = 0.01$ kip

For girder AB: $M^{Y}_{AB} = -0.04$ ft-kip and $M^{X}_{AB} = -3.20$ ft-kips

Similarly, reactions and moments at other points on the frame may be computed.

3a. Component of lateral wind load acting parallel to the X-axis = $P \cos\phi$ = 70.7 kips or p = 0.95 kip/ft. (Fig. 13):

Here $k = EI_c/GJ_c = 2A = 1.3225$

For $h_c/b = 1$ and $r = 0.5$:

From Table I: $C_{33} = 0.40081$; $C_{34} = C_{43} = 0.08538$; and $C_{44} = 1.11588$

From Table II: $A_{22} = 2.98189$; $A_{23} = A_{32} = -2.06155$; and $A_{33} = 3.16811$

From Fig. 9: $F.E.F._{AB}^{X} = 1.125\ pa = 4.975$ kips

and $F.E.F._{BA}^{X} = 2.875\ pa = 12.705$ kips

Substituting the above constants and forces into Equations (22), (27), and (28), the following values are obtained

$$\Delta X_B = \Delta X_B = -1468.0/E, \quad \beta_A = 53.0/E \text{ and } \beta_B = 27.5/E;$$

and the corresponding end reactions are:

For column AA_1: $M_{AA1}^{Y} = -128.0$ ft-kips and $F_{AA1}^{X} = -15.35$ kips

For column BB_1: $M_{BB1}^{Y} = -189.4$ ft-kips and $F_{BB1}^{X} = -19.8$ kips

For girder AB: $M_{AB}^{X} = 114.5$ ft-kips and $M_{AB}^{Y} = 64.0$ ft-kips

Similarly, reactions and moments at other points on the frame may be determined.

3b. Component of lateral wind load acting parallel to the Y-axis = -p = -0.95 kip/ft:

By noting that the sign of p is reversed, stresses at various points on the frame for this component may be evaluated from the results obtained above.

4a. Component of moment load acting about the Y-axis = $M' \cos \phi = M^Y = 1414.22$ ft-kips:

The magnitude of equivalent anti-symmetrical vertical load w_3 at a distance "a" from the Y-axis due to this component (Fig. 14) may be approximately computed as follows:

$$w_3 = M^Y/47.29a^2 = 1.38 \text{ kips/ft.}$$

The fixed-end moments with reference to coordinates X and Y may be obtained from Figs. 7 and 8 for $h_c/b = 1$ and $r = 0.5$, as follows:

$$F.E.M_{AB}^{Y} = 0.0825\ w_3a^2 = 2.46 \text{ ft-kips;}$$

$$F.E.M_{AB}^{X} = 2.9425\ w_3a^2 = 88.00 \text{ ft-kips;}$$

$$F.E.M_{BA}^{Y} = -1.9925\ w_3a^2 = -59.5 \text{ ft-kips;}$$

$$F.E.M_{BA}^{X} = 0.2050\ w_3a^2 = 6.00 \text{ ft-kips}$$

The solution of Equations (29), (33), and (34) then gives

$$\Delta X_A = \Delta X_B = -85.8/E; \quad \beta_A = 0.62/E \text{ and } \beta_B = 15.88/E;$$

and the resulting moments and reactions are as follows:

For column AA_1: $M^Y_{AA1} = -13.51$ ft-kips and $F^X_{AA1} = -1.33$ kips

For column BB_1: $M^Y_{BB1} = -11.18$ ft-kips and $F^X_{BB1} = 1.33$ kips

For girder AB: $M^X_{AB} = 123.80$ ft-kips and $M^Y_{AB} = 6.77$ ft-kips

Similarly, the reactions and moments at other points on the frame may be computed.

4b. Component of moment load $M^X = M' \sin\phi = -1414.22$ ft-kips acting about the X-axis:

Similar to case 3b, all reactions and moments for this component may be obtained from the results achieved in case 4a above. Finally, the total shears and moments are algebraically "summed." Table III and Fig. 16 (solid lines) show respectively the values of total moment, torsion, and vertical shear, and their corresponding diagrams for one-half of the unfolded girder, using the following sign conventions:

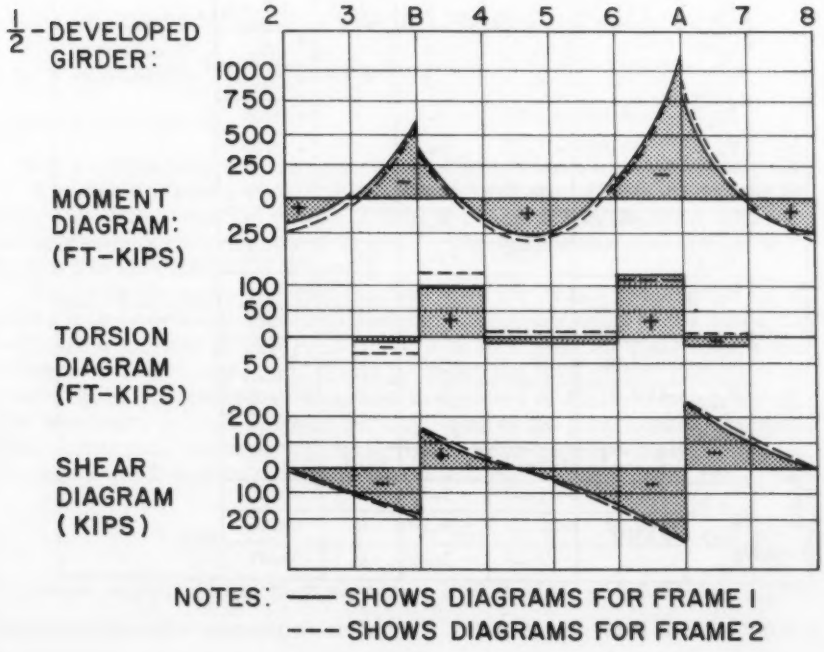

Fig. 16
Comparison of Moment, Torsion, and Shear for Frames I and II

TABLE III - SUMMARY OF STRESSES IN GIRDER OF FRAME I

Stress \ Load		Vertical Load	Wind Load	Moment Load	Haunch Loads	Total	Remarks
MOMENT	M^h_2	218.03	31.23	-63.21	0.10	186.15	Moments in ft-kips
	M^h_{3-2}	- 20.15	31.23	-14.05	-0.10	- 3.07	
	M^h_{3-B}	- 15.32	26.15	-10.13	-0.10	1.20	$\not\subset = 45^\circ$ for wind and moment loads
	M^h_{B-3}	-730.11	26.15	127.01	-3.20	-580.15	
	M^h_{B-4}	-730.11	234.14	96.12	-3.20	-403.05	
	M^h_{4-B}	- 15.32	99.32	29.02	-0.10	112.92	
	M^h_{4-5}	- 20.15	135.03	27.21	-0.10	141.99	
	M^h_5	218.03	0	0	0.10	218.13	
TORSION	T_2	0	0	0	0	0	Torsions in ft-kips
	T_{3-2}	0	0	0	0	0	
	T_{3-B}	14.02	-18.21	4.13	0	- 0.06	
	T_{B-3}	14.02	-18.21	4.13	0	- 0.06	
	T_{B-4}	-14.07	90.34	16.42	0	92.69	
	T_{4-B}	-14.07	90.34	16.42	0	92.69	
	T_{4-5}	0	-7.26	-9.92	0	-17.18	
	T_5	0	-7.26	-9.92	0	-17.18	
VERTICAL SHEAR	V_2	0	0	0	0	0	Shears in kips
	V_{3-2}	-102.08	0	15.03	0	-87.03	
	V_{3-B}	-102.08	0	15.03	0	-87.03	
	V_{B-3}	-205.13	0	39.06	-2.03	-168.10	
	V_{B-4}	205.13	-29.12	-21.11	2.03	157.93	
	V_{4-B}	102.08	-29.12	- 9.10	0	63.86	
	V_{4-5}	102.08	-29.12	- 9.10	0	63.86	
	V_5	0	-29.12	- 5.15	0	-34.27	

Beam convention is used for moments, i.e., negative when they cause tension in the top fibers.

Torsions are positive for a clockwise rotation of the section when looking along the girder in a clockwise sense.

Vertical shears are positive when they are directed upward. Since the vertical deflection at the mid-span of the girder members due to static loads may govern the serviceability of the frame, it is often desirable to evaluate its numerical value. With the aid of the data given in the appendix, the deflection Δz_2 at point "2" for the given vertical load and the computed moment at the mid-points of the girder may be computed as follows:

Here $w_1 = 21.94$ kips/ft and $w_2 = 0.92$ kip/ft,

and $w_1/w_2 = 0.0417$

$$M_2^h = 0.4574\ w_1 a^2$$

For $h_c/b = 1$ and $r = 0.5$; from Table V, $\lambda_{13} = -0.0228$

from Fig. A-2, $\lambda_{14} = -0.9542$

and from Fig. A-3, $\lambda_{15} = 1.3935$

Assuming $E = 3 \times 10^6$ psi ($f'_c = 3000$ psi), Equation A.2 yields

$$\Delta z_2 = -0.3172\ w_1 a^4 / EI_c^X = 0.087 \text{ in.}$$

Analysis of Frame II

For a comparison between the results derived for a haunched frame and for a prismatic frame, an analysis has also been carried out for Frame II (Fig. 17). The prismatic girder section of Frame II has the same area as the maximum girder section of Frame I. The loading that was applied to Frame I is also applied to Frame II.

Following the same procedure as that used for Frame I, using the appropriate frame constants and fixed-end forces corresponding to the shape factor ($h_c/b = 1.5$, and haunch ratio (r) = 0 in this case, the final shears and moments are then computed. Table IV shows the final numerical values so obtained; the corresponding diagrams are plotted in Fig. 16 (dotted lines). The maximum vertical deflection at mid-span of the girder members due to static loads amounts to -0.058 inch. The results from the analyses of Frames I and II may be briefly listed as follows

ITEM	FRAME I	FRAME II	$\frac{\text{FRAME I}}{\text{FRAME II}}$
Maximum negative moment at support	1062 ft-kips	1043 ft-kips	1.016
Maximum positive moment at center	250 ft-kips	301 ft-kips	0.830
Maximum torsion at support	121 ft-kips	146 ft-kips	0.820
Maximum vertical shear at support	257 kips	265 kips	0.970
Maximum vertical deflection	0.087 in.	0.058 in.	1.500
Material required for girder	38.050 c.y.	50.700 c.y.	0.750

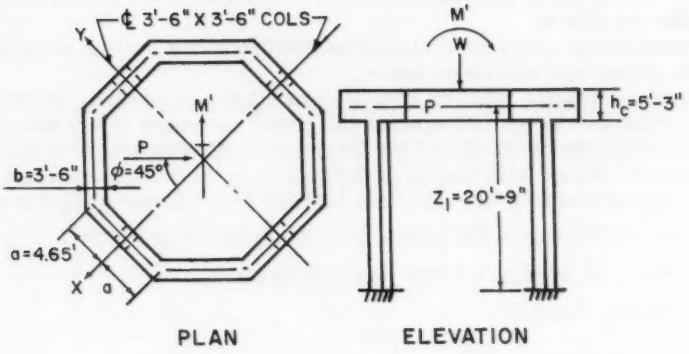

Fig. 17 Dimensions and Loads for Frame II

From this comparison it may be concluded that the 25% material saving in the girder of Frame II resulted in a 50% increase in deflection, while the major stresses were changed only slightly. If the absolute deflection is not objectionable, the selection of Frame I is suggested, inasmuch as it will have a better appearance at lower cost.

Stress Variations for Different Wind Directions

In the foregoing stress analyses, an arbitrary direction was assumed to exist for wind and its associated moment load. For the governing design of the frame, however, an understanding of the critical direction which produces maximum stress response of the members is essential. A study has been made to ascertain the stress variations versus variations in wind direction for frames with: (1) bending stiffness of column, (2) bending stiffness of girder and (3) torsional stiffness of girder approximately in the ratio of 1:1:1/2. Using the X-axis as the reference direction for wind (Fig. 18), the results of this investigation are summarized below:

1. Stress variations due to lateral wind load only:

   a. Stress in the girder members:

      When the wind is acting at $\phi = 45^{\circ}$, maximum bending moment, torsion, and vertical shear occur simultaneously at the ends of the side members whose middle segment is parallel to the direction of wind, whereas the stresses at the supports of both windward and leeward members are reduced to a minimum. Maximum bending at mid-span of the latter members, however, occurs approximately at an angle $\phi = 30^{\circ}$. Figures 19 and 20 show the pattern of variations.

   b. Stresses in the columns:

      There are two wind positions which induce equal combined stress in the columns, namely, $\phi = 45^{\circ}$ and 26°. $\phi = 45^{\circ}$ gives maximum combined

TABLE IV - SUMMARY OF STRESSES IN GIRDER OF FRAME II

Stress \ Load		Vertical Load	Wind Load	Moment Load	Total	Remarks
MOMENT	M^h_2	274.03	50.13	77.21	246.50	Moments in ft-kips; $\phi = 45^\circ$ for wind and moment loads
	M^h_{3-2}	25.12	50.13	-28.15	37.10	
	M^h_{3-B}	20.34	39.24	-20.04	39.54	
	M^h_{B-3}	-728.07	39.24	116.32	-572.51	
	M^h_{B-4}	-728.07	227.35	98.02	-402.70	
	M^h_{4-B}	20.34	87.11	28.14	135.59	
	M^h_{4-5}	25.12	142.03	31.03	198.18	
	M^h_5	274.03	0	0	274.03	
TORSION	T_2	0	0	0	0	Torsions in ft-kips
	T_{3-2}	0	0	0	0	
	T_{3-B}	-18.21	-32.15	14.32	-36.04	
	T_{B-3}	-18.21	113.21	15.04	146.46	
	T_{B-4}	18.21	113.21	15.04	146.46	
	T_{4-B}	18.21	113.21	15.04	146.46	
	T_{4-5}	0	18.24	-10.21	8.03	
	T_5	0	18.24	-10.21	8.03	
VERTICAL SHEAR	V_2	0	0	0	0	Shears in kips
	V_{3-2}	-107.12	0	15.06	-92.06	
	V_{3-B}	-107.12	0	15.06	-92.06	
	V_{B-3}	-214.22	0	39.01	-175.11	
	V_{B-4}	214.22	-30.11	-21.07	163.03	
	V_{4-B}	107.12	-30.11	- 9.21	67.80	
	V_{4-5}	107.12	-30.11	- 9.21	67.80	
	V_5	0	-30.11	- 5.34	-35.45	

stress due mainly to the bending in both horizontal axes. Hence it is also the governing angle for the design of columns. $\phi = 26^\circ$, on the other hand, produces the average response of the frame as a whole. Figure 21 shows the general characteristics of the variations.

2. Stress variations due to wind moment:

   a. Stresses in the girder members:

      Both maximum moment and torsion occur at the supports of the girder when $\phi = 0^\circ$. On the other hand, maximum vertical shear at the supports and maximum bending at mid-span are both given by $\phi = 45^\circ$.

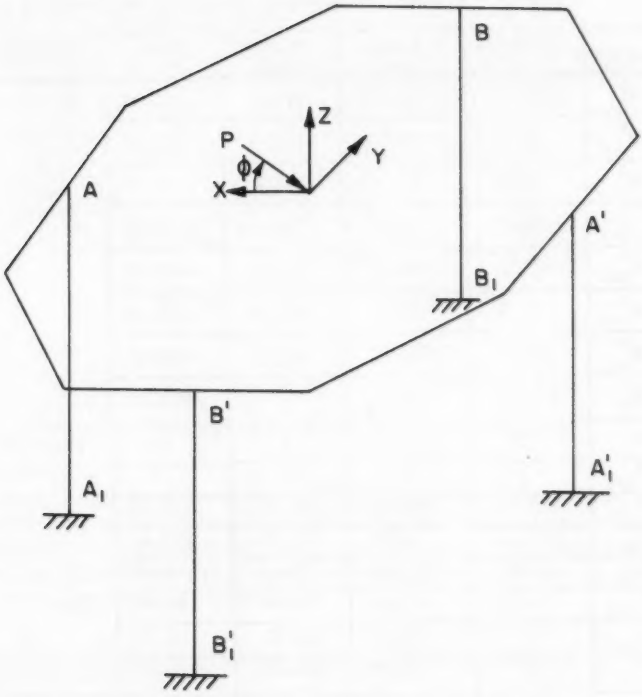

Fig. 18 Frame Subjected to Arbitrary Horizontal Load

b. Stresses in the columns:

Since the bending and shear stresses are usually small in the columns, because of this particular loading, the direct stress alone dominates the response. Maximum uplift or compression occurs in the front and rear column respectively for $\phi = 0^{o}$, which is approximately 37% greater than that for $\phi = 45^{o}$.

ACKNOWLEDGMENTS

The writer is indebted to Professors L. C. Maugh and B. G. Johnston of the University of Michigan for their valuable suggestions and general guidance. The writer also greatly appreciates the assistance given by Lockheed Aircraft Corp. in the preparation of this paper.

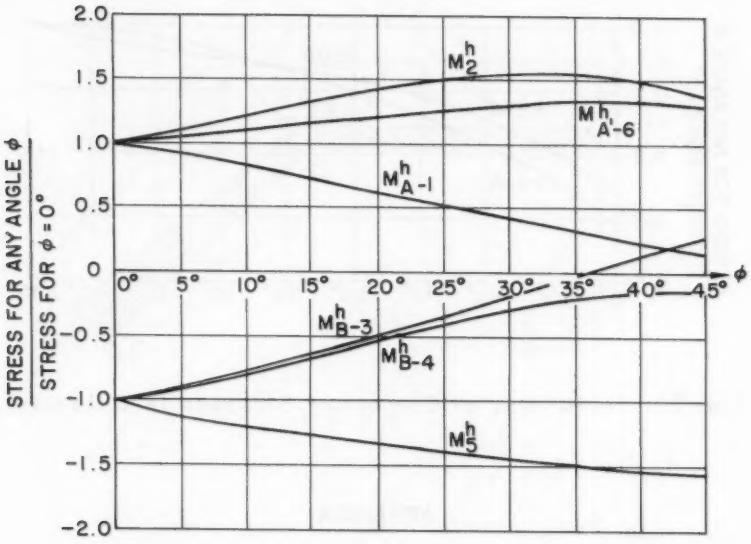

Fig. 19 Variations of Moments in Girder

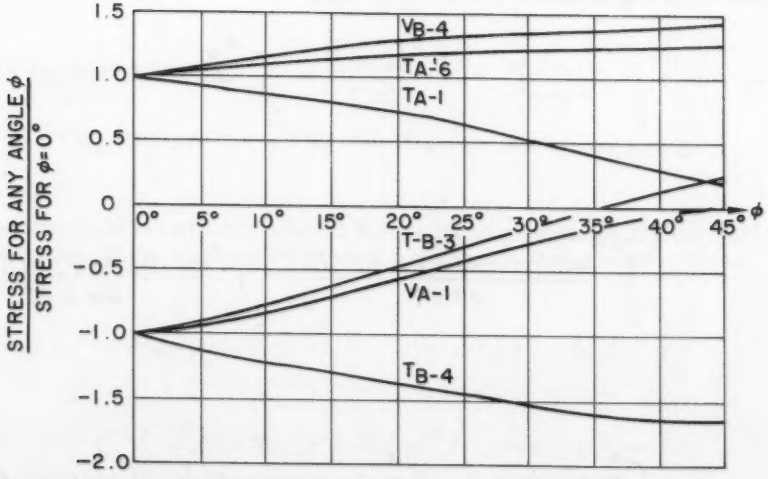

Fig. 20 Variations of Shears and Torsions in Girder

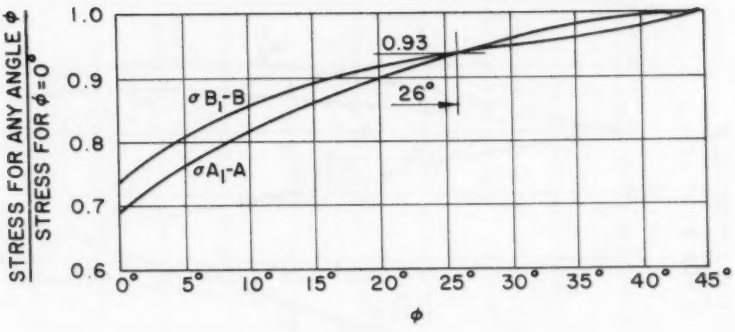

Fig. 21 Variations of Combined Stresses in Columns

APPENDIX

Evaluation of Deflection at Mid-Span of Polygonal Girder Due to Vertical Loads

The vertical deflection at the center of any haunched polygonal girder due to the haunch load (w_2), uniformly distributed vertical load (w_1), and the induced moment (M_E) can be expressed in terms of the applied loads and properties of the girder as follows (Fig. A.1):

$$\Delta Z_E = -\int_E^C \frac{w_1 s^2 ds}{2EI_c^x} + \int_E^C \frac{M_E s\, ds}{EI_c^x} - \int_C^A \frac{(\frac{a}{2}\cos\theta + s)(a\cos\theta + s)\, ds}{EI_s^x}$$

$$- \int_C^A \frac{w_1 (a\cos\theta + s) s^2 ds}{2EI_s^x} - \int_C^A \frac{w_2 (a\cos\theta + s) s^3 ds}{6aEI_s^x}$$

$$- \int_C^A \frac{w_1 a^3 \sin^2\theta\, ds}{2GJ_s} + \int_C^A \frac{M_E \cos\theta(\cos\theta + s)\, ds}{EI_s^x} + \int_C^A \frac{M_E \sin^2\theta\, ds}{GJ_s} \quad \text{(A.1)}$$

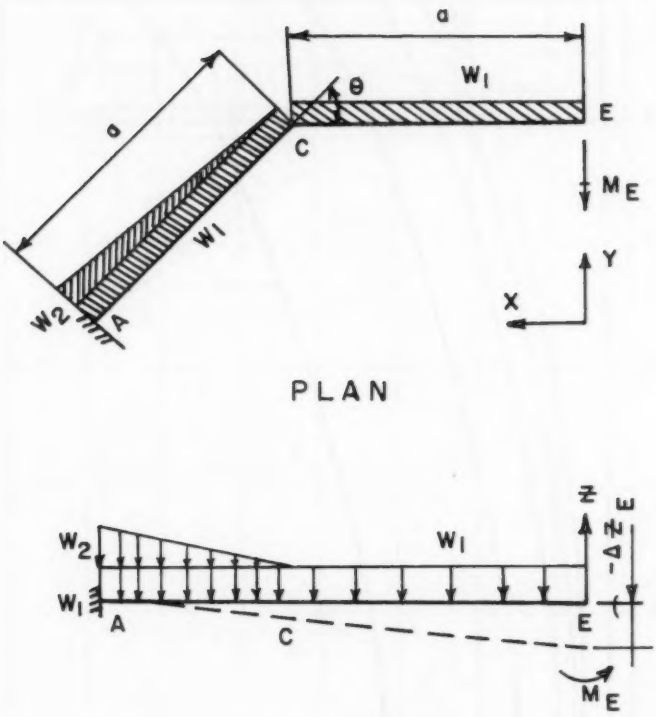

Fig. A-1 Deflection of Girder Due to Vertical Loads

Equation (A.1) is perfectly general for the basic member of any polygonal girder frame. If the shape of the girder is octagonal, then $\theta = 45^0$. Using the relation

$$k_s = EI_c^x / GJ_s = 0.575(1+u)[1+(h_s/b)^2],$$

or $$GJ_s = EI_c^x / 0.69[1+(h_s/b)^2] \quad \text{for } u = 0.20$$

Equation (A.1) finally takes the following form after integration

$$\Delta Z_E = -\lambda_{13} \frac{W_2 a^4}{EI_c^x} - \lambda_{14} \frac{W_1 a^4}{EI_c^x} + \lambda_{15} \frac{M_E a^2}{EI_c^x} \qquad \text{(A.2)}$$

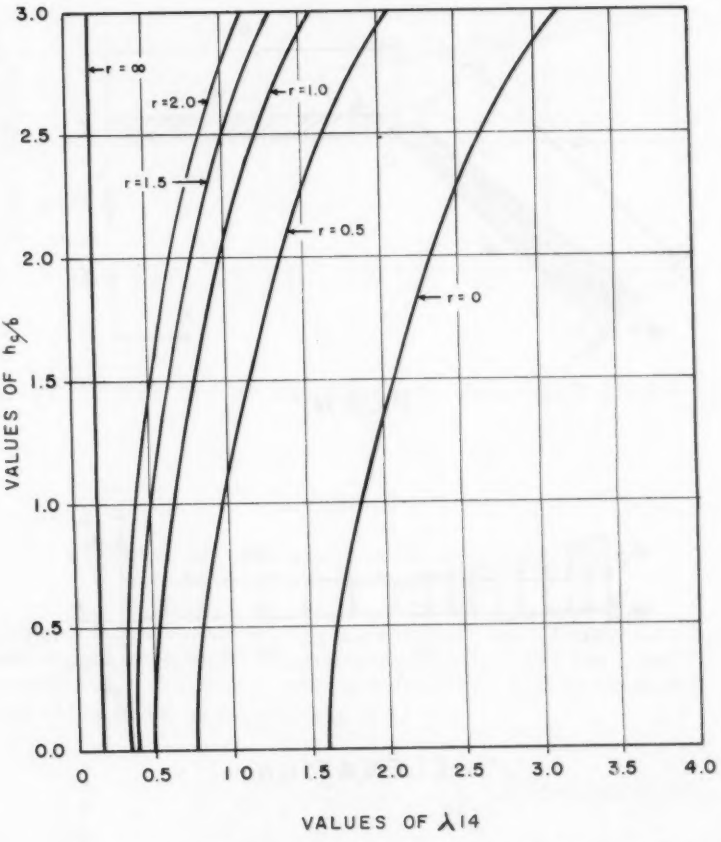

Fig. A-2 Deflection Coefficient Due to Uniform Vertical Load

In which

$$\lambda_{13} = \frac{0.15112}{r^4}\left[\frac{5}{2} + r - 3Ln(1+r) - \frac{3}{1+r} + \frac{1}{2(1+r)^2}\right.$$

$$\left. + \frac{1}{6r^5}\left[\frac{(1+r)^2}{2} - 4(1+r) + 6Ln(1+r) + \frac{4}{1+r} - \frac{1}{2(1+r)^2}\right]\right. \qquad \text{(A.3)}$$

$$\lambda_{14} = \frac{1}{8} + \frac{0.25r + 1.56051}{2(1+r)^2} + \frac{1.35355}{r^3}\left[Ln(1+r) - \frac{r(2+3r)}{2(1+r)^2}\right]$$

$$+ \frac{1}{2r^4}\left[\frac{5}{2} + r - 3Ln(1+r) - \frac{3}{1+r} + \frac{1}{2(1+r)^2}\right] \qquad \text{(A.4)}$$

$$+ \frac{0.17153}{r}\left[\frac{r(2+r)}{2(1+r)^2} + \left(\frac{h_c}{b}\right)^2 Ln(1+r)\right]$$

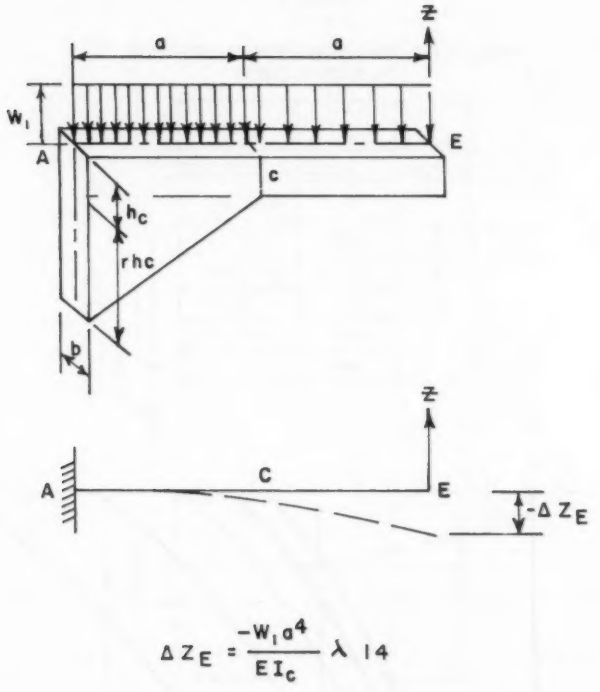

$$\Delta Z_E = \frac{-W_1 a^4}{E I_c} \lambda_{14}$$

Fig. A-2
Deflection Coefficient Due to Uniform Vertical Load (Cont.)

$$\lambda_{15} = \frac{1}{2} + \frac{0.5r + 1.70711}{2(1+r)^2} + \frac{0.34306}{r}\left[\frac{r(2+r)}{2(1+r)^2} + \left(\frac{h_c}{b}\right)^2 Ln(1+r)\right] \qquad (A.5)$$

Values of λ_{13} for various haunch ratios are listed in Table V, while values of λ_{14} and λ_{15} for different haunch ratios and the shape factors of the girder are respectively shown in Figs. A.2 and A.3. By means of this table and the accompanying figures, the maximum vertical deflection for the octagonal girder can be evaluated without difficulty.

REFERENCES

1. Disario, P. C.; Podolan, J. A.; Weil, N. A., "The Octagonal Girder Four Column Space Frame," ASCE Proceedings, Vol 80, Separate No. 542 (1954).

TABLE V

VALUES OF THE DEFLECTION COEFFICIENT FOR HAUNCH LOADS

hc/b	r	λ_{13}
All Values	0	0.06278
	0.5	0.02278
	1.0	0.01101
	1.5	0.00617
	2.0	0.00383
	∞	0

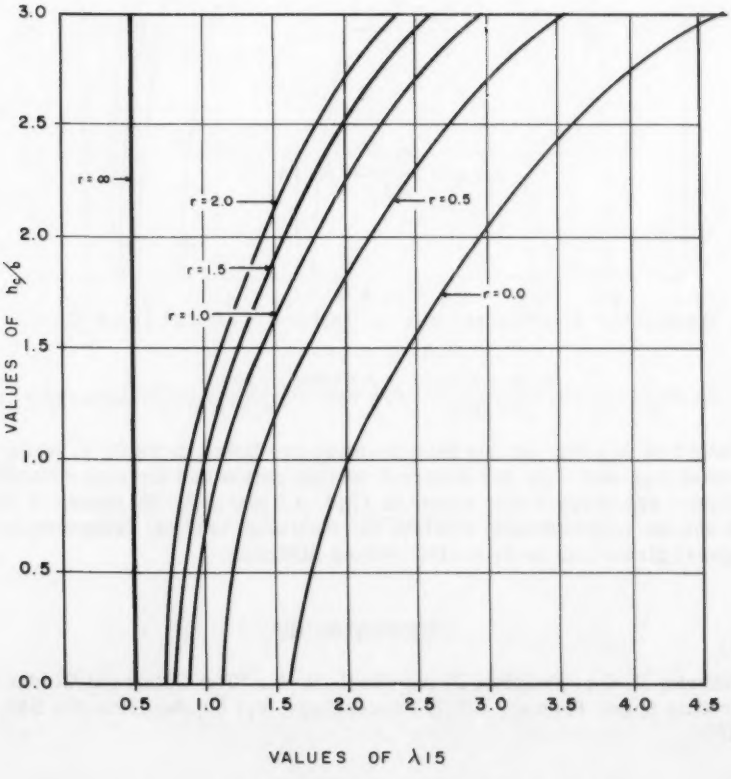

Fig. A-3 Deflection Coefficient Due to Moment

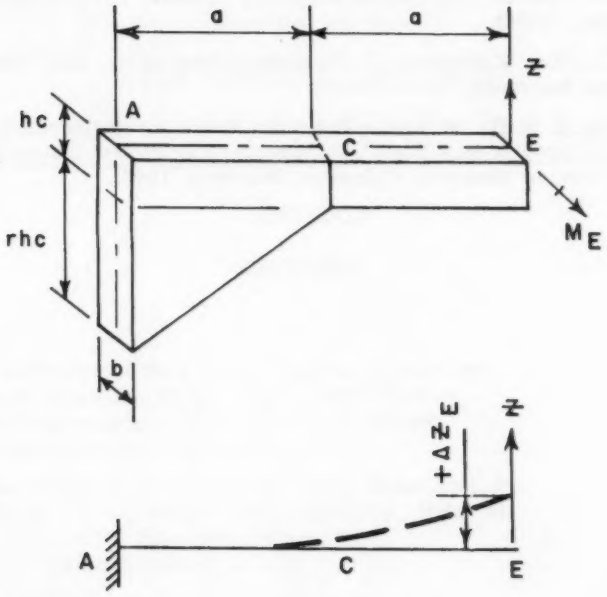

$$\Delta z_E = \frac{+M_E a^2}{E I_C} \lambda_{15}$$

Fig. A-3 Deflection Coefficient Due to Moment (Cont.)

2. Maugh, L. C., "Statically Indeterminate Structures," John Wiley & Sons Co., New York, N.Y. p. 132 (1948).

3. Saint Venant, B., "Mémoire sur le calcul de la résistance et de la flexion pièces solides à simple ou à double courbure, en prenant simultanément in consideration les divers efforts auzquels elles peuvent être soumises dans tous les sens," Comptes-Rendus de l'Académie des Sciences de Paris, France, Vol. 17, p 942 (1843).

4. Navier, "Résumé des Lecons," 3rd Ed, Notes and Appendices by St. Venant (Artical 5 on 'Torsion' presents St. Venant's studies in complete form).

5. Andersen, P., "Rectangular Concrete Sections under Torsion," ACI Proceedings, Vol. 34 (1937).

6. Grinter, L. E., "Theory of Modern Steel Structures," MacMillan Co., New York, N. Y. Vol. II, p. 241 (1949).

7. Timoshenko, P., "Theory of Elasticity," McGraw-Hill Book Co., New York, and London, p. 245 (1934).

8. Tsui, Y. W., "A Study of Stress Distribution in Haunched Polygonal Girder Space Frames with Column Supports," Thesis, Univ. of Michigan, Ann Arbor, (1956).

9. Unold, G., "Der Kreistrager," Forschungsarbeiten No. 255, Verein Deutscher Ingeniere, Berlin (1922).

10. Moorman, R. B. B., "Influence Lines for Horizontally Curved Fixed-End Beams of Circular-Arc Plan," Engineering Experiment Station Bulletin No. 35, Univ. of Missouri, Columbia, Missouri (1947).

Journal of the
STRUCTURAL DIVISION
Proceedings of the American Society of Civil Engineers

CONTENTS

DISCUSSION

Page

A Method of Design of Reinforced Concrete Section, by Panagiotis D. Moliotis. (Proc. Paper 1509, January, 1958. Prior discussion: 1827. Discussion closed.)
by Panagiotis Moliotis (closure) 43

Earthquake Design Criteria for Stack-Like Structures, by John E. Rinne. (Proc. Paper 1696, July, 1958. Prior discussion: 1857, 1922. Discussion closed.)
by John E. Rinne (closure) 45

Biaxially Loaded Reinforced Concrete Columns, by Tung Au and Algis Pabarcius. (Proc. Paper 1865, December, 1958. Prior discussion: 1988. Discussion closed.)
by Frederick Norman Pannell. 47

Direct Design of Optimum Indeterminate Trusses, by Louis M. Laushey. (Proc. Paper 1867, December, 1958. Prior discussion: 1952, 2043. Discussion closed.)
by A. J. Francis. 55

Review of Limit Design for Structural Concrete, by C. W. Yu and Eivind Hognestad. (Proc. Paper 1878, December, 1958. Prior discussion: 1952. Discussion closed.)
by Aron Zaslavsky 59
by W. W. L. Chan. 64
by Shaukat Miraz 65
by Henry J. Cowan 68

(Over)

Note: Paper 2075 is part of the copyrighted Journal of the Structural Division, Proceedings of the American Society of Civil Engineers, Vol. 85, ST 6, June 1959.

Page

Elasti-Plastic Analysis of Continuous Frames and Beams, by L. P. Johnson and H. A. Sawyer. (Proc. Paper 1879, December, 1958. Prior discussion: none. Discussion closed.)
by Giuliano Augusti 71
by Tullio Renzulli 74
by Emilio Rosenblueth 77
by A. A. Eremin 81

Shear Strength of Reinforced Concrete Beams, by Sidney A. Guralnick. (Proc. Paper 1909, January, 1959. Prior discussion: 2009. Discussion closed.)
by Robert F. Warner 83
by Henry J. Cowan 84
by Bela Goschy and George Balazs 85

On the Solution of Rigid Frames on the Column Analogy, by D. Y. Fok and Tung Au. (Proc. Paper 1914, January, 1959. Prior discussion: 2009. Discussion closed.)
by John Sherman 89

Analysis of a Two Way Truss System, by John A. Sbarounis and Michael P. Gaus. (Proc. Paper 1940, February, 1959. Prior discussion: none. Discussion open until July 1, 1959.)
by David Dario Brillembourg Bravo 97
by R. Schjödt 99
by John A. Sbarounis and Michael P. Gaus (corrections) 102

A METHOD OF DESIGN OF REINFORCED CONCRETE SECTION[a]

Closure by Panagiotis Moliotis

PANAGIOTIS D. MOLIOTIS,[1] M. ASCE.—Mr. Plaehn is of the opinion that the method of calculating any section of a reinforced concrete member of a structure as explained in Proceedings Paper 1509, is a difficult one. Mr. Plaehn bases this opinion mainly on the use of the factors which he considers difficult to understand and consequently the designer runs the risk of misinterpretation on application. He furthermore suggests that such problems be solved step by step instead of using formulas containing various factors.

Perhaps Mr. Plaehn did not have clear in his mind the role of each factor and therefore considers them to be difficult to understand. The role of each factor is clear and is not subject to any misunderstanding or misinterpretation.

There are basically 4 factors in the writer's study i.e. ρ, ρ', K_1, K_2. The factors ρ and ρ' depend on the distribution of the tensile and compression reinforcement in the reinforced concrete section under consideration. Factor K_1 determines the influence of the shape of the compressed part of the section of the concrete on the force C in comparison with the force C on the corresponding equivalent rectangular section with the same neutral axis. Factor K_2 also determines the influence of the compressed part of the section of the concrete on the determination of the point of application of the force C.

Finally the factors ρ, ρ', K_1 and K_2 influence the first member of the equation which expresses the balance of the moments of the forces which act on the section thus determining the auxiliary moments $\bar{M}_u$ and M_u^0 and the designation of the equivalent moment M_t which acts on the section of the concrete member. They also participate in the second member of the general equation for calculating rectangular sections, for the determination of the tensile and compressive reinforcement of the section considered.

The writer is of the opinion that for certain types of sections the auxiliary tables in conjunction with the corresponding basic tables of calculation of rectangular sections, will considerably facilitate design and will save repeating considerable calculations.

---

a. Proc. Paper 1509, January, 1958, by Panagiotis Moliotis.

1. Dr. Civ. Eng. Asst., National Technical Univ., Athens, Greece.

EARTHQUAKE DESIGN CRITERIA FOR STACK-LIKE STRUCTURES[a]

Closure by John E. Rinne

JOHN E. RINNE,[1] M. ASCE.—The additional detail and background of the response of simple one-mass structures given by Mr. Housner is appreciated. As he points out, the spectral responses of acceleration, velocity, and displacement are interrelated. Any one of these defines the elastic response of a one-mass system of constant natural period. Actually, in a major earthquake, the behavior of a structure is neither completely elastic, nor does the period stay constant. However, the period of a stack-like structure is not likely to change as much as a building period in the same earthquake. This is mentioned only to emphasize that the response spectra for idealized one-mass structures should not be accepted quantitatively without considerable reservations. Qualitatively, however, it is important to know that the characteristic shapes of the response curves are given by Mr. Housner's Figs. 1 and 2, for velocity and acceleration spectra, respectively.

The use of the velocity spectrum is particularly useful in the energy approach to the stresses induced in the structure. The big advantage in the energy method is that recognition can be given to the big energy absorption in the non-linear deformations, or the plastic range of the materials. But it should be kept in mind that the spectra, on the assumptions on which they are developed, are basically elastic responses. The assignment of large velocity damping factors, like 20% of critical damping, is not really consistent with the behavior of structures nor of the materials of which they are made. Judiciously selected, the damping factor might give an over-simplified but right-order-of-magnitude response of a given structure. But let us not get trapped into thinking that because the idealized, simplified structures can be analyzed very precisely, that this same precision and quantitative results apply equally well to real structures involving quite different conditions. This is not to belittle the spectrum analyses, which the writer is the first to acknowledge has become a most useful tool in the analysis of earthquake records.

The response of a distributed-mass structure, such as a stack, involves the superimposed responses of the different modes in which the structure can vibrate. By representing each of these modes by an equivalent one-mass system, the spectra can apply to each mode. The relative modal responses in shear and moment were obtained in the writer's paper, and the design criteria were established as the sum of these modal responses. Hence, it is not to be expected that combined modal response criteria would follow the spectrum which represents the response of a single one-mass system. Perhaps with

---

a. Proc. Paper 1696, July, 1958, by John E. Rinne.

1. Civ. and Structural Engr., Standard Oil Co. of California, San Francisco, Calif.

the aid of electronic computers analyses of combined responses can be made to test the validity of adding the modal responses. It is recognized that the peak, or spectral responses in the significant modes do not necessarily occur at the same instant. Nevertheless, it is believed that this assumption provides reasonable criteria for design. Perhaps Mr. Housner's curve A (his Figs. 3 and 4) does represent a better design criterion, but the writer has considerable doubt that it takes care of the combined modal responses adequately. Further analyses seem to be needed.

Mr. Housner also makes reference to the experience with stack-like structures in the 1952 Arvin-Tehachapi (Kern County, California) earthquake. A number of vertical stack-like vessels stretched their anchor bolts and some skirt buckling was evident. The buckling was associated with the detail of the anchor bolt attachment, which unfortunately did not provide a continuous horizontal ring plate around the vessel in the plane of the top of the anchor bolts. The writer recommends such ring plates and anchor bolts with sufficient projection out of the foundation so they can yield and absorb significant energy if need be. In a structure of this type, it is much more tolerable to accept yielding of the anchor bolts, with the energy absorption and damping attendant thereto, than to hazard a buckling of the shell or skirt of the vessel. An inherent and desirable "weakness" is built into the structure, selectively permitting yielding where it is not harmful. In earthquake-resistive design, it is preferable to permit overstress and yielding in desirable spots rather than to attempt to build a "one-horse shay" that will fail in all its parts. There seems to be an implication of the latter philosophy in Mr. Housner's opening comment: "All parts of a structure should have essentially the same factor of safety." For stack-like structures, as well as many others, this philosophy of design is unacceptable to this writer.

. . . . . .

The writer notes that Mr. Miller also comments on the omission of background material, some of which Mr. Housner has kindly supplied. Much of the background has been published, in ASCE proceedings and elsewhere. It was not considered essential to repeat what has already been very adequately documented in the literature of the profession.

. . . . . .

Mr. Degenkolb makes a point that the criteria proposed, involving higher-than-usual coefficients for shear, and two-thirds increase over normal allowable stresses instead of one-third as has been customary, would probably not be acceptable for building codes. The writer concedes this point but hastens to add that the best design practices are not necessarily reflected in our codes. There are many factors that go to make a code, and technical adequacy is only one of these.

BIAXIALLY LOADED REINFORCED CONCRETE COLUMNS[a]

Discussion by Frederick Norman Pannell

FREDERICK NORMAN PANNELL.[1]—Biaxially loaded columns occur in almost every reinforced concrete frame, and it is essential that some method of designing these members should be available. The authors are to be congratulated upon their effort to produce a completely general method of analysis, even if the actual application appears to be unsuitable for practical design purposes. One mild criticism of the paper concerns the statement that stress distributions can be predicted; since the form of the stress block in bending and compression cannot be defined with any accuracy—and indeed it is difficult to see that it can ever be so defined, for stresses are not measurable quantities—then no accurate determination of stresses can be obtained from measured strains. It is precisely this difficulty which has led to the adoption of ultimate load methods.

Few examples of the analysis of biaxially loaded columns are available, but it is noteworthy that the column sections chosen in these cases have a nearly equal amount of steel in each face. This is an understandable and economic choice, such as most practical designers would adopt. This fact may be used to advantage.

The writer has produced a method of designing such columns; the design can be carried out with almost complete accuracy in a matter of minutes. The approach is fundamentally different from that first outlined by Whitney and Cohen,(1) systematised by Au,(2) and completely generalised by the authors. It may therefore be of interest to outline this approach and to indicate its application to the column section analysed in the paper.

The method involves the consideration of the interaction surface which would be formed by plotting in three-dimensional form the curves of failure load against corresponding moment for all possible axes of the column. Although the actual surface could only be obtained with extreme difficulty, its fundamental nature is such that certain operations may legitimately be performed upon it. There is a whole family of such surfaces for a section varying in breadth-to-depth ratio only, and the writer has demonstrated that all these surfaces can be telescoped into one. There is a further family of such telescoped surfaces for varying steel cover ratios, and these in their turn can also be reduced to one surface.

The one remaining surface—representing a family of families of surfaces—can now be transformed and rectified until it closely coincides with the surface of revolution formed by rotating the major Y-axis interaction curve through 360°. The transformed surface can then be defined by one curve, and this

a. Proc. Paper 1865, December, 1958, by Tung Au and Algis Pabarcius.
1. Lecturer, Dept. of Structural Eng., College of Science and Technology, Manchester, England.

curve, reduced to non-dimensional form, can then be used to predict the failure load for any rectangular column with an equal and uniformly distributed area of steel in each face, having any practical breadth-to-depth ratio and cover-to-depth ratio, and loaded with any combination and eccentricity of loads. The curve of course related to one particular steel ratio; it has unfortunately been found impracticable to telescope all steel ratios into one.

The design curve is therefore the one for bending about a major axis. A set of such curves for a multi-bar column—based on the stress and strain values adopted by the authors—for one to four per cent of steel is given in Fig. 1. A definite ultimate concrete stress has been adopted for simplicity in comparison, although the curves may readily be prepared in more general form. A Whitney stress block was used in deriving the equations, and some allowance made for the area of concrete displaced by steel in compression.

The equation for transforming the actual moments to conform to the design surface is:

$$M_g = \frac{F\, M_y \sec\theta}{1 - N(\sin 2\theta)^2}$$

in which the symbols may be defined as follows:

$$\theta = \tan^{-1} \frac{\phi\, M_x}{M_y} \quad \text{where}$$

M_x and M_y are the components on the X and Y axes respectively of the actual radial moment, and

ϕ is the ratio $\frac{M_{by}}{M_{bx}}$ of the 'balanced' failure moments when the failure load acts in the planes of the Y and X axes respectively.

F is a factor adjusting for steel cover ratio, obtained from $F = \frac{M_{bb}}{M_{ba}}$ in which M_{ba} is the 'balanced' failure moment for the actual steel cover ratio used and M_{bb} is the equivalent moment for the ratio upon which the design curve is based, when the failure load in each case acts in the Y axis plane.

N is a deviation factor for the point of maximum deviation of the actual interaction surface from the idealized design surface, and which can be obtained graphically.

$(\sin 2\theta)^2$ is an empirical expression for the shape of the deviation path.

M_g is the moment to be used in conjunction with the required failure load P to check the section on the design curve.

Values of N, F, and ϕ can be obtained and plotted as in Fig. 2.

The accuracy of the method has been investigated by means of a large number of case-analyses. Defining the problem as being to find the load which will bring the column to the point of failure when applied at a given radial eccentricity, the standard of prediction has been taken as the ratio $\frac{Pg}{P}$ in which

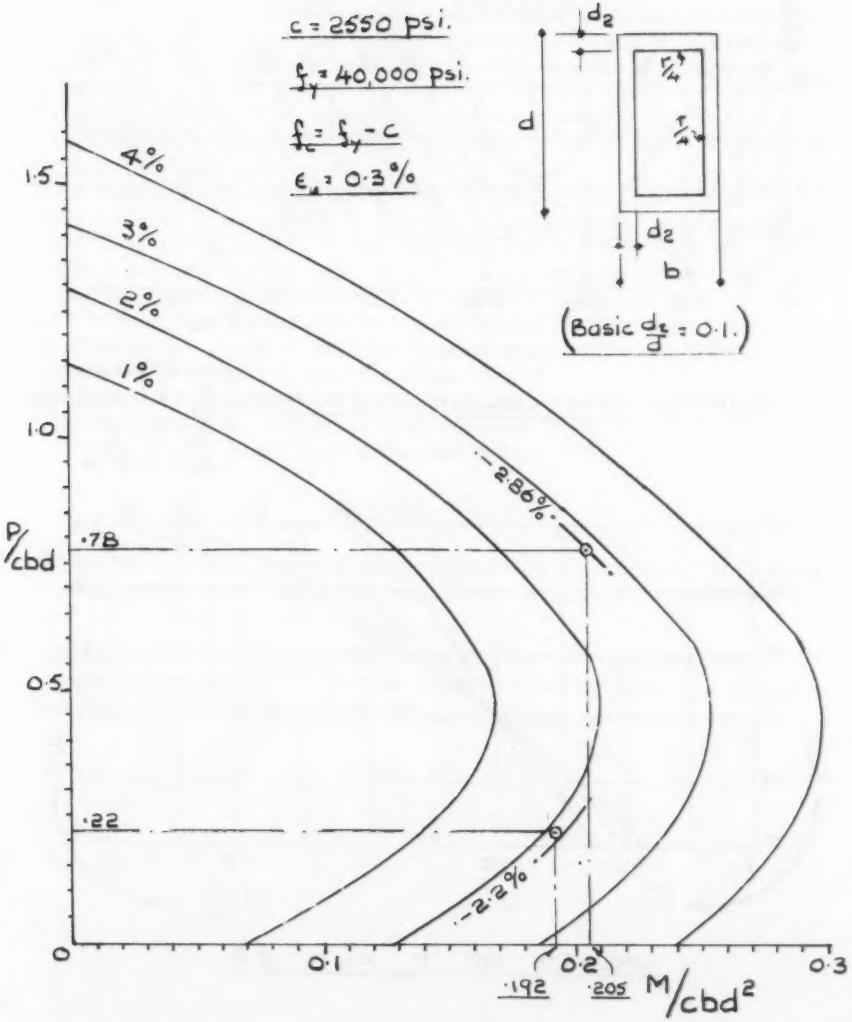
c = 2550 psi.
f_y = 40,000 psi.
$f_c = f_y - c$
ϵ_u = 0·3%
d_2
d
b
(Basic $\frac{d_2}{d}$ = 0·1.)
4%
3%
2%
1%
2·86%
2·2%
1·5
1·0
0·5
0
P/cbd
·78
·22
0·1
0·2
0·3
·192
·205
M/cbd²

Fig. 1

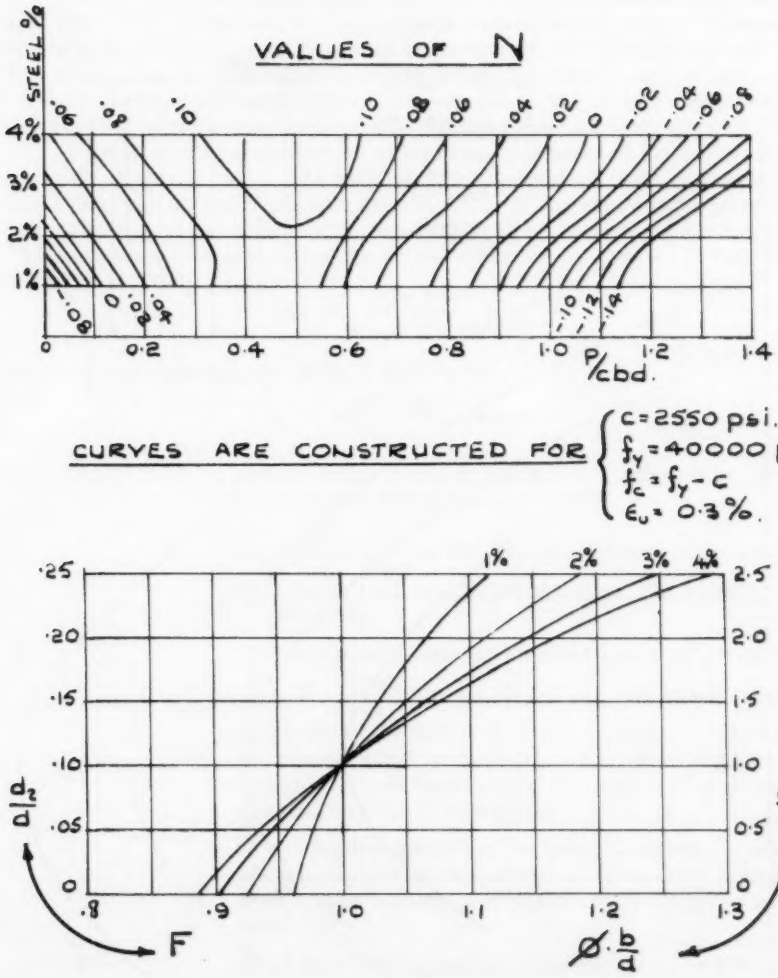
VALUES OF N
STEEL %
4%
3%
2%
1%
0
0·2
0·4
0·6
0·8
1·0
1·2
1·4
P/cbd.
CURVES ARE CONSTRUCTED FOR
c = 2550 psi.
f_y = 40000 psi
$f_c = f_y - c$
ϵ_u = 0·3%.
1%
2%
3%
4%
·25
·20
·15
·10
·05
0
·8
·9
1·0
1·1
1·2
1·3
2·5
2·0
1·5
1·0
0·5
0
d/d₂
d/D
F
$\phi \cdot \frac{b}{d}$
VALUES OF F AND $\phi \frac{b}{d}$

Fig. 2

Pg is the failure load predicted from the graph, and P is the failure load derived from a theoretical analysis.

Of the 127 non-dimensional cases analysed, to the nearest 1% 82 had no significant error, 35 had a 1% error, 8 a 2% error, and 1 a 3% error. The cases cover all possible ranges of position of the neutral axis.

It was found that for columns with twelve or more bars the steel distribution may be taken to be in the form of a steel ring without significant error. For eight or four bar columns special curves appropriate to these patterns must be used.

Turning to the column section analysed in the paper, the calculations necessary to check the section are given in Fig. 3; the section calculated by Au is also considered, in Fig. 4.

The resulting moments M_g are plotted in Fig. 1. The prediction given in the first example is some 0.5% in error because the steel is not quite equally distributed in the four faces, as has been assumed in constructing the design curve; this error is about a quarter of that which would be induced by neglecting the area of concrete displaced by compression steel. In the second example the steel distribution is even further from that assumed, causing an error of about 2%, which in this case is about equal to the error induced by the originator in neglecting concrete displacement.

The foregoing derives from research carried out in the Structural Engineering Department of the College of Science and Technology, Manchester, and is drawn from a thesis to be submitted in May, 1959.

REFERENCES

1. "Guide for Ultimate Strength Design of Reinforced Concrete" by Charles S. Whitney and Edward Cohen. Journal of the American Concrete Institute Nov. 1956, No. 5, Vol. 28.

2. "Ultimate Strength Design of Rectangular Concrete Members Subject to Unsymmetrical Bending", by Tung Au, Journal of the American Concrete Institute, Feb. 1958, No. 8, Vol. 29.

EXAMPLE 1.

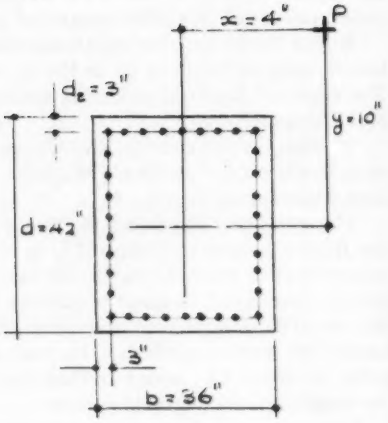

Data.

P = 3000 kips
Px = 12000 kip. ins.
Py = 30,000 kip. ins.
Steel Ratio r = 2.86%
d_2/d = .0715
d/b = 1.167
c = 2550 psi.
cbd = 3860 kips

Calculations

$$P/_{cbd} = \frac{3000}{3860} = \underline{\underline{0.78}}$$

From Fig. 2 N = .05 F = .97
ϕ = 1.02 × 1.167 = 1.19.

$$\text{Tan } \theta = 1.19 \times \frac{12000}{30000} = .476 \qquad \theta = 25^\circ 27$$

Sec θ = 1.107

$$M_g = \frac{.97 \times 30000 \times 1.107}{1 - .05 \times .602} \qquad \sin^2 2\theta = .602$$

= 33,200.

$$\frac{M_g}{cbd^2} = \frac{33,200}{3860 \times 42} = \underline{\underline{0.205}}$$

Fig. 3

EXAMPLE 2.

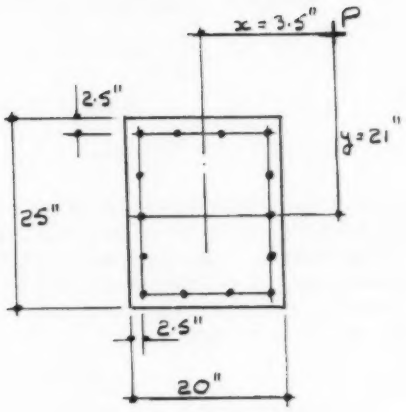

Data.

P = 280 kips.
Px = 980 kip.ins.
Py = 5880 kip.ins
Steel ratio r = 2.2%
d_2/d = 0.1
d/b = 1.25
c = 2550 psi.
cbd = 1275 kips

Calculations

$$P/cbd = \frac{280}{1275} = \underline{0.22}.$$

From Fig. 2 N = .065 F = 1.0

$$\phi = 1.025 \times 1.25 = 1.28$$

$$\text{Tan}\,\theta = \frac{1.28 \times 980}{5880} = .214$$

$\theta = 12^\circ 6$

Sec θ = 1.023

$\text{Sin}^2 2\theta = 0.168$

$$\frac{Mg}{cbd^2} = \frac{5880 \times 1.023}{1275 \times 25\,(1 - .065 \times .168)} = \underline{0.192}.$$

Fig. 4

DIRECT DESIGN OF OPTIMUM INDETERMINATE TRUSSES[a]

Discussion by A. J. Francis

A. J. FRANCIS.[1]—It is always interesting to observe how divergent are the courses pursued by two research workers proceeding independently from the same point. The basic concept on which Mr. Laushey's paper is built is identical with that stated by me in two papers a few years ago;[1,2] but his development differs considerably from mine, and our work is really complementary.

Mr. Laushey's investigation of the problem of satisfying the basic Eq. (2)

$$\sum s \cup L \quad = 0$$

is more thorough than my own. In particular, his use of the relationship $\Sigma uL = 0$ which holds for certain cases is most interesting. This equation is a special case of the author's Eq. (3)

$$\sum FL \quad + \quad \sum (P,R)\, d \;=\; 0$$

This relationship, due to Van den Brock, between the internal forces in a truss and the external loads and reactions is a remarkable one, and apparently very little known. But I am dubious as to the validity of the proof put forward by Mr. Laushey, and prefer an approach by way of the principal of virtual work, as follows:

Consider a statically indeterminate framework (Fig. 1(a)) with a redundant member EG and redundant reactions at B and C, acted on by loads P_1 and P_2 which produce a force F in a typical member MN. The reactions at B and C have horizontal and vertical components X_B, Y_B and X_C, Y_C. Tensile forces are assumed positive.

Now consider the same truss with all loads and external reactions removed. Let us assume that the plane in which the truss lies undergoes a uniform expansion relative to some point or pole 0. All lines in the plane (including the bars of the truss) increase in length by a uniform ratio α, but do not change in direction. Then the displacement of any joint of the truss such as D will be in the direction OD, away from O, to a point D' where $DD' = \alpha .OD$. (Fig. 1(b)). We assume that $\alpha << 1$.

According to the theorem of virtual work in finite form,

$$\sum (P,\, R)\, \Delta \quad = \quad F \;\bullet$$

where P, R are external loads and reactions, and F is a bar force, in the first state (Fig. 1(a)), and Δ and e are a component of displacement of a loaded point in the direction of a load or reaction and a bar extension respectively, in the second state (Fig. 1(b)).

---

a. Proc. Paper 1867, December, 1958, by Louis M. Laushey.

1. Head, Dept. of Civ. Eng., Univ. of Melbourne, Melbourne, Australia.

Hence we have:

$$\sum (P, R) \propto OD \cos\theta = \sum F \propto L$$
$$\text{or} \quad \sum (P,R) \quad QD = \sum F L \qquad (1)$$

A term (P, R) Q D is positive if the component of P or R in the direction of the pole acts away from the pole, and a term FL is positive if F is tensile. The terms FL include all members of the truss including the redundant member (s). Eq. (1) holds for non-elastic as well as for elastic behaviour of the truss under the loads P, so long as the relation between load and change of length of each bar is single-valued.

Applying this procedure to the truss shown in Fig. 2(c) of the paper (see my Fig. 2), we may conveniently choose as our pole the joint A, since we automatically eliminate the term involving the reaction at A by so doing. Then we have:

$$P_1 (0) + P_2 (0) - P_3 . AC \cos\theta + R_B . (0) = FL$$

Or,

$$- P_3 . y = FL$$

as in Mr. Laushey's paper.

Again, taking Mr. Laushey's Fig. 2(a) (my Fig. 3) and assuming, as he in fact does, that $X_A = X_B = \frac{1}{2\sqrt{2}}$, we have

$$- 1. AC \cos\theta + \frac{1}{2\sqrt{2}} . AB = \sum FL$$
$$\text{or} \quad - \quad d \quad = \sum FL,$$

again as in the paper.

Apropos the discussion of the minimum weight of trusses it may be interesting to mention that Sved[3] has shown that the framework of minimum weight to support a given set of loads with specified bar stresses is always statically determinate; in other words, indeterminacy always adds to the weight, even if full stressing is possible. The same conclusion does not necessarily apply to a truss designed for several different loading conditions. The question of optimum design in this case is much more difficult, and although Mr. Laushey has tackled this problem in his paper his ad hoc approach, while yielding reasonable results in the examples he gives, could lead in special cases to substantial overstressing in some members under one or other loading condition.

The procedure put forward—that of picking out the only fully stressed members under each system of loads and making a composite structure out of them—has no rational basis, there being no assurance that the stresses will be as assumed.

Schmidt, working in the Department of Civil Engineering at Melbourne University, has recently tackled this problem in an interesting paper.[4] He derives the conditions for minimum weight design under alternative load systems and gives example of how such a design may be undertaken. A solution can only be reached by a series of successive adjustments to initial trial designs.

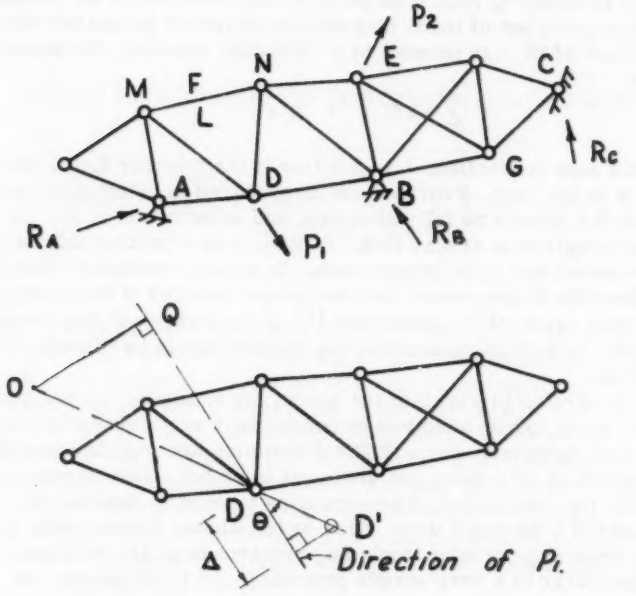

FIG. 1

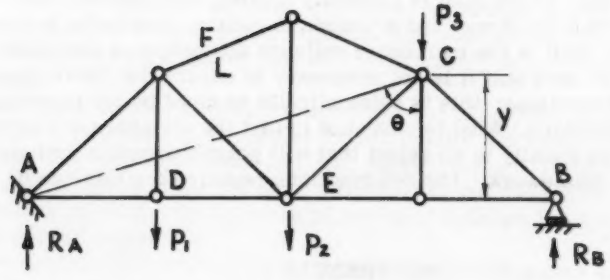

FIG. 2

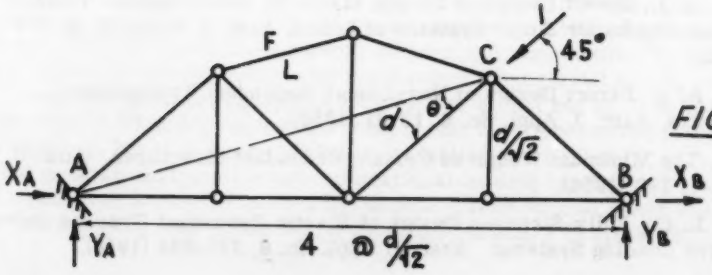

FIG. 3

The difficulty of securing maximum permissible stresses in all members of a truss under a given set of loads may be circumvented in another way. When an initial lack of fit λ is present in a redundant member, the author's Eq. (2) becomes

$$\sum sv\mathrm{L} \cdot \lambda E \qquad (2)$$

in which, with my sign convention, λ is positive if the member is too short and negative if it is too long. Provided one is prepared to admit such lack of fit, all members can always be fully stressed, and substitution in Eq. (2) will give the value of required to ensure this. Another way of putting this is that the redundant member has to be prestressed. In a multi-redundant structure it is perfectly feasible to prestress each redundant member if necessary, and examples have been given of the procedure.(1) If the redundant is a reactive force at a support, lack of fit means that the support has to be displaced in the required direction.

In the truss illustrated in Fig. 6 of the paper, for example, the full stress t or c in each member can be achieved by producing a vertical displacement at each of the inner supports. Remarkable economics are possible in arches by the simple expedient of jacking one abutment in or out. This seems to open up a vast field for the application of prestressing to framed structures.

In a later paper(2) I extended these ideas to non-linear frameworks, and showed that the general principles, including prestressing, are still applicable. This leads in particular to a very simple procedure for limit design. A reasonable system of internal forces which satisfies equilibrium is assumed, and each member is assigned the limit stress, from which the sectional areas may be calculated. As the load is gradually applied, one member after another reaches the limit stress and proceeds to deform plastically in tension or compression, until at the moment of collapse all members are at the limit stress. It will be seen that it is not necessary to ensure that there is compatibility of deformations: this is automatically ensured by the plastic deformation of the members. What <u>is</u> essential is that the members are actually able to deform plastically to an extent that will permit complete redistribution of stress in the framework. The deformations required for this can be calculated.

REFERENCES

1. Francis, A. J., Direct Design of Elastic Statically Indeterminate Triangulated Frameworks for Single Systems of Loads, Aust. J. Appl. Sc. <u>4</u>, 175-185 (1953).

2. Francis, A. J., Direct Design of Non-Linear Redundant Triangulated Frameworks, Aust. J. Appl. Sc. 6, 13-31 (1955).

3. Sved, G., The Minimum Weight of Certain Redundant Structures. Aust. J. Appl. Sc. <u>5</u>, 1-9 (1954).

4. Schmidt, L. C., Fully-Stressed Design of Elastic Redundant Trusses under Alternative Loading Systems. Aust. J. Appl. Sc. <u>9</u>, 337-348 (1958).

REVIEW OF LIMIT DESIGN FOR STRUCTURAL CONCRETE[a]

Discussions by Aron Zaslavsky, W. W. L. Chan, Shaukat Miraz, and Henry J. Cowan

ARON ZASLAVSKY.[1]—Ultimate strength design may be regarded as a first step towards limit design allowing for the different limitations of the concrete (low plasticity, danger of excessive cracking under service loads etc.).

Incorporation of limit design in the Code may be still far away, but it is hoped it will not result in three alternative design methods being simultaneously available for use: elastic, ultimate strength and limit design. Even now, various dubious combinations of the elastic and ultimate-strength methods have been used with a view to obtaining economical sections. (It may be recalled that according to the former ACI Code the design of beams with compression reinforcement involved elastic design for tensile steel and plastic design for compression steel).

As for current practices in different countries, one may justify ultimate strength design based on an elastic moment distribution, since this is one of the many possible collapse moment diagrams; but elastic design of sections based on plastically redistributed moments (in consequence of the appearance of plastic hinges) seems rather illogical, even though numerical results may be acceptable.

A more detailed definition of the term "plastic hinge" would read:—a beam section where yielding has developed in both tensile and compression zones. The plastic hinge develops when the (full) plastic moment is applied; it is capable of rotation as if the member were hinged, but the plastic moment is maintained at the hinge. In the case of reversed rotation the response is elastic from the outset.

The contention that strengthening some of the sections may actually weaken the structure as a whole is very interesting. The writer was aware of such cases in the elastic range, but not in limit design.(1) For example, consider a rectangular (a x b) mild steel bar in axial tension P (Fig. 1a; σy = yield stress). Fig. 1b shows the variation of the maximum elastic (P_y) and plastic (P_{cr}) carrying capacity when additional eccentric material (x - a) is added.(2) It is seen that additional material may reduce P_y but not P_{cr}. In other cases (e.g.(3,4)) additional reinforcement may not increase the plastic carrying capacity, but it is assumed that no reduction takes place.

Shake-down analysis for non-proportional loading has been mentioned in the review but it may be interesting to note that in special cases even proportional loading may produce non-monotonic changes of stresses.

---

a. Proc. Paper 1878, December, 1958, by C. W. Yu and Eivind Hognestad.

1. Sr. Lecturer, Technion - Israel Inst. of Technology, Haifa, Israel.

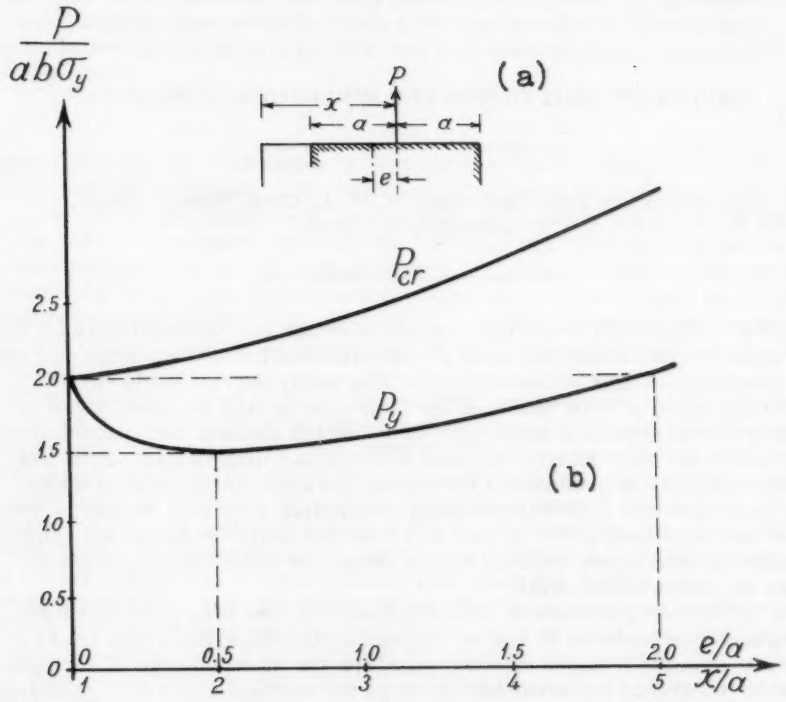

Fig. 1

Take for example the above steel bar under eccentric tension (Fig. 2a) with force P inside the section core (say e = a/9). Fig. 2b shows the non-monotonic stress variation at the far fibre (2) with increasing P.

Another example is an ideal plastic two-span beam of variable cross-section (Fig. 3a).[2] The loading history shows (Fig. 3b) that a plastic hinge forms at D, rotates and ceases to rotate, and a decrease of stress takes place before collapse.

The exact moment coefficients (for total, i.e. dead + live, load) of the Russian Code[5] are shown in Fig. 4. These recommendations apply to one-way slabs and secondary beams in cases of spans differing by not more than 10%. The support coefficients refer to the reduced moment due to width of supports. It is also required that reinforcement at the support be not too heavy, the ratio of depth of the neutral axis to effective depth being limited to not more than 0.3; this is to ensure against brittle (compression) failure.

In conclusion, some remarks on the criterion of ultimate-strength and limit designs! Both methods are based on the concept of strength in the sense that calculations are carried out in terms of critical stresses (yield stress, crushing-strength stress etc.). But in the last resort it is the limiting deformation that defines the "structural usefulness" (referring to authors' definition) of the structure. A single-span steel beam does not actually collapse

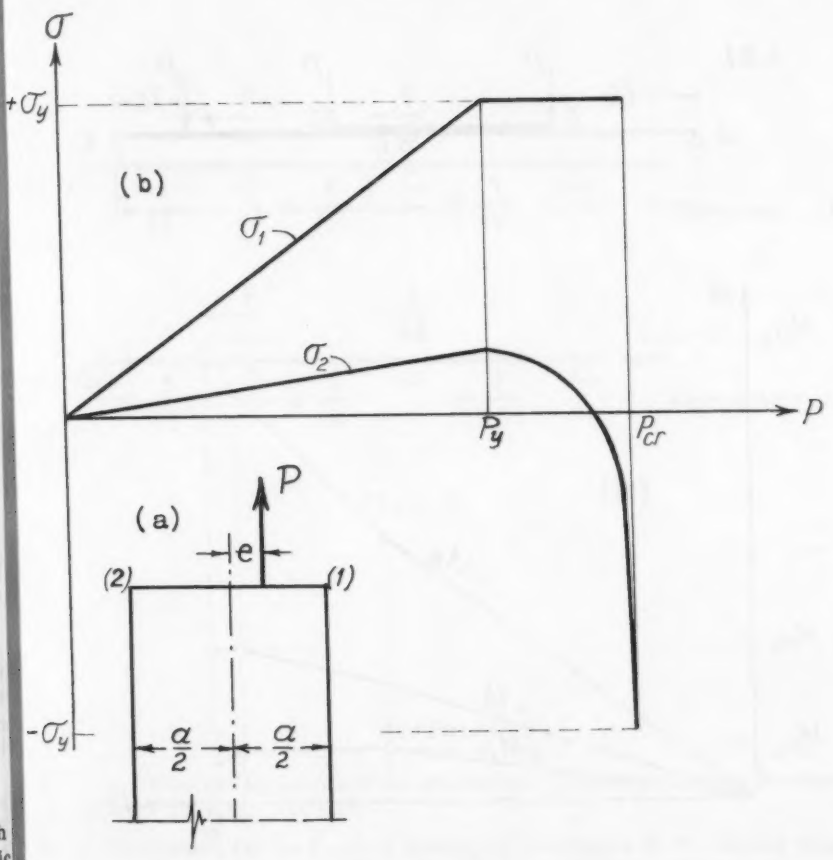

Fig. 2

when a plastic hinge has formed at its most stressed section. If, still, this state is defined as the critical collapse state, it can only be justified on the grounds that deflections have become so excessive as to render the structure totally unserviceable (no local buckling assumed).

In reinforced concrete structures, although the ultimate plastic moment may cause the actual crushing of the concrete, it is again the deformation rather than the strength (stress) criterion that counts—in view of the restrictions imposed on plastic hinge rotations, width of cracks etc. It may be also noted that there are wide discrepancies in the definition of concrete crushing (design) strength in flexure. According to the ACI Code it is 85% of the cylinder strength; according to the British Code it is 2/3 of the cube strength; the Russian Code assumes it to be 25% higher than the prism strength. While the ultimate bending moment depends very little on concrete strength, this is not the case in sections subjected to the combined action of bending moment and axial force.

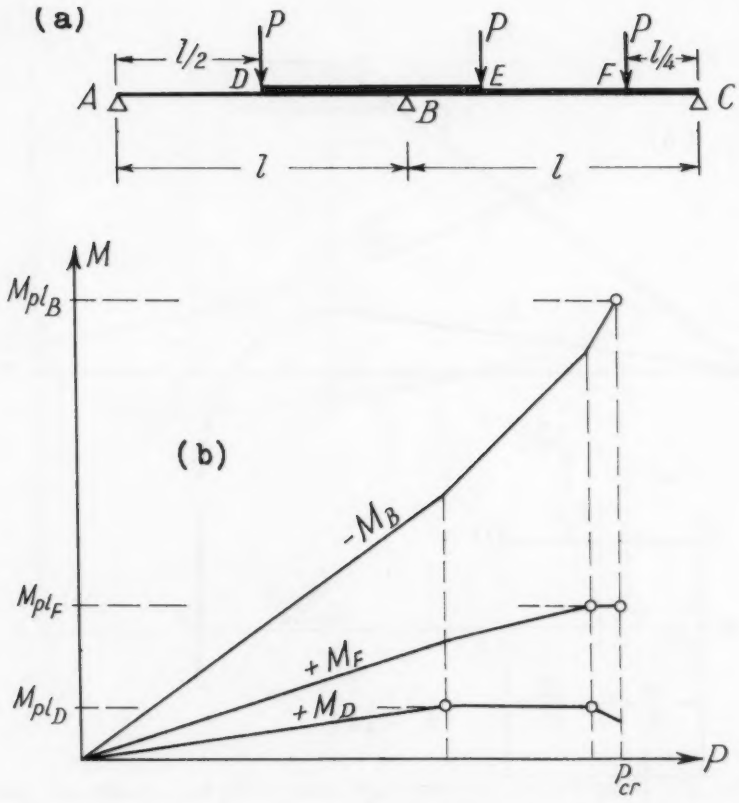

Fig. 3

The term "ultimate load design" may, therefore, be more appropriate than "ultimate strength design".

The above considerations may have led to the modified ultimate strength design method adopted by the Austrian Code in 1953.[6] According to this Code, the carrying capacity of a section is exhausted when a certain limit compressive strain E_c^* in the concrete or a certain tensile yield strain E_y^* in the steel has developed. E_c^* approximately represents the peak of the stress/strain diagram of the concrete; E_y^* denotes the initial stage of the yielding capacity of the steel. Ultimate strength is then related to a stress distribution (σ_c^* ; σ_v^*) corresponding to the E* values and a specified safety factor is required against the appearance of the limit deformations mentioned above.

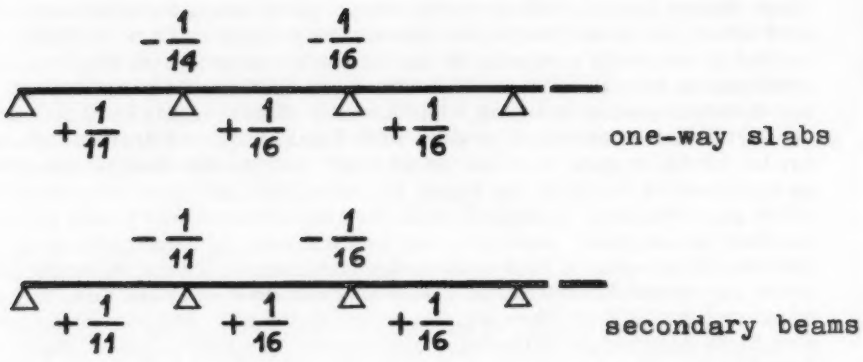

Fig. 4

REFERENCES

1. D. C. Drucker, Limit Analysis and Design, Applied Mechanics Reviews, October 1954, pp. 421-423.
2. A. Zaslavsky, On the Loading History of Structures in the Elastic Plastic Range, In the Field of Building No. 53, Israel Institute of Technology 1958 (in Hebrew).
3. Eugene Guillard, Ultimate Resisting Moment of Beams with Compression Reinforcement, Journal ACI, March 1958.
4. A. Zaslavsky, Discussion of above, Journal ACI, Part 2, Sept. 1958.
5. K. V. Sachnovsky, Reinforced Concrete Structures, Moscow, 1959 (in Russian).
6. K. Jäger, Die Bemessung der Stahlbetonbauteile nach Önorm B 4200, Vienna 1953 (in German).
7. A. Zaslavsky, Ultimate Load Design of Steel and Reinforced Concrete Structures, The Association of Engineers and Architects in Israel, 1956 (in Hebrew).

W. W. L. CHAN.[1]—The authors have given a valuable survey, with comments, of the existing knowledge in this field. It is, however, regrettable that the results of much research work listed in the References and the Plastic Hinge Theory have not been properly compared to assess the extent of accuracy which can be achieved by the latter. The promoter of a novel design method is invariably compelled to sacrifice some accuracy (so long as this is small and on the safe side) in order that his method may be simple to apply and therefore popular in appeal. For instance, Baker's early work on moment re-distribution as described on page 1878-7 was a rigorous approach which can be carried to great accuracy of solution. On the other hand, his later work as expressed in Eq. (3) of the Paper, is a simplified and powerful method in which approximations inherently exist, the magnitudes of which have yet to be carefully investigated. Amongst other implications, the assumption of an idealised elasto-plastic load-deformation curve drawn always below the actual curve may result in an actual structure which is over-stiff, and this, as pointed out on page 1878-20, does not always err on the safe side, especially for structures designed for differential settlement. The Plastic Hinge Theory is therefore an advance in the basic concept of a structure as a whole, accompanied by loss of accuracy which is inherent whatever refinements are made to the "safe-limiting" parameters. The objective of future development of the Plastic Hinge Theory is thus to establish the amount of inaccuracy which is acceptable, and the "Concluding Remarks" should be qualified in this light.

With regard to the approximate elastic solution, it is surprising that the Paper accepts without further comment the ability of the Limit Design method "to satisfy both the ultimate load, and the working load conditions of the structure" (page 1878-13). As is well known, an elastic solution however "exact", has little meaning in steel structures and even less so in concrete structures. Thus an elastic solution does not generally indicate even approximately the conditions of servicibility, but rather adds to the simple Limit Design method the work of solving a set of simultaneous equations which even by approximate relaxation techniques is tedious, and detracts from the merit of simplicity. It would seem far more realistic and convenient to discard this labour and instead, establish from tests such limiting criteria as load factors, minimum slenderness ratios and steel percentages, which would result in satisfactory working-load conditions for structures designed by ultimate load considerations alone; this seems to have been considered in the Russian recommendations.

Turning now to the rotation capacity of plastic hinges, the Paper suggests on page 1878-12 that Baker's Eq. (5) neglects the elastic deformation. This is incorrect, since s_p (Baker's notation) is defined as the "strain of concrete at compression edge, which occurs under increasing load between the steel yielding and the concrete crushing."

It is further stated, without evidence, that Chan's method for calculating plastic hinge rotation based on flexural analysis is highly theoretical because other complex deformations could occur within a structural junction next to a hinge. This observation is confused, since rotation developed along the member and inside the junction are largely two separate and independent phenomena, the sum of which constitute the total available rotation. Chan's analysis and experiments have been recently verified by Prasad,(1) which showed

1. Sr. Engr., Sir Bruce White, Wolfe Barry & Partners, Cons. Engrs., London, England.

that the method is valid for plastic hinges occurring in members that are flexible compared to their adjacent structural junctions, where little rotation is developed inside the junctions. Tests carried out by Ernst (Reference 52 of the Paper) also confirmed Chan's conclusions in those cases, and established further important conclusions as to the spread of plastic rotations into structural junctions for a wide variety of cases.

Another important omission in the Paper is the effect of axial load on the spread of plastic hinge length, such as occurs in columns. Chan's method considers this, (References 26 and 31) and based on test results, a simple interaction formula has further been proposed:(2)

$$l_{pc} = l_p \left(1 + 0.25 \frac{P}{P_u}\right) \quad (1)$$

where P = column load;

P_u = ultimate strength of column under axial load only.

Summing up the knowledge available to date on plastic hinge rotation, Baker's and Chan's methods can be reconciled with the experimental work of Ernst, and all combined into a simple formula (see Fig. A). Based on Eq. (5a) by Baker, l_p is determined as a variable according to Chan's concept, the numerical parameters being established from tests. This results in a formula for l_p of the form:

$$l_p = c\left(Z - \frac{B}{2}\right) + l_s \quad (2)$$

where Z = distance from hinge to point of contraflexure;

B = width of support;

l_s = spread of plasticity into junction, and can be taken in the case of over-reinforced beams as the lesser of 2d or $\frac{B}{2}$, and as zero for balanced and under-reinforced beams;

c = a constant which varies from about 0.25 to 0.35.

This method is general and takes into account all the principal variables contributing to plastic hinge rotation. It has the further advantage that no reference has to be made to the values of M_E and $(EI)_e$.

REFERENCES

1. P. J. Prasad, "An Experimental and Analytical Investigation of Post-tensioned Joints in Continuous Prestressed Concrete Frames", M.Sc. Thesis, University of London, 1958.

2. W. W. L. Chan, Discussion on a Paper, "Ultimate Load Design of Reinforced and Prestressed Concrete Frames", Symposium on the Strength of Concrete Structures, Cement and Concrete Association, London, 1956.

SHAUKAT MIRZA.[1]—The paper "Review of limit design for structural concrete" by Mr. C. W. Yu and Eivind Hognestad has been very

1. Graduate Student, Univ. of Wisconsin, Madison, Wis.

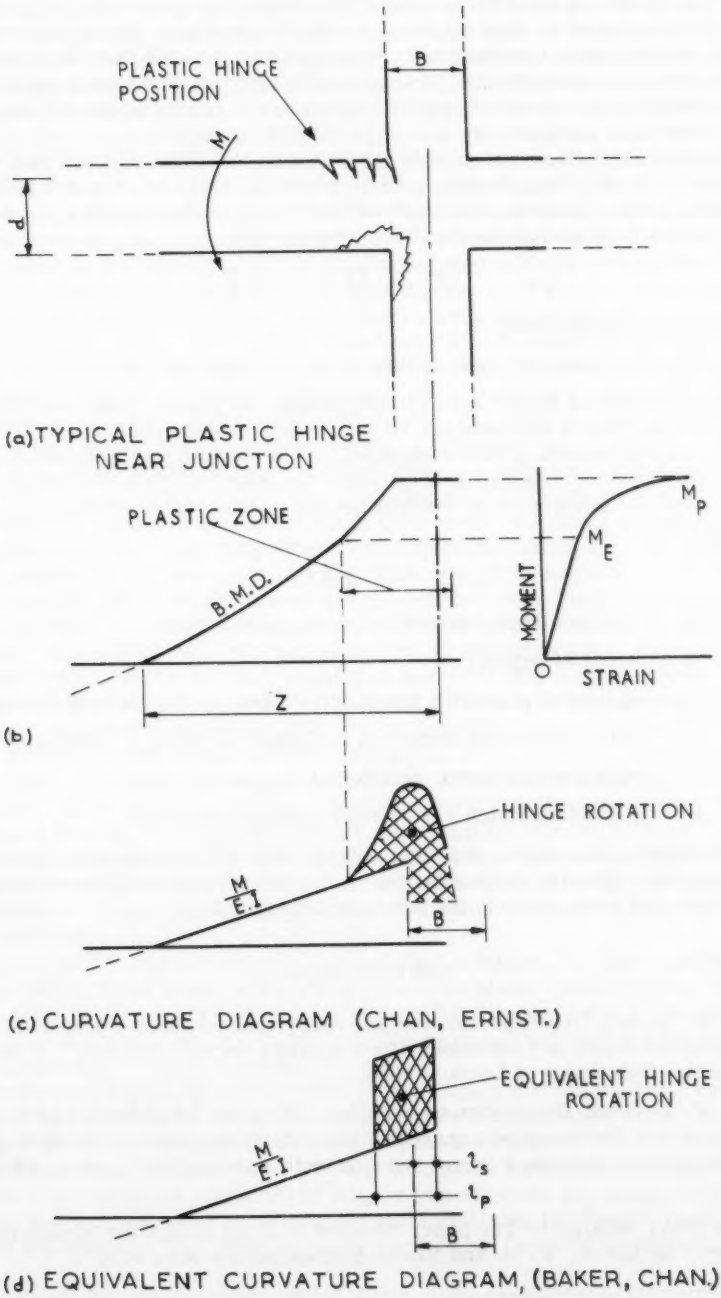
PLASTIC HINGE POSITION
B
M
d
(a) TYPICAL PLASTIC HINGE NEAR JUNCTION
PLASTIC ZONE
B.M.D.
Z
(b)
M_P
M_E
MOMENT
STRAIN
HINGE ROTATION
$\frac{M}{E.I}$
B
(c) CURVATURE DIAGRAM (CHAN, ERNST.)
EQUIVALENT HINGE ROTATION
$\frac{M}{E.I}$
l_s
l_p
B
(d) EQUIVALENT CURVATURE DIAGRAM, (BAKER, CHAN.)

Fig. A

comprehensively and systematically reproduced. The setup of the paper is sufficiently vivid and appealing. Apart from the many good points of the paper there are some phases which I feel have not been elucidated and given due attention. The phenomenon of plastic hinges in concrete is complex and should have been expressed more clearly. Referring to the first assumption on page 9 of the paper the authors write that "plastic yield is concentrated at a hinge" which does not completely specify the conditions. Now if we consider a frame to be increasingly loaded, plasticity will develop in the members. This process goes on as the load increases and the plasticity travels longitudinally for a short length of the member finally causing a drop. This localized yield or drop results in a discontinuity or change of slope of the member. The change of slope in the immediate vicinity of the short plastic length may be looked into as the rotation of the hinge. The moment at the support attains the maximum value first and if the plastic length is small and confined then the moment at the centre goes on increasing and the beam continues dropping until the failure occurs, while during all this time the support moment is constant. It can be said that the concrete in the plastic length acts as a confined fluid which automatically dictates that there is no strain variation in that region. This then leads to the assumption that plastic hinges are concentrated at the point. The above condition is highly idealised because the deformation takes place over a finite length. It will not be out of the place to mention that the assumption of formation of n hinges before failure of the unit leads to the conclusion that the load causing the nth hinge to form is the ultimate load, since after this stage failure occurs.

Besides the assumptions mentioned in the paper there are other important assumptions which need mention and are as follows:

1. In the unit under consideration, the moment varies linearly with the increasing load. This however is not true near the hinges. Because in the plastic concrete as mentioned earlier in the discussion, the moment remains constant.
2. Ultimate strength of concrete in over reinforced case and yield strength of steel in under reinforced case are responsible for the moments in the plastic hinge. It should also be seen that the cracks in the unit produced due to the increasing load should not be too wide. To take account of this cracking Mr. A. L. L. Baker has made use of the ratio F, the ratio of average strain near the tensile steel to the maximum strain in the concrete near the steel at its yield stress. Value of 'F' ranges from I to 0.I for the extreme cases.

The formula (4) on page 1878-10 of the paper is based on the approximation that M_r (the moment due to a unit moment at the hinge in the direction of X_r on the frame made statically determinate) is equal to unity, which is evidently not justifiable. The result can easily be deduced from Eq. (3) mentioned on page 1878-9, taking into consideration the plastic yield length 1_p and the elastic length in between the two hinges.

$$\Theta r=\left(\int_{l-l_p}^{l}\frac{M_o\,M_r}{(EI)_p}\,dx-\int_{l-l_p}^{l}\frac{M_o\,M_r}{(EI)_1}\,dx\right)+\bar{X}_1\left(\int_{l-l_p}^{l}\frac{M_1\,M_r}{(EI)_p}\,dx-\int_{l-l_p}^{l}\frac{M_1\,M_r}{(EI)_1}\,dx\right)$$

$$+\ldots\ldots\ldots+\bar{X}_n\left(\int_{l-l_p}^{l}\frac{M_n\,M_r}{(EI)_p}\,dx-\int_{l-l_p}^{l}\frac{M_n\,M_r}{(EI)_1}\,dx\right)$$

which may be written as;

$$\theta_r = \int_{1-1\rho}^{1} M_r M \left[\left(\frac{I}{EI}\right)_p - \frac{I}{(EI)_1}\right] dx.$$

$$\text{Where } M = M_0 + M_1 \bar{X}_1 + M_2 \bar{X}_2 + \ldots\ldots\ldots + M_n \bar{X}_n .$$

The above equation is to be integrated throughout the structure, but it will be sufficiently accurate if only the rth term is taken, the other terms do not contribute much. Thus the final equation reduces to:

$$\theta_r = \int_{1-1\rho}^{1} \frac{M_r M}{(EI)_p} dx - \int_{1-1\rho}^{1} \frac{M_r M}{(EI)_1} dx$$

The equation mentioned above seems to yield better result than the Eq. (4) as indicated in the paper. The writer also agrees with the remark made by the authors on page 1878-15 about the complexity of stresses near the joint and the unability of Chan's analysis to coordinate with the actual conditions.

REFERENCES

1. Baker, A. L. L., "Recent Research in Reinforced Concrete and Its Application to Design". Journal of Institution of Civil Engineers. V 35, No. 4.
2. Baker, A. L. L., "Further Research on Reinforced Concrete and Its Application to Design". Proceedings of Inst. of Civil Engineers, Vol. 2, Part 3, No. 2.
3. Baker, J. F., "The Design of Steel Frames". The Structural Engineer V. 27, No. 10.
4. Chan, W. W. L., "The Ultimate Strength and Deformation of Plastic Hinges in Reinforced Concrete Frameworks". Magazine of Concrete Research, V. 7, No. 21.
5. Mirza, Shaukat., "Ultimate Load Design Theory for Indeterminate Structures". M. S. Thesis to be submitted to University of Wisconsin.

HENRY J. COWAN,[1] A. M. ASCE.—This review of limit design for concrete structures is timely and most welcome. It seems to the writer, however, that there are more gaps in our knowledge at present than this paper implies.

As the authors point out, limit design can be applied to reinforced concrete frames with several redundancies only if the hinges can sustain, without disintegration of the concrete, the rotation required for the formation of further hinges.

It is theoretically possible to design a structure in which all the plastic hinges form at the same load. This is comparatively easy to achieve if the theory set out by the authors is valid. The resistance moment of reinforced concrete can be varied simply by altering the disposition of the reinforcement without changing the overall dimensions of the section: in this respect it

1. Prof. of Architectural Science, Univ. of Sydney, Sydney, Australia.

differs from structural steel in which a change of section is frequently inconvenient and sometimes impracticable. If the hinge sections are designed so that all hinges form at the same load, the hinges need sustain, theoretically, only very little plastic deformation. Can the authors say if there is adequate experimental corroboration that this holds true for reinforced concrete?

The authors' reference to the use of spiral reinforcement as a means of extending the capacity of concrete for plastic deformation is entirely convincing. The writer wonders, however, whether this in fact is an acceptable device for normal reinforced concrete construction. It is worth noting that the theory of the use of spiral reinforcement in the compression zone of reinforced concrete beams has been included in German language textbooks on reinforced concrete (Saliger, Probst, etc.) for some decades. In spite of that it hardly appears to have been used, except in conventional hinges (i.e. two-hinged or three-hinged arches). Do the authors consider that spiral reinforcement in the compression zone of beams would be an economical form of construction?

Even if it is practicable to employ these two devices, however, it seems to the writer necessary to extend limit design before it can be generally accepted for reinforced concrete. G. de Kazinczy (author's reference No. 1) pointed out as long ago as 1933, and emphasized again at the Fourth International Congress of Bridge and Structural Engineering (Cambridge 1952) that the capacity of reinforced concrete to sustain large rotations is essentially a property of the steel (assuming no spiral reinforcement is used). J. F. Baker in a discussion on a paper by A. L. L. Baker (Jnl. Institution of Civil Engineers, London, Vol. 35, p. 315, 1951), pointed out that the load carried by an under-reinforced beam was maintained after hinge formation, but that it fell off rapidly in the case of an over-reinforced beam. The writer also has observed that full redistribution of moments occurred in simple portals with low percentages of reinforcement (Jnl. Inst. Civ. Eng., Vol. 36, p. xiii, 1951; Engineering, London, Vol. 174, p. 277, 1952; Constructional Review, Sydney, Vol. 30, No. 7, p. 30, 1957), but he has found little redistribution in two over-reinforced portals.

It seems to the writer therefore that there are two main problems to be solved: (i) how much rotation can a given reinforced concrete section sustain without causing a falling-off in the resistance moment? and (ii) how much rotation is required at the first hinge to allow all the other hinges to form in accordance with the authors' theory?

It may well be that in the case of reinforced concrete these two problems must be solved separately, since the scale model approach so successfully employed by J. F. Baker's team on steel structures is hardly practicable for concrete structures.

With regard to the first problem, the information given by the authors is very limited in scope, and it seems to the writer that the recent experiments by Ernst (Jnl. American Concrete Institute, Vol. 28 (1957) pp. 1119-1144), which are not included in the authors' comprehensive bibliography, are the most informative carried out so far.

The second problem, viz. the angle of rotation needed in a given multi-bay rigid frame for the formation of the requisite number of hinges, seems to the writer most important, and he would appreciate it if the authors would work out a typical numerical example using the method in the paper.

Since the authors make reference to a number of non-American design codes, it may be of interest to mention that the new Australian Standard Rules

for the Use of Reinforced Concrete in Buildings (CA 2, Standards Association of Australia, Sydney, 1958) admit a 15 per cent adjustment of bending moments in continuous beams, like the British Code. The Australian Code furthermore states that "the design of slabs spanning in two directions may be based on the assumption that failure occurs along a pattern of yield lines at which the full ultimate moment of resistance of the reinforced concrete section is developed. The yield-line pattern shall be chosen so as to give the lowest possible ultimate load for the slab."

ELASTI-PLASTIC ANALYSIS OF CONTINUOUS FRAMES AND BEAMS[a]

Discussions by Giuliano Augusti, Tullio Renzulli, Emilio Rosenblueth and A. A. Eremin

GIULIANO AUGUSTI.[1]—In this paper, the moment effects caused by the plastic portion of the curvature are computed assuming that these curvatures are angle changes concentrated at the point of maximum moment. On the contrary, the writer has in some numerical examples realized that this shortcoming causes sometimes not negligible errors.

Therefore it is better to remove the mentioned shortcoming, and to calculate the moment effect of the plastic curvatures taking them in consideration as distributed, as they actually are. This computation can easily be made by means of the moment influence lines for travelling distortions.

The moment influence line in section S for a travelling distortion is a diagram that gives the bending moment in S caused by a concentrated distortion θ_i, with its ordinate m_i read in correspondence of the section in which the θ_i is applied and multiplied by the value of the θ_i. (1).

If the concentrated distortions are more than one, their moment effect in S is given by the sum $\Sigma_i m_i \theta_i$; if, instead of some concentrated distortions, there are infinite elementary distortions μds, distributed in a zone of length Δ, the following moment in S is given by $\int_\Delta \mu m \, ds$.

Therefore, we assume the moment effects of plastic curvatures to be like the moment effects of elementary distributed distortions ($\phi_p = \mu$); so we have at once the moment at any section - if we know the moment influence line for that section - by $\int_\Delta \phi_p m \, ds$. (2)

Of course, to get the whole moment diagram caused by plastic curvatures in a rectilinear span frame or in a continuous beam, it is sufficient to compute its values at the joint sections. Thus, it is necessary to draw the influence lines only for these sections: this does not require a greater preliminary work than Looney's procedure for unbalanced moment distribution, recommended by the AA.

The reason of the difference in evaluation of moment effects caused by concentrated or distributed plastic curvatures is shown in the example of Fig. 1. The actual moment diagram for a given load, which doesn't attain its ultimate value, is given in Fig. 1-b; the plastic curvature diagram is given in Fig. 1-c, assuming the moment-curvature relationship of Fig. 2; the moment influence line in section B for a travelling angle change is given in Fig. 1-d.

In evaluating moment effects, when we consider the plastic curvatures ϕ'_p and ϕ''_p as two angle changes concentrated at points of maximum moment (i.e.

a. Proc. Paper 1879, December, 1958, by L. P. Johnson and H. A. Sawyer.

1. Asst. Engr., Bridge Const. Inst., Univ. of Naples, Naples, Italy.

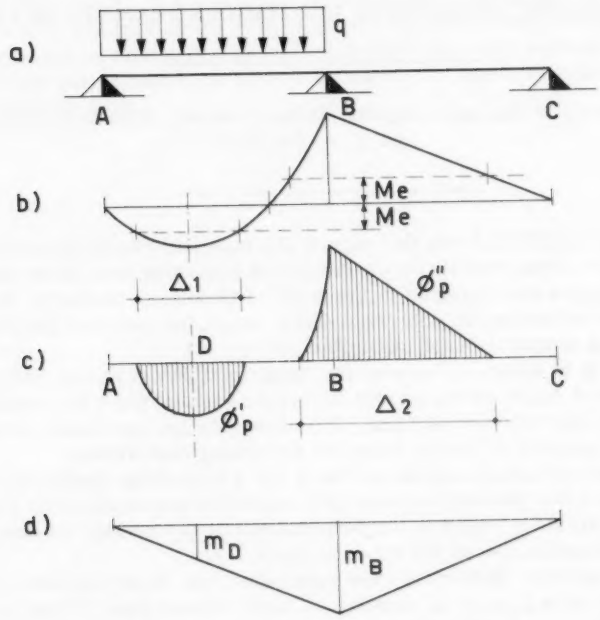
a)
q
A
B
C
b)
Me
Me
Δ1
Ø"p
c)
D
A
B
C
Ø'p
Δ2
d)
mD
mB

Fig. 1

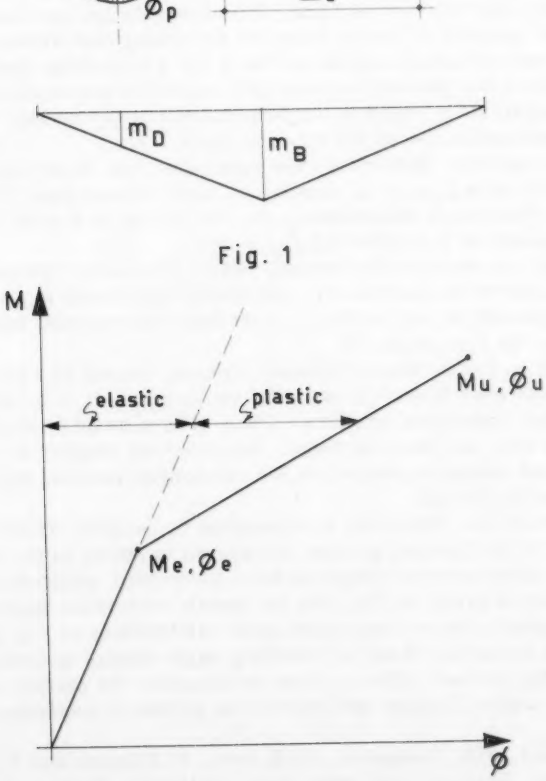
M
elastic
plastic
Mu, Øu
Me, Øe
Ø

Fig. 2

D and B), we compute areas $\int_{\Delta 1}\phi'_p\,ds$ and $\int_{\Delta 2}\phi''_p\,ds$ (3) and then we multiply them by the ordinates m_D and m_B of influence line, instead of calculating directly integrals $\int_{\Delta 1}\phi'_p\,m\,ds$ and $\int_{\Delta 2}\phi''_p\,m\,ds$. But from Fig. 1 we have easily:

$$(a) \qquad \int_{\Delta_1}\phi'_p\,m\,ds = m_D\int_{\Delta_1}\phi'_p\,ds \;;$$

$$(b) \qquad \int_{\Delta_2}\phi''_p\,m\,ds < m_D\int_{\Delta_2}\phi''_p\,ds \;.$$

The writer has in some examples ascertained that the moment evaluated with the integrals on the right side of equalities and/or disequalities (a), (b) may sometimes be even two or three times greater than the exact moment, as evaluated with integrals on the left side. It occurs sometimes, however, that —especially in the case of concentrated loads—when substituting right sides of (a), (b) for the left ones, we incur errors of opposite sign and of same magnitude, so that the final error is actually negligible; but this is only a lucky chance.

It is possible to draw moment influence lines also in the case of frames with sway. This allows the use of recommended procedure, with a greater time expenditure only in preliminary work.

When we can envisage plastic curvatures being only around few joint sections in a highly statically indeterminated frame, it is possible to combine our procedure with that of MM. Johnson and Sawyer; in so doing we get at the same time good approximation and quickness in computation.

If plastic curvatures are expected to be only around joint sections A, B, C, . . . , we compute moment effects of plastic curvatures in the same sections by means of corresponding moment influence lines.

In calculating moment effects at the other joint sections, it is possible—on the contrary—to consider the plastic curvatures in A, B, C, . . . as concentrated angle changes θ_i. The moment in all these sections caused by the θ_i, is easily determinated when we remember that the influence lines, already computed, coincide with the moment diagrams caused by an angle change $\theta = +1$, applied in A, B, C respectively. Thus, we can compute moments in all these sections by superposition of effects of individual angle changes in A, B, C, . . .

Notes

1. According to Betti's generalized theorem, the moment influence line in S for a travelling angle change θ_i coincides with the moment diagram caused by an angle change $\theta = +1$, applied at S. (See: A. Galli, Scienza delle Costruzioni, Vol. 3°, Cap. 25°, Napoli 1957; V. Franciosi, Lezioni di Ponti, Cap. 3°, Napoli 1954.) The angle change θ_i—with the common algebraic sign convention—is positive when the positive moment makes for it a positive work.

2. The expression of this integral may be found in advance for the most common moment diagrams and a given moment-curvature relationship. We must remember the assumed algebraic sign convention (note 1). For example, in Fig. 1-c, assumed positive the moment stretching lower fibers, the ϕ'_p are negative distortions, the ϕ''_p positive ones.

3. For the sign, see note 2.

TULLIO RENZULLI.[1]—The procedure proposed for the calculation of a frame is without doubt more exact than those which are based on a limited stress-strain diagram, or those which take no account of the elastic strains in comparison with plastic ones. This exactness, however, is linked to more extended calculations.

A similar method, though based on a less general moment-curvature relationship, has been proposed for rigid-frame calculations.(1,2)

One should take into consideration the possibility of (1) discharge phases at any section, that is, moment decreasing during a phase of structural loading, and (2) the simultaneous presence of normal and shearing stresses.(3)

Starting with an ideal stres-strain relationship composed of two straight lines, the second of which stops at the value of the fracture strain, Fig. 1, the moment curvature $(M - \frac{1}{r})$ diagram is straight while the strains are in the elastic range and becomes curvilinear starting from the point of coordinates M_e, $\frac{1}{r_e}$ and reaches its highest value at the point C of coordinates M_i, $\frac{1}{r_i}$ (Fig. 2).

With increasing curvature we have the fracture of elements of the section where $\epsilon \geq \epsilon_r$, and consequently the moment decreases and asymptotically approaches zero.

The stress-strain relationships are as shown in Fig. 3a, b, d, where the curvature is contained in one of the intervals $0 - \frac{1}{r_e}, \frac{1}{r_e} - \frac{1}{r_i}, \frac{1}{r_i} - \infty$. For $\frac{1}{r} = \frac{1}{r_i}$ we have the diagrams in Fig. 3c.

For a rectangular section the moment-curvature relationship is

$$M = \tfrac{1}{4} b\sigma_0 h^2 - \tfrac{1}{3} b\sigma_0 \varepsilon_0^2 r^2 \qquad \text{for} \quad M \leq M_i \tag{1}$$

$$M = b\sigma_0 \varepsilon_R^2 \left[1 - \tfrac{1}{3}\left(\frac{\varepsilon_0}{\varepsilon_R}\right)^2\right] r^2 \qquad \text{for} \quad M \geq M_i \tag{2}$$

The highest value of the moment, termed by the authors M_u, is

$$M_i = \tfrac{1}{4} b\sigma_0 h^2 \left[1 - \tfrac{1}{3}\left(\frac{\varepsilon_0}{\varepsilon_R}\right)^2\right] \tag{3}$$

which depends on the highest stress δ_0 and the fraction E_0/E_r. When E_r approaches infinity we obtain the known value

$$M_i = \tfrac{1}{4} b\sigma_0 h^2 \tag{3'}$$

Similar expressions can be derived for different sections.

If we substitute a straight line for the curve in the interval O-C of Fig. 2, analytical operations are remarkably simplified.

For a beam section in the elasti-plastic range, for which $M > M_e$ over a plastic length of Δs, the plastic angle is

$$\varphi_p = \int_{\Delta S} \frac{1}{r_p}\, ds = k \int_{\Delta S} (M - M_e)\, ds \tag{4}$$

and the plastic curvature is

1. Assistente alla cattedra di Scienza delle Costruzioni della Facoltá di Ingegneria di Napoli-Libero Docente.

$$\frac{1}{r_p} = k\,(M - M_e) \tag{5}$$

where K is a constant whose value can be obtained from Eq. (5) with $M = M_i$. For a straight or parabolic distribution of moment corresponding to an unloaded or uniformly loaded region (with uniform load p), we have

$$\varphi_p = \frac{k}{2}\,(M^* - M_e)\,\Delta s \tag{6}$$

$$\varphi_p = \frac{k}{2}\left(M^* - M_e - \frac{p}{6}\,\Delta s^2\right)\Delta s \tag{7}$$

where M^* is the highest ordinate of the moment diagram in the region.

If we consider two spans, h and h + 1, of a rigid frame, Fig. 4, the four-moment equation can now be generalized so as to be applicable to the elasti-plastic range. Blackened portions of the moment diagram represent regions where the moment exceeds M_e. Treating the plastic angles as concentrated and using as isostatic structures the two spans hinged at their ends, the angles of rotation of the members of the joint may be equated to obtain

$$\varphi_B^h + \varphi_A^{h+1} = \varphi_{Bh} + \varphi_{A(h+1)} + \sum_i^{3,4} \int_{\Delta S_i} \frac{1}{r_p}\,ds - \sum_i^{2,5} \int_{\Delta S_i} \frac{\ell_i - \xi_i}{\ell_i}\,\frac{1}{r_p}\,ds \tag{8}$$

where φ_B^h, φ_A^{h+1} = hinge angles caused by external loads and settlements

φ_{Bh}, $\varphi_{A(h+1)}$ = hinge angles caused by joint moments

ξ_i = distance of region Δs_i from the joint

ℓ_i = length of the span

Direct solution of Eqs. (8) is not possible, as the lengths and the positions of the regions Δs_i are not known. It is better to use a trial and error method: starting with a bending moment diagram calculate the plastic angles, from which, by substitution in Eq. (8), a system of linear equations solvable for the joint moments is obtained.

For homogeneous and reinforced concrete sections the $M - \frac{1}{r}$ relationship indicates that the plastic curvatures can be ignored with respect to the plastic ones. (Fig. 5). In this case, with increased external loads, we take into consideration only plastic curvatures. Then Eq. (8) reduces to the geometric relationship shown in Fig. 6

$$\vartheta_2 = \vartheta_1 + \vartheta_3 \tag{9}$$

It is remarkable that, starting from the $M - \frac{1}{r}$ diagram of Fig. 5 and neglecting elastic strains, we calculate a rigid frame as proposed by Greenberg and Prager,[4] moreover taking into account the limitation on strain.

For this purpose, we complete a calculation based on a limited $M - \frac{1}{r}$ relationship and obtain, for an n-degree hyperstatic frame, the positions of the n + 1 hinges necessary for rigid collapse. The angle between any two sections linked by a plastic hinge i is α_i. These angles are known through a proportionality constant. We obtain the plastic angles $\mathcal{V}_{pi}$ using Eq. (4) or

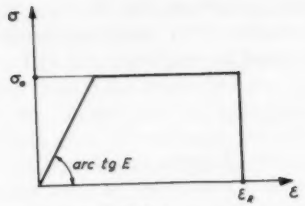

FIG. 1

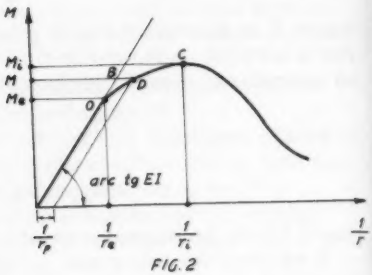

FIG. 2

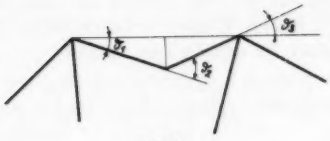

FIG. 6

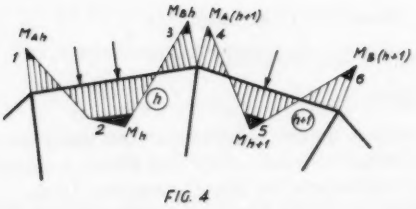

FIG. 4

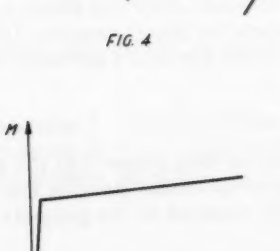

FIG. 5

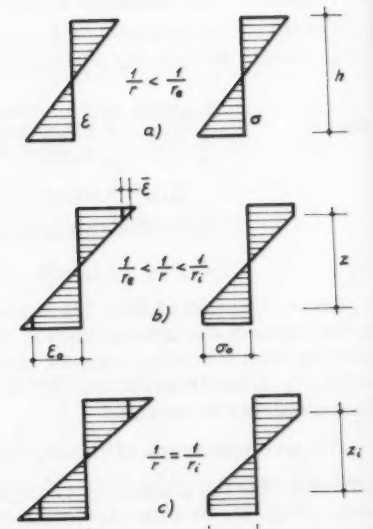

FIG. 3

Eqs. (6) and (7), and we can state that the greatest strain in the material is reached at the section t where the value α_t/φ_{pt} is highest.

At collapse (which we consider occurs when M_i is attained at any section), in the broken hinge $\alpha_t = \varphi_{pt}$. In the others the plastic angles are obtained knowing the values α_i/α_t, and are indicated with φ_i^*. In hinge t the bending moment is M_i. In the other hinges moments, M_i^*, may be calculated, knowing the plastic angle φ_i^*, by the relation

$$\varphi_i^* = k \int_{\Delta s_i} (M_i^* - M_e)\, ds \tag{12}$$

and in particular cases of an unloaded or uniformly loaded region by the relations

$$\varphi_i^* = \frac{k}{2} (M_i^* - M_e)\, \Delta s_i \tag{13}$$

$$\varphi_i^* = \frac{k}{2} \left(M_i^* - M_e - \frac{p}{6} \Delta s_i^2\right) \Delta s_i \tag{14}$$

In Eqs. (13) and (14) the lengths Δs_i are obtained by trial moment diagrams, then, considering the moments M_i^* so obtained, these lengths are recalculated and the new values substituted.

REFERENCES

1. A. Galli T. Renzulli: Contributo alla evoluzione del metodo delle cerniere plastiche-Giornale del Genio Civile Roma 1954 nº 11-12.
2. T. Renzulli: Sul calcolo delle strutture monodimensionali in regime elastoplastico-Rend. Acc. di Scienze Fis. e Mat. Napoli Serie 4-1954.
3. V. Franciosi: Il teorema fondamentale del calcolo a rottura - L=Ingegnere Milano 1955 nº 12.
4. H. Y. Greenberg, W. Prager: Limit design of beams and frames - Proceedings of the Am. Soc. of Civ. Eng. 1951 nº 59 Vol. 77.

EMILIO ROSENBLUETH,[1] A. M. ASCE.—The authors have presented a neat and useful method of analysis applicable to continuous beams and frames constituted by members having any moment-curvature diagrams, which lead to curved relations between bending moment and angle change at inelastic hinges. Due to its generality the method might well have been termed "inelastic analysis". As pointed by one of the authors in an earlier paper(1) (of which the present one may be regarded as a generalization) the advantage of idealizing a moment-curvature diagram as formed by two or three straight lines lies in the feasibility of resorting to the relatively simple tabulated formulas for the plastic angle change θ_p in terms of the bending moment diagram.

Usually the error associated with such idealizations is quite tolerable.(1) But this is not necessarily the case in all instances. When one must retain curved relations between moment and curvature, θ_p may be obtained from a plot as a function of M. The plot is conveniently calculated by a numerical

1. Director, Inst. of Eng., Univ. of Mexico, Mexico City, Mexico.

ST 6

procedure (e.g., Newmark's[2] for the three types of moment diagram considered in the authors' Fig. 2.

For structures with a large number of joints it is possible to develop a method which often involves less computational work than the authors'. It requires knowledge of the distribution constants for prismatic members having elastic hinges.

Consider the member in the writer's Fig. 1. It is a prismatic beam of span L, having hinges connected by springs. These are located at distances $\xi_1 L$, $\xi_2 L$, . . . from the left support, and at $\eta_1 L$, $\eta_2 L$ . . . from the right-hand support. It is easily shown that the carry-over factor from left to right is

$$t_{ab} = \frac{0.5 + \Sigma \alpha_i \eta_i}{1 + \Sigma \alpha_i \xi_i} \tag{1}$$

and the left-hand stiffness, when the right-hand support is fixed against rotation, is

$$K_a = \frac{3EI/L}{(1 + \Sigma \beta_i \eta_i)(1 - t_{ab} t_{ba})} \tag{2}$$

where

$$\alpha_i = \frac{3EI\xi_i}{k_i L},$$

$$\beta_i = \frac{3EI\eta_i}{k_i L},$$

and k_i is the stiffness (moment over angle change) of the ith spring.

If the right-hand end is simply supported, Eq. (2) becomes

$$K'_a = \frac{3EI/L}{1 + \Sigma \beta_i \eta_i}. \tag{3}$$

The stiffness of the beam (shear over lateral displacement), when its supports are displaced laterally without rotation, is found to be

$$\frac{V}{\delta} = \frac{1 + \Sigma \frac{EI}{k_i L}}{1 + \Sigma \frac{EI}{k_i L}(1 - 3\xi_i + 3\xi_i^2)} \cdot \frac{12EI}{L^3} \tag{4}$$

where V denotes the shear corresponding to a displacement δ.

Eqs. (1) to (4) permit a straightforward moment distribution in frames with elastic hinges and/or semi-rigid connections. The method proposed consists in, first, estimating the redundances so as to obtain a preliminary moment diagram. The structure is then dimensioned and, at every region where the bending moment exceeds the elastic-limit moment, an inelastic hinge is placed. A moment-rotation diagram can be drawn for every inelastic hinge, such as the solid curve in the writer's Fig. 2. From the preliminary moment diagram, the bending moment at the hinge has in effect been estimated and one can draw a secant (OA in Fig. 2) through the origin. The slope of the secant defines a preliminary stiffness of the hinge and one can carry out a first moment distribution using Eqs. (1) to (4).

Results of the moment distribution provide a new moment diagram, which in general will differ from the original. The final moment diagram will

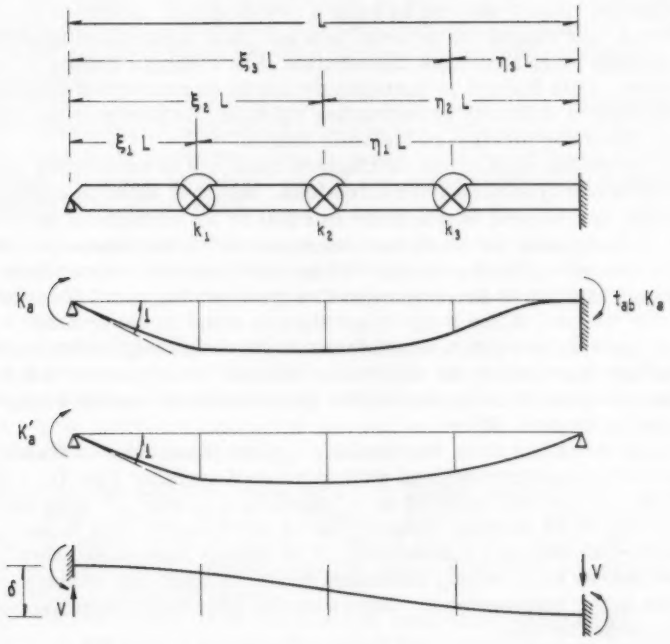

ROSENBLUETH ON JOHNSON AND SAWYER.
FIG. 1.- BEAM WITH ELASTIC HINGES.

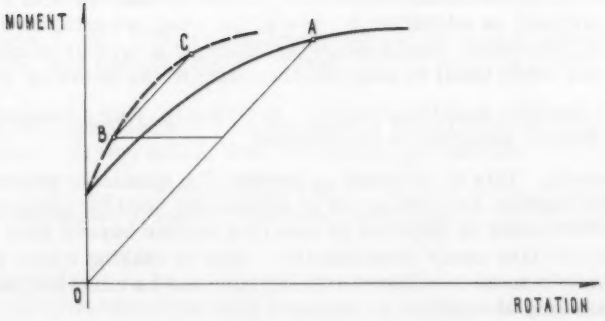

ROSENBLUETH ON JOHNSON AND SAWYER.
FIG. 2.- MOMENT-ROTATION CURVES AT ELASTIC HINGE.

usually be intermediate between the original and that found from moment distribution. Hence one can assume a new diagram, closer to the solution of the frame, and repeat the process in a series of successive approximations. At any stage after a moment distribution it is a simple matter to redesign the structure. This feature is particularly useful in reinforced-concrete frames, where there is difficulty in estimating off-hand the points of bar cut-off, which in turn affect the location of inelastic hinges.

The proposed method can be changed from one of successive approximations to one of successive corrections. Say that, after distributing moments, the moment at one hinge is equal to the ordinate of point B in Fig. 2 while the originally assumed moment equalled the ordinate of A. In the figure, point B has been placed on a revised moment-rotation curve (dashed line), which corresponds to the new estimated moment diagram. If in the new diagram the moment at the hinge in question is equal to the ordinate of point C (on the same dashed line), a correction to the originally estimated diagram is obtained by distributing the difference between the ordinates of A and B (and similar differences in the rest of the hinges) with an assumed hinge stiffness equal to the slope of BC.

This process has been successfully applied to analysis of frames having inelastic semi-rigid connections without need of applying Eqs. (1) - (4). The connection is merely replaced by a "phantom member",[3] with stiffness equal to the slope of its moment-rotation curve and a carry-over factor of -1 (in the static-moment sign convention). It is equally successful when the position of most hinges is correctly estimated from the start and redesign at mid-analysis is not contemplated. Otherwise the successive-approximations version is preferable.

In essence the operations carried out in the proposed method are the same as those in the authors' but are performed in a manner that seems more efficient when the number of joints is large. Conversely, in frames with a small number of joints the labor involved in distributing a unit moment applied successively at each of the joints is not excessive, and the authors' method offers greater advantages.

Following A. L. L. Baker,[4] it would seem that moment-angle change diagrams for reinforced concrete members might be adequately approximated for design purposes by two straight lines, the first through the origin, coinciding with perfectly elastic behavior, and the second horizontal, with limited rotation. This proposal is attractive in view of the many uncertainties involved when failure is impending. Again following Baker, this type of moment-rotation diagram lends itself to analysis according to the following steps.

1. Invent a solution satisfying statics. In this step, four considerations usually govern selection of the solution:
   a. Economy. This is achieved by keeping the maximum moment down in rectangular sections so as to obviate the need for compression reinforcement or increase in concrete section beyond what is required to take shear economically. Also by making minor adjustments so as to utilize the reinforcement as close as possible to its working stress.
   b. Ease for placing concrete.
   c. Minimum deflections and crack formation. To this end the solution should be close to the elastic solution (although the latter need not be computed accurately). Test results and application of Baker's

proposed load factors indicate that as much as 33 per cent reduction in design bending moments may be tolerated with respect to the elastic solution without special provisions, so long as statics are satisfied.

d. Uniformity in bar lengths. For instance, the design moment over the first interior support of a continuous beam or girder having several equal spans can often be made equal to that over other interior supports so that all except end spans require the same distribution of reinforcement.

2. Assuming elastic behavior, compute "dislocations" (finite angle changes) required at plastic hinges to satisfy continuity elsewhere in the frame. Tables of end slopes of simple beams are helpful in this step.
3. Compare with allowable dislocations (ultimate hinge rotations). If computed angle changes are smaller than these, the frame has been solved. Otherwise apply end moments to close the gaps sufficiently to keep them within allowable limits, or else add stirrups, ties, or spirals to increase allowable angle changes.

For routine analysis of reinforced concrete frames this method seems preferable to most others. But, even though it could easily be extended to more general moment-rotation curves, it would loose its simplicity and conceivably be no longer advantageous over the authors' method or over the one described earlier in this discussion.

Whatever method is chosen for analysis in connection with design, it is important that it be adapted to permit changes in the structure at intermediate stages of the analysis. Fortunately the authors' method as well as the two procedures described above apparently lend themselves to such adaptation. The writer hopes that in their closing discussion the authors will more fully describe this aspect of their proposed method.

REFERENCES

1. Sawyer, Jr., H. A., "Elasti-plastic design of single-span beams and frames", Proc. ASCE, Vol. 81, paper 851 (Dec. 1955).
2. Newmark, N. M., "Numerical procedure for computing deflections, moments, and buckling loads", Trans. ASCE, Vol. 108 (1943), pp. 1161-1234.
3. Sholtz, W., Discussion of "Elastic properties of riveted connections", by J. Rathbun, Trans. ASCE, Vol. 101 (1936), pp. 568-569.
4. Baker, A. L. L., "Ultimate Load Theory Applied to the Design of Reinforced and Prestressed Frames", Concrete Publications Ltd. (London, 1956).

A. A. EREMIN,[1] A. M. ASCE.—In this paper the authors have shown the method of distribution of bending moments in rigid frames by considering the elasti-plastic deformations.

1. Associate Bridge Engr., California State Highways, Sacramento, Calif.

It is interesting to note that the operations of distributing the plastic moments is similar to distributing elastic moments. The same elastic properties of rigid frame members were considered in both cases.

For checking purposes and also for visual presentation of the elastic properties of the continuous beam in the illustrative example shown by the authors in their Fig. 5, the moments were determined by graphical distribution.

Distributing of elastic bending moments from the given loading is shown in Fig. 20a and the graphical distribution of the plastic bending moments is shown in Fig. 20b.

The final resulting bending moments for the elasti-plastic condition of the continuous beam are determined by summation of the elastic bending moments in Fig. 20a and one half of value of plastic bending moments from Fig. 20b. The final bending moment closing line is shown in Fig. 20a by line AEFD.

It may be noted that the final bending moments determined with the graphical constructions vary from the moments computed by the authors less than 6 per cent.

With the graphical constructions the effect of the elastic properties of the members of the continuous beams may easily be revealed.

The characteristic points in the beam, Fig. 20a are determined by the graphical construction termed "three line polygon".(1,2)

REFERENCES

1. "Simplified Graphical Distribution of Bending Moments", by A. A. Eremin, 1948.

2. Transaction ASCE, 1950, p. 630, discussion of "Arches and Bents".

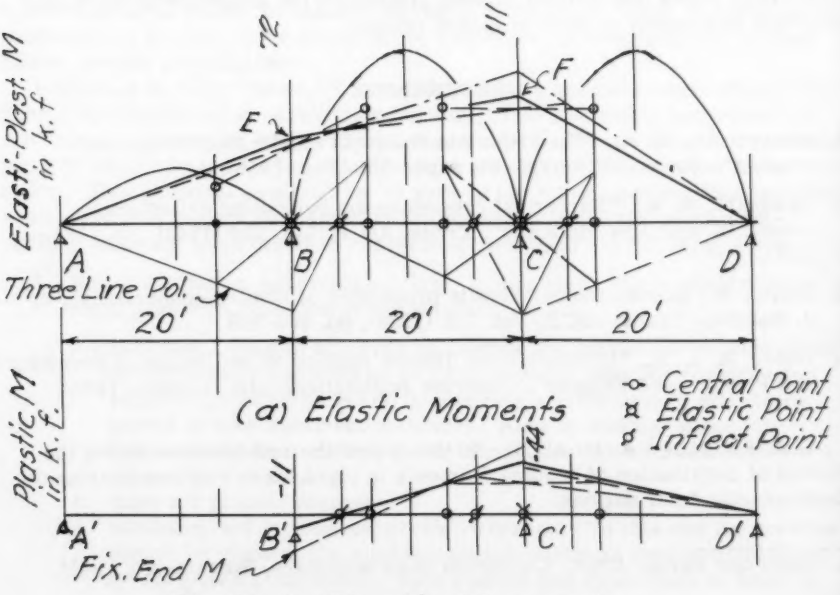

Fig. 20-b. Plastic Moments

4/20/59
By A.A.Erem

SHEAR STRENGTH OF REINFORCED CONCRETE BEAMS[a]

Discussions by Robert F. Warner, Henry J. Cowan, and Bela Goschy and George Balazs

ROBERT F. WARNER.[1]—The author is to be congratulated for his paper dealing with shear failure in reinforced concrete beams. His application of the Mohr failure theory to the concrete in the stress block above the inclined crack is a useful contribution to our understanding of the "shear-compression" failure which is commonly observed in laboratory tests. It is interesting to note that in another, independent investigation Walther(1) also used the Mohr failure theory to obtain the critical stresses above the inclined crack. The author's treatment is more general than Walther's, in that it takes into account variations in the ratio of the tensile to compressive strength of concrete.

In dealing specifically with the shearing strength of concrete beams however, the author has made an omission which, it is thought, severely restricts the usefulness of the theory. The author does not state a compatibility condition in his paper, and hence gives no indication of how the depth of the neutral axis at failure, defined by the dimensionless parameter k_u, is to be determined. This quantity occurs explicitly in Eqs. (27) and (18).

$$K_p = \frac{1 - k_2 k_u}{M/V_d} \cdot \frac{f'_c}{v'_c} \qquad (27)$$

$$V_c = v\, b\, k_u\, d \qquad (18)$$

Probably there would be no great error involved in letting

$$(1 - k_2 k_u) = 0.9$$

in Eq. (27) to avoid the use of a specific k_u value, but in Eq. (18), where any error in k_u will cause a proportional error in V_c the ultimate shearing force resisted by the section, no such approximation can be used.

Although it is not explicitly stated in the paper, the author appears to have avoided using a compatibility condition in the table of calculations (Table 2) by assuming that the longitudinal reinforcing steel has yielded at the time of failure. This assumption, which was also made by Bresler and Pister,(2) is unjustified, for if the steel reaches yield, the flexural strength of the beam has been achieved and the problem of premature shear failure does not arise. Bresler and Pister foresaw this objection and showed that their computed values for shearing strength, based on the assumption of yielding in the steel, were significantly lower than the computed flexural strengths. This is not a

a. Proc. Paper 1909, January, 1959, by Sidney A. Guralnick.
1. Research Asst. in Civ. Eng., Lehigh Univ., Bethlehem, Pa.

justification for the assumption of yielding in the steel (which is contrary to the experimental evidence of many shear tests); it is an indication that there is a second compensating error in the formulation of the theory.

The problem of finding a rational compatibility condition for the failure region appears now to be the one major obstacle to a satisfactory theory for the shear-compressive strength of prestressed and reinforced concrete beams. A promising approach has been made by Walther,(1) who stipulates a "shear rotation" about the neutral axis, coupled with a pull-out effect of the longitudinal steel relative to the surrounding concrete. However, the present formulation of this theory does not correlate test data so well as the purely empirical approach suggested by Sozen.(3)

With the attention currently being given to the problem and with the increased understanding achieved by papers such as the one being discussed, this writer is hopeful that a completely satisfactory solution for shear-compressive strength will be obtained in the near future. However, he feels it is important that the shear-compression failure be not considered as the only "shearing" type of failure which can occur in prestressed and reinforced concrete beams.

Ferguson(4) has already demonstrated experimentally that the shear strength of a beam, when loaded through side stubs, can be as low as 37 per cent of its strength when loaded on the top surface of the concrete. Whether failure will be in shear-compression or diagonal tension when moving point loads, distributed loads, side shear loads, and other "practical" loading conditions are involved, can only be determined by more tests in which the loading conditions are varied. It is quite possible that the shear-compression failure occurs only under conditions similar to those existing in the typical laboratory shear tests, in which stationary point loads are applied to the top surface of the beam. More research work is urgently required in this area to determine the proper limitations to the use of the concept of shear-compression failure.

REFERENCES

1. Walther, Rene E., The Shear Strength of Prestressed Concrete Beams; Session 1, Paper No. 9, Third Congress of the Federation Internationale de la Precontrainte, Berlin 1958.
2. Bresler, B., Pister, K., Strength of Concrete under Combined Stresses; Journal, American Concrete Institute, September 1958.
3. Sozen, M. A., Strength in Shear of Prestressed Concrete Beams without Web Reinforcement; Ph.D. Thesis, August 1957, University of Illinois, Urbana, Illinois.
4. Ferguson, Phil M., Some Implications of Recent Diagonal Tension Tests; Journal, American Concrete Institute, August 1956.

HENRY J. COWAN,[1] A. M. AMSE.—The author is to be complimented on a successful theoretical approach to an important problem.

1. Prof. of Architectural Science, Univ. of Sydney, Sydney, Australia.

The problem of combined bending and transverse shear, even though more important in practice, presents much greater difficulties than the related problem of combined bending and torsion, largely because it is much easier to separate the effect of bending in the case of torsion. It is gratifying, if not unexpected, to find that the author obtained for shear similar results to those previously obtained for torsion by Nylander(1) and later by Armstrong and the writer.(2)

The author's observations on the relation between the tensile and the compressive strength of concrete are most helpful, and the writer would be interested in the correct reference to the author's work in this field, (54) being apparently a typographical error.

The writer finds himself in agreement with the author's statement that the tensile and compressive strength of concrete are two separate physical constants of the material. However, this would suggest to the writer the use of two separate failure criteria. Although the author refers to the writer's work (Author's reference 7) and uses similar illustrations, the writer did in fact use two failure criteria, viz. the maximum stress criterion for primary tension failure and the Mohr criterion for primary compression failure. The effect of using only the Mohr criterion becomes apparent if one refers to the author's Fig. 7, which is grossly out of scale for the range of values of a given by the author. The author's footnote suggests a ratio $f'_c/f'_t = 10$, whereas the figure shows a ratio of only 2.8. For a ratio of 10 the angle θ would be very much larger. The writer finds it difficult to reconcile this angle with the work of Balmer (author's reference 2) or the earlier work of Richart, Brandtzaeg and Brown(3) assuming that a straight line envelope with a constant angle of inclination is to be used for the entire range of stress combinations investigated by the author. It seems to the writer that the angle θ requires adjustment. This would alter the curves in Fig. 13, although it would not make a fundamental difference to author's conclusions.

REFERENCES

1. H. Nylander: Vridning och vridningsinspänning vid betongkonstruktioner. Stockholm. States Kommitte für Buggnadsforskning. 1945. Meddelanden 3. pp. 138.

2. H. J. Cowan and S. Armstrong: Experiments on the strength of reinforced and prestressed concrete beams and of concrete-encased steel joists in combined bending and torsion. Magazine of Concrete Research, Vol. 7 1955), pp. 3-20.

3. F. E. Richart, A. Brandtzaeg, and R. L. Brown: A study of the failure of concrete under combined compressive stresses. University of Illinois. Engineering Experiment Station Bulletin 1928, No. 185, pp. 104.

BELA GOSCHY[1] and GEORGE BALAZS.[2]—The author has proposed the application of Mohr's failure theory to determine the rupture condition in the compression zone of reinforced concrete beams subjected to bending and shear. Although the application of Mohr's fracture theory for concrete has

1. Civ. Engr., Budapest, Hungary.
2. Civ. Engr., Budapest, Hungary.

been widely criticized, the investigations of Bresler and Pister proved the validity of the practice. The relation between shear and compression stress in state of rupture according to Mohr's theory can be expressed in the following way

$$V = \frac{fc'}{1+\alpha}\sqrt{\alpha 2 + (1-\alpha)\alpha\frac{f}{fc'} - \alpha\frac{f^2}{fc12}}\ ;\ \alpha = \frac{ft'}{fc'} \qquad (1)$$

another form of Eq. (14a) deduced by the author. Or by considering the results of Bresler and Pister which can be formulated with a good approximation as:

$$\frac{f1}{fc} + \frac{f2}{ft'} = 1 \qquad (2)$$

and substituting

$$f1 = f;\ f2 = \frac{f}{2} - \sqrt{\frac{f^2}{4} + v^2}$$

one obtains:

$$V = \alpha fc'\sqrt{1 + \left(\frac{1}{\alpha} - 2\right)\frac{f}{f'_c} - \left(\frac{1}{\alpha} - 1\right)\frac{f^2}{f'^2_c}} \qquad (3)$$

The difference between Eqs. (1) and (3) by different values of α is below 10%.

For a completer view of the problem it has to be mentioned that Eq. (1) can be deduced by introducing the idea of the "reduced stress" (f_r) as well.

According to Mohr's theory the value of the reduced stress is

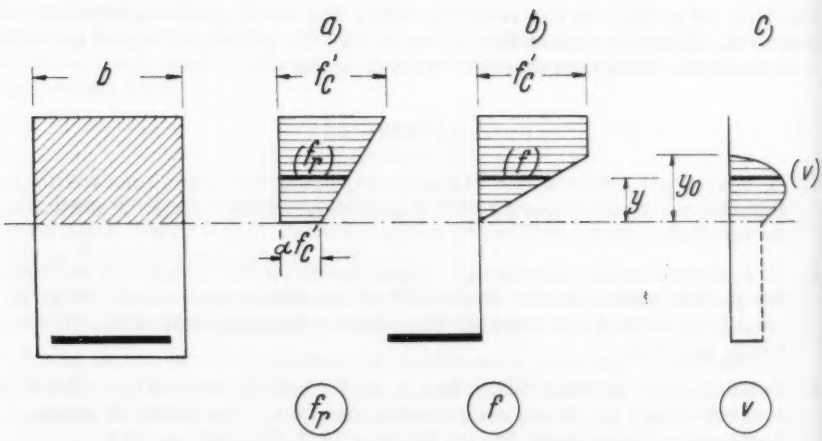

Figure 1.

a) Distribution of the reduced stress
b) " " " compressive stress (bending)
c) " " " shear stress

$$f_r = f_1 - \alpha f_3 = \frac{1-\alpha}{2} f + \frac{1+\alpha}{2} \sqrt{f^2 + 4v^2} \qquad (4)$$

The extreme values of f_r and the stress distribution in the compression zone is shown in Fig. 1.

v can be expressed from Eq. (4) as follows:

$$v = \frac{fr}{1+\alpha} \sqrt{1 - (1-\alpha)\frac{f}{fr} - \alpha \frac{f^2}{fr^2}} \qquad (4a)$$

and for

$$f = \frac{fc'}{y_o} y$$

the corresponding value of f_r is

$$f_r = \alpha f_c' + \frac{fc' - \alpha fc'}{y_o} y$$

By elimination of the parameter y/y_o one obtains the Eq. (1).

Remarks

1. The average shear stress in the compression zone can be discussed not only by its degree of approximation but also by its universal validity. Using other stress distribution theories like those of Westergard (square shape) shear stress in the compression zone by rupture is impossible and the assumption of diagonal cracks (Sachnowski) does not give any results for the failure shear. It is much more adequate to determine the failure shear from

$$Q_{max} = \int_0^{yo} v\, b\, dy$$

in which the function of v is given by Eq. (1) with the following substitution

$$\frac{f}{f_c'} = \frac{y}{y_o}$$

(See Fig. 1.)

2. The shear distribution below the neutral plane is not a question of cracks (i.e. the elastic shear theory in the II. state of stress) but it depends only on the connection between steel and concrete; when slip is impossible the shear stress distribution extends to the reinforcement (See: G. Kani, Der Bauingenieur No. 10, 1958.)

ON THE SOLUTION OF RIGID FRAMES ON THE COLUMN ANALOGY[a]

Discussion by John Sherman

JOHN SHERMAN,[1] M. ASCE.—The authors proof of the column analogy consists of demonstrating that the column analogy satisfies the conditions assumed for the redundancy of the frame. It does not show the physical meaning of the column analogy for the unsymmetrical case, and is unnecessarily complicated.

The column analogy is simply an extension of the method first used by Mueller-Breslau for the analysis of fixed arches, and can, therefore be readily developed from this method. Molitor[2] states that Mueller-Breslaue, and others, used a cantilever, a pair of cantilevers and a simple beam for the basic determinate structure. These three types are shown in Fig. 1, the redundants being applied at some arbitrary point 0 and connected to the cut portion of the frame by a rigid arm. The conception of the rigid arm is not used in the column analogy, and the type of basic determinate structure is arbitrary.

The Mueller-Breslau method consists of the simplication of the following work equation.

$$X_a\delta_{aa} + X_b\delta_{ba} + X_c\delta_{ca} = -\delta_a \qquad (1a)$$

$$X_a\delta_{ab} + X_b\delta_{bb} + X_c\delta_{cb} = -\delta_b \qquad (1b)$$

$$X_a\delta_{ac} + X_b\delta_{bc} + X_c\delta_{cc} = -\delta_c \qquad (1c)$$

The deflections in Eqs. (1) represent the move-of point 0 in Fig. 1. The deflections bearing subscripts with two letters are due to $X_a = 1$, $X_b = 1$ and $X_c = 1$ applied one at a time to the basic determinate structure. The deflections bearing single letter subscripts are due to the external loading applied to the basic determinate structure, and act at the point of application and in the direction of the redundant bearing the same lettered subscript.

The deflections bearing double letter subscripts are due to, and act at the point of application and in the direction of, the reduntant subscripted with the same letter.

The deflections bearing subscripts with different letters are the component deflections of the redundant indicated by the first letter, and act at the point of application and in the direction of the redundant indicated by the second letter. Maxwells law states that

---

a. Proc. Paper 1914, January, 1959, by D. Y. Fok and Tung Au.

1. Engr. American Bridge Div. U. S. Steel; retired, Roanoke, Va.

2. Kinetic Theory of Engineering Structures.

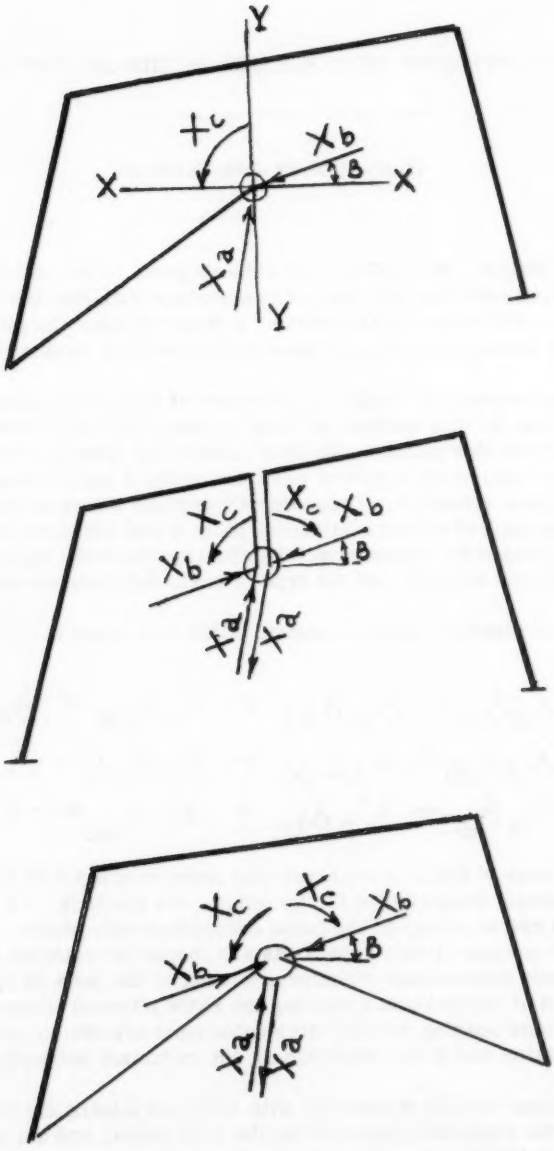
Y
Xc
Xb
B
X
X
Xa
Y
Xc
Xc
Xb
Xb
B
Xa
Xa
Xc
Xc
Xb
Xb
B
Xa
Xa

$$\delta_{ab} = \delta_{ba} \tag{2a}$$

$$\delta_{ac} = \delta_{ca} \tag{2b}$$

$$\delta_{bc} = \delta_{cb} \tag{2c}$$

Assuming any location for point 0 and denoting the sum of the lengths of the members of the frame and $\frac{1}{EI}$ by w_c, then in reference to the X and Y axes passing through point 0,

$$\delta_{cc} = \int_0^S w_c \, ds \tag{3a}$$

$$\delta_{cx} = \int_{-X}^{X} w_c x \, ds \tag{3b}$$

$$\delta_{cY} = \int_{-y}^{y} w_c y \, ds \tag{3c}$$

Eq. (3a) is equal to the total moment area of the frame for $X_c = 1$. Eqs. (3b) and (2c) are the statical moment of this moment area about the Y and X axes respectively becoming zero when point 0 is located at the center of gravity of w_cs. Point 0 will satisfy this condition when located at distances x" and y" from the Y and X axes respectively passing through the assumed point 0, where

$$X_o = \frac{\delta_{cx}}{\delta_{cc}} \quad , \quad y_o = \frac{\delta_{cY}}{\delta_{cc}} \tag{4}$$

The values of the deflections due to X_a and X_b are calculated to agree with the final location of point 0 and the component deflection eliminated by taking X_a to act vertically and inclining X_b an angle B from the X axis where

$$\tan B = \frac{\delta_{ab}}{\delta_{aa}} \tag{5}$$

Using the above arrangement of the redundants the following work equations can be used

$$X_a \delta_{aa} = -\delta_a \, , \; X_b \delta_{bb} = -\delta_b \, , \; X_c \delta_{cc} = -\delta_c \tag{6}$$

Since it is more convenient to use a horizontal shearing force H than the inclined X_b, the value of H is

$$H = X_b \cos B \tag{7}$$

from which the vertical shearing force V becomes

$$V = X_a + H \tan B \tag{8}$$

The foregoing is a brief description of the Mueller-Breslau method, from which the column analogy differs only in its notation and that X_a is inclined so as not to produce any horizontal movement. In the above terminology the angle that X_a makes with vertical is denoted by A, where

$$\tan A = \frac{\delta_{ab}}{\delta_{bb}} \tag{9}$$

Taking for the present H and V as the redundants then for the deflections due to H and V equal one the following values and analogies exist

$$\delta_{cc} = w_c s = A \tag{10a}$$

$$\delta_{xx} = \int_{-x}^{x} w_c x^2 ds = I_x \tag{10b}$$

$$\delta_{yy} = \int_{-y}^{y} w_c y^2 ds = I_y \tag{10c}$$

$$\delta_{xy} = \int_{-y}^{y}\int_{-x}^{x} w_c x y ds = I_{xy} \tag{10d}$$

In which A is the area of the analogous column section which has the same shape as the frame and a width $\frac{1}{EI}$, I_X and I_Y are the moments of inertia of A about the Y and X axes respectively, and I_{XY} is the product of inertia of A about point 0.

Denoting the moment area due to the loading on the basic determinate structure by P and the distances of the centroid of P from the Y and X axes by x_o and y_o respectively, the deflections due to the loading have the following values and analogies;

$$-\delta_a = \int_{-y}^{y} m_s w_c y ds = P y_o = M_Y \tag{11a}$$

$$-\delta_B = \int_{-x}^{x} m_s w_c x ds = P x_o = M_X \tag{11b}$$

Noting that the component deflections due to X_C are zero the values of H and V can be determined by the simultaneous solution of Eqs. (1a) and (1b) and expressed in terms of the above analogies. This procedure while correct obscures the physical meaning.

In Fig. 2, which is an enlarged picture of point 0 I_{XY} is taken as positive. The values of I_X and I_Y are positive, therefore the tangents of angles A and B are positive and X_a and X_b act in the direction shown. When I_{XY} is negative the direction of X_a and X_b is shown by the dash lines.

Recalling that the direction of the deflection is normal to the moment arm of the moment area, then H and V can be calculated by measuring the abscissas x' and y' horizontally and vertically from the inclined axes, where

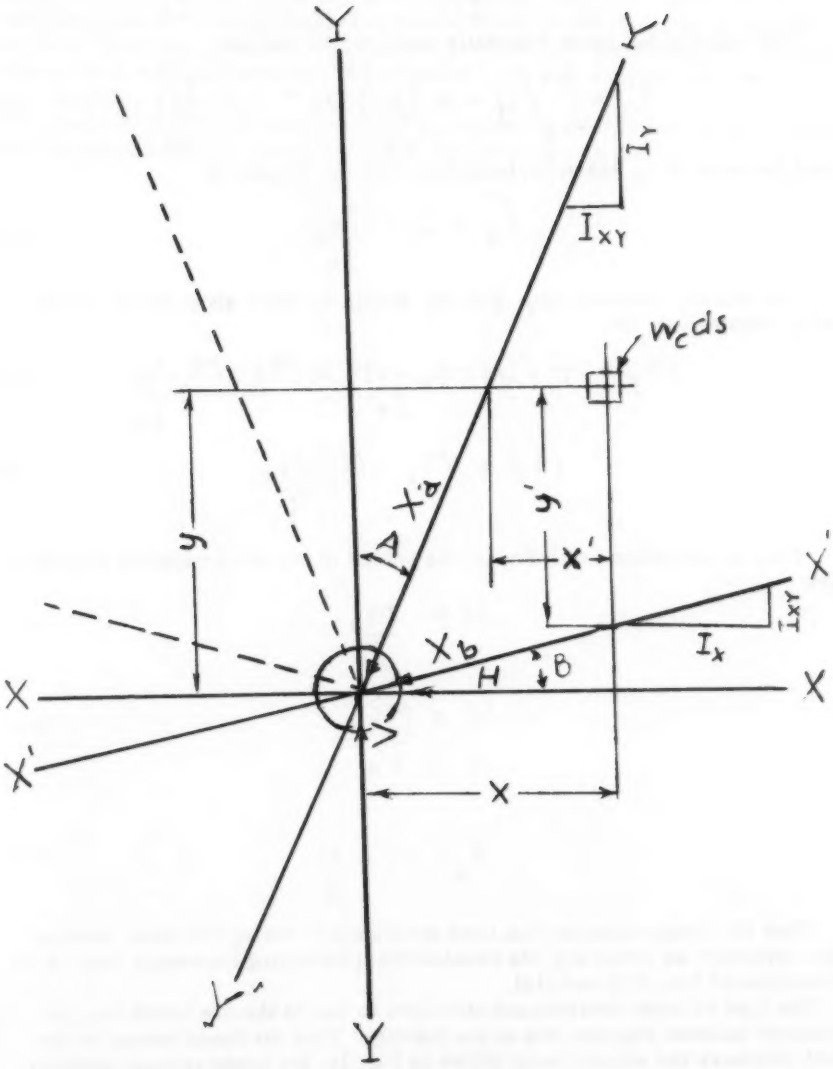
Y
Y'
I_Y
I_{XY}
$w_c ds$
x'_a
A
y
y'
x'
X'
I_{XY}
I_X
X_b
H
B
X
X
X'
Y'
Y
x

$$x' = x - y\frac{I_{XY}}{I_Y} \quad , \quad y' = y - x\frac{I_{XY}}{I_X} \tag{12}$$

The value of I'_Y taken vertically about the X' axis is

$$I'_Y = \int_{-y}^{y}\left(y - x\frac{I_{XY}}{I_X}\right)^2 ds = I_Y - \frac{I_{XY}^2}{I_X} \tag{13}$$

and the value of I'_X taken horizontally about the Y' axis is

$$I'_X = I_X - \frac{I_{XY}^2}{I_Y} \tag{14}$$

The statical moments M'_Y and M'_X similarly taken about the X' and Y' axes respectively are

$$M'_Y = P\left(y_o - x_o\frac{I_{XY}}{I_Y}\right) = M_Y - M_X\frac{I_{XY}}{I_X} \tag{15}$$

$$M'_X = M_X - M_Y\frac{I_{XY}}{I_Y} \tag{16}$$

Then in accordance with Eq. (6) the values of the forces applied at point 0 are

$$H = \frac{M'_Y}{I'_Y} \tag{17a}$$

$$V = \frac{M'_X}{I'_X} \tag{17b}$$

$$X_c = m = \frac{P}{A} \tag{17c}$$

Thus the column analogy has been developed by taking the basic determinate structure as arbitrary, its consideration becoming necessary only in the evaluation of Eqs. (15) and (16).

The type of basic determinate structure to use is the one which has the simplest moment diagram due to the loading. Thus for loads lateral to the roof members the simple beam shown in Fig. 1c, for loads applied laterally to a column the cantilever shown in Fig. 1a, and couples applied to the columns the two cantilevers shown in Fig. 1b will give the simplest moment diagrams.

When the frame is hinged at one end, this end is taken as the origin of the coordinates, as the authors state, and the choice of the basic determinate structure is limited to the simple beam or the cantilever.

When both ends are hinged the basic determinate structure is the simple beam.

When the supports are at different elevations for the two hinged frames the authors equation Eq. (21) which is based on rotating the x and y axes results in the redundant force being applied in the direction of the line connecting the base of the columns. It is much simpler to take the line connecting the column bases as the X axis and measure y' vertically from this inclined axis and obtain H directly.

The general method as described can be applied to a truss and beam combination by calculating the elastic loads for the truss members.

DAV
the pro
directl
Profes
If w
and we
each be
ing rel
Momen

ω

where
nate th
$\Delta^2 x W_2$
the ber
pressi
momen
we can

from

Δ^2_x

a. Pr
Ga
1. Pa

ANALYSIS OF A TWO WAY TRUSS SYSTEM[a]

Discussions by David Dario Brillembourg Bravo and R. Schjödt
Corrections by John A. Sbarounis and Michael P. Gaus

DAVID DARIO BRILLEMBOURG BRAVO,[1] A. M. ASCE.—The solution to the problem of the grid of orthogonal members in flexure as been obtained directly in terms of the loads and moments acting on the structure by Professor Anatole Zagustin of the Universidad Central de Venezuela.(1)

If we consider the group of eight joints around a central point 0 of a grid, and we assume that the loads act at the joints only, the moment diagram for each beam in the grid is lineal between joints, and we can establish the following relationship between deflections and moments by applying the Three Moments Equation:

$$\omega_3 - 2\omega_2 + \omega_1 = \frac{h^2}{6E}\left(\frac{M_{3x}}{D_{23}} + \frac{2M_{2x}}{D_{23}} + \frac{2M_{2x}}{D_{21}} + \frac{M_{1x}}{D_{21}}\right)$$

where h is the grid spacing and D the relative inertia of each span. We designate the left hand side of this equation as the curvature of the horizontal beam: $\Delta^2_x W_2$ at the joint 2, and from the right side we see that it is a function of the bending moments on the horizontal beam. We can also form a similar expression for the curvature of the vertical beams and those will depend on the moments on the vertical beams only. In total with a given set of nine joints, we can write six expressions for curvatures:

$$\Delta^2_x \omega_2 = \omega_3 - 2\omega_2 + \omega_1$$
$$\Delta^2_x \omega_0 = \omega_4 - 2\omega_0 + \omega_8$$
$$\Delta^2_x \omega_6 = \omega_5 - 2\omega_6 + \omega_7$$
$$\Delta^2_y \omega_4 = \omega_3 - 2\omega_4 + \omega_5$$
$$\Delta^2_y \omega_0 = \omega_2 - 2\omega_0 + \omega_6$$
$$\Delta^2_y \omega_8 = \omega_1 - 2\omega_8 + \omega_7$$

from which we can obtain

$$\Delta^2_x \omega_2 - 2\Delta^2_x \omega_0 + \Delta^2_x \omega_6 = \Delta^2_y \omega_4 - 2\Delta^2_y \omega_0 + \Delta^2_y \omega_8$$

a. Proc. Paper 1940, February, 1959, by John A. Sbarounis and Michael P. Gaus.

1. Partner Guinand and Brillembourg, C. A., Caracas-Venezuela.

That can be expressed as:

$$\Delta^2_y \Delta^2_x w_o = \Delta^2_x \Delta^2_y w_o$$

This expression Dr. Zagustin calls the Compatibility Equation—which expressed in words reads: The second difference in the vertical sense of the curvature of the horizontal beams is equal to the second difference in the horizontal sense of the curvature of the vertical beams. The left hand of this expression contains only moments on the horizontal beams, and the right side of the equation moments in the vertical beams only. This equation is the extension to a plan of the Three Moments Equation. We can point out that it is an exact relationship as long as the loads are applied at the joints only.

The compatibility equation can be applied at the interior points of the grid only and if expressed in terms of the unknown forces of interaction between beams at a joint, will lead to a set of equations equal to the number of dissimilar interior ponts and having the same number of unknown interaction forces.

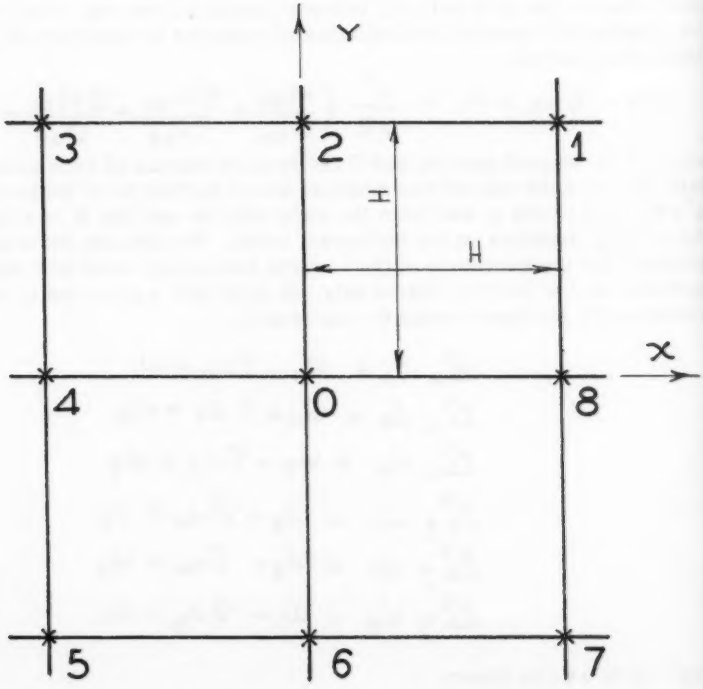

FIG-1 GRID NOTATION

In the Truss presented, we would obtain six unknowns for the equivalent grid or fortyfive for the original system, all expressed in term of the interacting forces at the joint.

We can also evaluate very easily the effect of a change in design on the coefficients of the unknowns, through the changes in curvature of the beams. When the number of interior points is too great for direct solving of the equations, a procedure of successive approximations has been described, which completely eliminates the need for constructing the equations.(1)

REFERENCES

1. A. Zagustin. Teoria y Calculo del Entrepiso Reticular. Editorial Arte. Caracas. 1958.

R. SCHJÖDT,[1] M. ASCE.—This analysis is an interesting and useful one. The nature of the structure, which makes it possible to ignore the torsional moments, and the check on the results made possible by the two methods presented, combine to make the paper very instructive.

The results of the two methods check adequately for members located at some distance from the supports and edges. For members close to these, however, the differences are more than 40% at most points, and even reach 87% at one point. This is of no practical importance for the design in this particular case, when the sections are adequate to carry the stresses resulting from the more unfavorable solution.

But this result is, of course, most unsatisfactory as far as the general usefulness of the methods is concerned, and it serves as an excellent illustration of an error which is frequently made when difference equations are used for the solution of physical problems. The authors cannot be criticized, as the point to be made here lies in the evolution of the difference equations, which the authors take as their starting point.

As an illustration, the equation

$$\frac{d^2M}{dx^2} = -p \qquad \text{(A)}$$

as used in Eq. (11) can be considered. When going from this differential equation to the corresponding difference equation, one writes

$$M_4 + M_2 - 2M_0 = -ph^2 \qquad \text{(B)}$$

with the notations used by the authors. If, however, the equilibrium conditions for the section 4-0-2 are written, one finds:

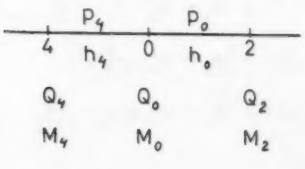

$$Q_0 - Q_2 = p_0 h_0 \qquad Q_0 = Q_2 + p_0 h_0$$

1. Technician, Norwegian Bldg. Research Inst., Oslo-Blendern, Norway.

Fig. A.
Beam notation.

$$M_2 - M_0 = Q_2 h_0 + p_0 \frac{h_0^2}{2}$$

$$Q_2 = \frac{M_2 - M_0}{h_0} - p_0 \frac{h_0}{2}$$

$$M_0 - M_4 = Q_0 h_4 + p_4 \frac{h_4^2}{2}$$

$$= (M_2 - M_0)\frac{h_4}{h_0} + p_0 \frac{h_0 h_4}{2} + p_4 \frac{h_4^2}{2}$$

$$M_4/h_4 + M_2/h_0 - M_6/(h_0 + h_4) = -p_0 \frac{h_0}{2} - p_4 \frac{h_4}{2} \quad (C)$$

If $h_4 = h_0$ and $p_4 = p_0$, then (C) = (B).

Now the point is that it is easy to proceed from Eq. (C) to (A), but impossible from (A) to (C). The left side of Eq. (C) may be arrived at from (A), but not the right side. In other words, in order to arrive at correct difference equations, it is necessary to start with the equilibrium conditions for the problem. Writing the differential equation as a difference equation will not always give a correct result, as the differential equations are evolved using certain assumptions as to the conditions in the immediate neighbourhood of the point in question, which may not always be made when the distances are finite.

Thus in Eq. (11) p is assumed to be constant, and in order to arrive at

$$\frac{d^2 w}{dx^2} = -\frac{M}{EJ} \quad (D)$$

which is used in the evolution of (9), the cross section is assumed to be constant, as can easily be shown. In the further work with (9), EJ is taken as variable, but with Eq. (D) as point of departure.

As will be understood from the above, the author's Eqs. (9) and (10) give correct difference equations for nets symmetrical about the point 0, but not in cases as for instance those shown in Fig. 10 and 12.

The difference equations for the truss system in question are perhaps most easily found by writing the deflections as second degree moments (the bending moment, divided by EJ, is considered as loading for calculating the second degree moments). With M_n and Q_n as the second degree moments at the point 0, and

$$C_h = Q_v + p_0 + R,$$

one finds:

Point 4 : $Q_m h_4 - M\frac{1}{2h_4 B_4^x} - Q_v \frac{1}{6B_4^x} = W_4 - W_0$

8 : $Q_m (h_4 + h_8) - M b_1 - Q_v b_2 = W_8 - W_0$

2 : $Q_m h_0 - M\frac{1}{2h_0 B_0^x} + Q_v \frac{1}{6B_0^x} + R\frac{1}{6B_0^x} = W_2 - W_0 - \frac{p_0}{6B_0^x}$

6 : $Q_m (h_8 + h_2) - M c_1 + Q_v c_2 + R c_2 = W_6 - W_0 - p_0 c_2 - \frac{p_2}{6B_2^x}$

Here :

$$b_1 = \frac{1+2h_8/h_4}{2h_4\,B_4^x} + \frac{1}{2h_8\,B_8^x}$$

$$b_2 = \frac{1+3h_8/h_4}{6\,B_4^x} + \frac{1+3h_4/h_8}{6\,B_8^x}$$

$$c_1 = \frac{1+2h_2/h_0}{2h_0\,B_0^x} + \frac{1}{2h_2\,B_2^x}$$

$$c_2 = \frac{1+3h_2/h_0}{6h_0\,B_0^x} + \frac{1+3h_0/h_2}{6h_2\,B_2^x}$$

R is the reaction from the truss in the x-direction, crossing at the point Zero, R = 0 gives an isolated truss in the x-direction. With R = 0, $h_n = h$, $p_n = p$ and $J_n = J$, the equations above give

$$w_6 - w_8 - 4w_2 - 4w_4 + 6w_0 = \frac{p}{B} ,$$

the difference equation for deflection of a one way truss with constant loading and section. (Note that p is now written as concentrated load at the section end).

The truss in the Y-direction naturally has the reaction - R in the point 0; apart from this the equations are the same as for the points 2, 4, 6, 8 with the

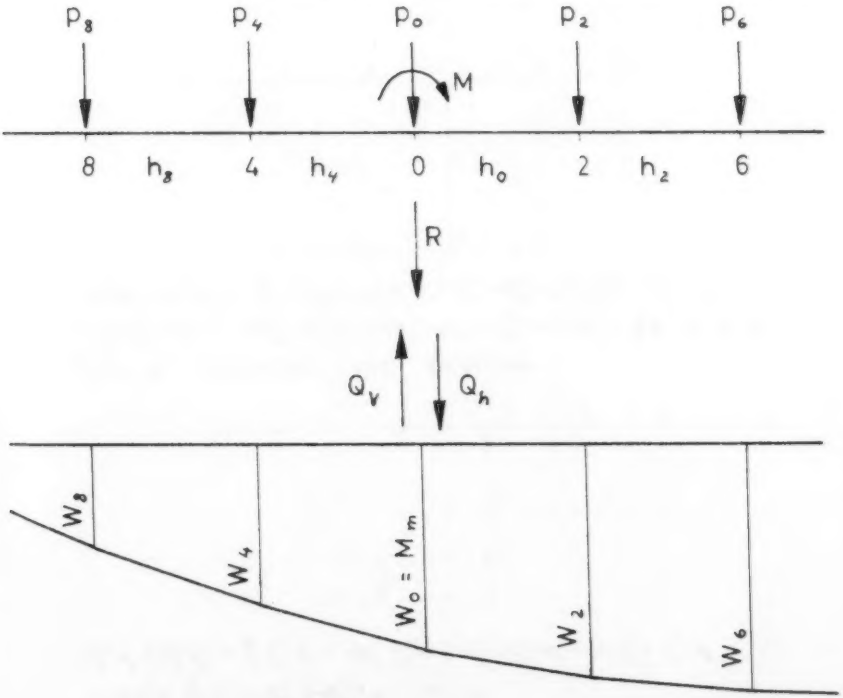

Fig. B
Beam deflections

ST 6

necessary change of numbering. If one therefore finds R from the four equations above, and puts it equal to the negative value of the same solution for the points 1, 3, 5, 7, one gets an equation containing only w_n and p_n, corresponding to (12). This solution is usually easily carried out, especially when all $h_n = h$ and $J_n = J$. In this case, Q_m and Q_v for instance are at once eliminated by summing the equations for the points 2 and 4.

With $h_n = h$ and $p_n = p$, these equations give the authors Eq. (12). For the case shown in Fig. 12, however, one finds

$$w_8 + w_7 - 2w_9 - 2w_3 + 2w_0 = \tfrac{4}{3}p$$

instead of equal to p . $B_n^x = B_n^y = 1$, for simplicity.

For the author's Fig. 10, one finds

$$w_8 + w_6 + \tfrac{1}{3}w_7 - 4w_2 - 4w_9 - \tfrac{2}{3}w_3 + 6\tfrac{1}{3}w_0 = \tfrac{19}{18}p \quad .$$

With this modification of the equations, the disagreements between the results of the two methods of analysis disappear.

CORRECTIONS.—In reviewing Proc. Paper 1940 in the February 1959 Journal of the Structural Division, the authors noted drafting errors in the subscripts in the equations in Figs. 15, 17, and 20. Corrected verions of these three figures are reproduced on the following page.

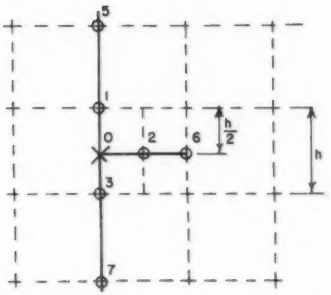

$$8B_2^X w_6 + \frac{8}{3}B_3^Y w_7 + \frac{8}{3}B_1^Y w_5 - 16B_2^X w_2 - (16B_0^Y + 8B_1^Y)w_1$$
$$-(16B_0^Y + 8B_3^Y)w_3 + (32B_0^Y + 8B_2^X + \frac{16}{3}B_1^Y + \frac{16}{3}B_3^Y)w_0 = p$$

FIG. 15 SPECIAL EQUATION FOR SUBDIVIDED GRID

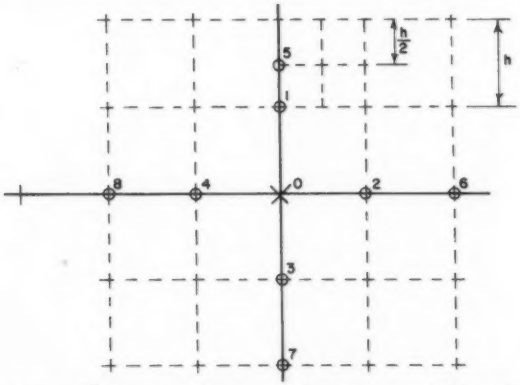

$$B_4^X w_8 + B_2^X w_6 + \frac{8}{3}B_1^Y w_5 + B_3^Y w_7 - 2(B_0^X + B_4^X)w_4 - 2(B_0^X + B_2^X)w_2$$
$$-(2B_0^Y + 4B_1^Y)w_1 - 2(B_0^Y + B_3^Y)w_3 + (4B_0^X + 4B_0^Y + B_4^X + B_2^X + B_3^Y + \frac{4}{3}B_1^Y)w_0 = p$$

FIG. 17 SUBDIVIDED GRID EQUATION

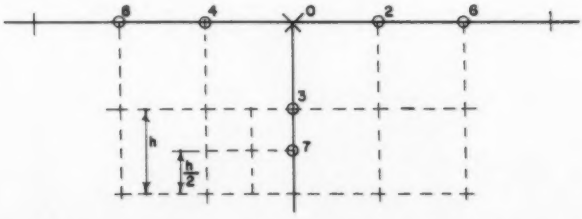

$$B_4^X w_8 + B_2^X w_6 + \frac{8}{3}B_3^Y w_7 - 4B_3^Y w_3 - 2(B_0^X + B_2^X)w_2 - 2(B_0^X + B_4^X)w_4$$
$$+ (4B_0^X + \frac{4}{3}B_3^Y + B_4^X + B_2^X)w_0 = p$$

FIG. 20 FREE EDGE POINT NEAR SUBDIVIDED GRID

PROCEEDINGS PAPERS

The technical papers published in the past year are identified by number below. Technical-division sponsorship is indicated by an abbreviation at the end of each Paper Number, the symbols referring to: Air Transport (AT), City Planning (CP), Construction (CO), Engineering Mechanics (EM), Highway (HW), Hydraulics (HY), Irrigation and Drainage (IR), Pipeline (PL), Power (PO), Sanitary Engineering (SA), Soil Mechanics and Foundations (SM), Structural (ST), Surveying and Mapping (SU), and Waterways and Harbors (WW), divisions. Papers sponsored by the Department of Conditions of Practice are identified by the symbols (PP). For titles and order coupons, refer to the appropriate issue of "Civil Engineering." Beginning with Volume 82 (January 1956) papers were published in Journals of the various Technical Divisions. To locate papers in the Journals, the symbols after the paper number are followed by a numeral designating the issue of a particular Journal in which the paper appeared. For example, Paper 1859 is identified as 1859 (HY 7) which indicates that the paper is contained in the seventh issue of the Journal of the Hydraulics Division during 1958.

VOLUME 84 (1958)

JUNE: 1658(AT1), 1659(AT1), 1660(HY3), 1661(HY3), 1662(HY3), 1663(HY3), 1664(HY3), 1665(SA3), 1666 (PL2), 1667(PL2), 1668(PL2), 1669(AT1), 1670(PO3), 1671(PO3), 1672(PO3), 1673(PL2), 1674(PL2), 1675 (PO3), 1676(PO3), 1677(SA3), 1678(SA3), 1679(SA3), 1680(SA3), 1681(SA3), 1682(SA3), 1683(PO3), 1684 (HY3), 1685(SA3), 1686(SA3), 1687(PO3), 1688(SA3)[c], 1689(PO3)[c], 1690(HY3)[c], 1691(PL2)[c].

JULY: 1692(EM3), 1693(EM3), 1694(ST4), 1695(ST4), 1696(ST4), 1697(SU2), 1698(SU2), 1699(SU2), 1700(SU2), 1701(SA4), 1702(SA4), 1703(SA4), 1704(SA4), 1705(SA4), 1706(EM3), 1707(ST4), 1708(ST4), 1709(ST4), 1710 (ST4), 1711(ST4), 1712(ST4), 1713(SU2), 1714(SA4), 1715(SA4), 1716(SU2), 1717(SA4), 1718(EM3), 1719 (EM3), 1720(SU2), 1721(ST4)[c], 1722(ST4), 1723(ST4), 1724(EM3)[c].

AUGUST: 1725(HY4), 1726(HY4), 1727(SM3), 1728(SM3), 1729(SM3), 1730(SM3), 1731(SM3), 1732(SM3), 1733 (PO4), 1734(PO4), 1735(PO4), 1736(PO4), 1737(PO4), 1738(PO4), 1739(PO4), 1740(PO4), 1741(PO4), 1742 (PO4), 1743(PO4), 1744(PO4), 1745(PO4), 1746(PO4), 1747(PO4), 1748(PO4), 1749(PO4).

SEPTEMBER: 1750(IR3), 1751(IR3), 1752(IR3), 1753(IR3), 1754(IR3), 1755(ST5), 1756(ST5), 1757(ST5), 1758 (ST5), 1759(ST5), 1760(ST5), 1761(ST5), 1762(ST5), 1763(ST5), 1764(ST5), 1765(WW4), 1766(WW4), 1767 (WW4), 1768(WW4), 1769(WW4), 1770(WW4), 1771(WW4), 1772(WW4), 1773(WW4), 1774(IR3), 1775(IR3), 1776(SA5), 1777(SA5), 1778(SA5), 1779(SA5), 1780(SA5), 1781(WW4), 1782(SA5), 1783(SA5), 1784(IR3)[c], 1785(WW4)[c], 1786(SA5)[c], 1787(ST5)[c], 1788(IR3), 1789(WW4).

OCTOBER: 1790(EM4), 1791(EM4), 1792(EM4), 1793(EM4), 1794(EM4), 1795(HW3), 1796(HW3), 1797(HW3), 1798(HW3), 1799(HW3), 1800(HW3), 1801(HW3), 1802(HW3), 1803(HW3), 1804(HW3), 1805(HW3), 1806(HY5), 1807(HY5), 1808(HY5), 1809(HY5), 1810(HY5), 1811(HY5), 1812(SM4), 1813(SM4), 1814(ST6), 1815(ST6), 1816(ST6), 1817(ST6), 1818(ST6), 1819(ST6), 1820(ST6), 1821(ST6), 1822(EM4), 1823(PO5), 1824(SM4), 1825(SM4), 1826(SM4), 1827(ST6)[c], 1828(SM4)[c], 1829(HW3)[c], 1830(PO5)[c], 1831(EM4)[c], 1832(HY5)[c].

NOVEMBER: 1833(HY6), 1834(HY6), 1835(SA6), 1836(ST7), 1837(ST7), 1838(ST7), 1839(ST7), 1840(ST7), 1841(ST7), 1842(SU3), 1843(SU3), 1844(SU3), 1845(SU3), 1846(SU3), 1847(SA6), 1848(SA6), 1849(SA6), 1850 (SA6), 1851(SA6), 1852(SA6), 1853(SA6), 1854(ST7), 1855(SA6)[c], 1856(HY6)[c], 1857(ST7)[c], 1858(SU3)[c].

DECEMBER: 1859(HY7), 1860(IR4), 1861(IR4), 1862(IR4), 1863(SM5), 1864(SM5), 1865(ST8), 1866(ST8), 1867 (ST8), 1868(PP1), 1869(PP1), 1870(PP1), 1871(PP1), 1872(PP1), 1873(WW5), 1874(WW5), 1875(WW5), 1876 (WW5), 1877(CP2), 1878(ST8), 1879(ST8), 1880(HY7)[c], 1881(SM5)[c], 1882(ST8)[c], 1883(PP1)[c], 1884(WW5)[c], 1885(CP2)[c], 1886(PO6), 1887(PO6), 1888(PO6), 1889(PO6), 1890(HY7), 1891(PP1).

VOLUME 85 (1959)

JANUARY: 1892(AT1), 1893(AT1), 1894(EM1), 1895(EM1), 1896(EM1), 1897(EM1), 1898(EM1), 1899(HW1), 1900(HW1), 1901(HY1), 1902(HY1), 1903(HY1), 1904(HY1), 1905(PL1), 1906(PL1), 1907(PL1), 1908(PL1), 1909(ST1), 1910(ST1), 1911(ST1), 1912(ST1), 1913(ST1), 1914(ST1), 1915(ST1), 1916(AT1)[c], 1917(EM1)[c], 1918(HW1)[c], 1919(HY1)[c], 1920(PL1)[c], 1921(SA1)[c], 1922(ST1)[c], 1923(EM1), 1924(HW1), 1925(HW1), 1926 (PL1), 1927(HW), 1928(HW1), 1929(SA1), 1930(SA1), 1931(SA1), 1932(SA1).

FEBRUARY: 1933(HY2), 1934(HY2), 1935(HY2), 1936(SM1), 1937(SM1), 1938(ST2), 1939(ST2), 1940(ST2), 1941(ST2), 1942(ST2), 1943(ST2), 1944(ST2), 1945(HY2), 1946(PO1), 1947(PO1), 1948(PO1), 1949(PO1), 1950(HY2)[c], 1951(SM1)[c], 1952(ST2)[c], 1953(PO1)[c], 1954(CO1), 1955(CO1), 1956(CO), 1957(CO1), 1958(CO1), 1959(CO1).

MARCH: 1960(HY3), 1961(HY3), 1962(HY3), 1963(IR1), 1964(IR1), 1965(IR1), 1966(IR1), 1967(SA2), 1968(SA2), 1969(ST3), 1970(ST3), 1971(ST3), 1972(ST3), 1973(ST3), 1974(ST3), 1975(ST3), 1976(WW1), 1977(WW1), 1978(WW1), 1979(WW1), 1980(WW1), 1981(WW1), 1982(WW1), 1983(WW1), 1984(SA2), 1985(SA2)[c], 1986 (IR1)[c], 1987(WW1)[c], 1988(ST3)[c], 1989(HY3)[c].

APRIL: 1990(EM2), 1991(EM2), 1992(EM2), 1993(HW2), 1994(HY4), 1995(HY4), 1996(HY4), 1997(HY4), 1998 (SM2), 1999(SM2), 2000(SM2), 2001(SM2), 2002(ST4), 2003(ST4), 2004(ST4), 2005(ST4), 2006(PO2), 2007 (HW2)[c], 2008(EM2)[c], 2009(ST4)[c], 2010(SM2)[c], 2011(SM2)[c], 2012(HY4)[c], 2013(PO2)[c].

MAY: 2014(AT2), 2015(AT2), 2016(AT2), 2017(HY5), 2018(HY5), 2019(HY5), 2020(HY5), 2021(HY5), 2022(HY5), 2023(PL2), 2024(PL2), 2025(PL2), 2026(PP1), 2027(PP1), 2028(PP1), 2029(PP1), 2030(SA3), 2031(SA3), 2032(SA3), 2033(SA3), 2034(ST5), 2035(ST5), 2036(ST5), 2037(ST5), 2038(PL2), 2039(PL2), 2040(AT2)[c]. 2041(PL2)[c], 2042(PP1)[c], 2043(ST5)[c], 2044(SA3)[c], 2045(HY5)[c], 2046(PP1), 2047(PP1).

JUNE: 2048(CP1), 2049(CP1), 2050(CP1), 2051(CP1), 2052(CP1), 2053(CP1), 2054(CP1), 2055(CP1), 2056 (HY6), 2057(HY6), 2058(HY6), 2059(IR2), 2060(IR2), 2061(PO3), 2062(SM3), 2063(SM3), 2064(SM3), 2065 (ST6), 2066(WW2), 2067(WW2), 2068(WW2), 2069(WW2), 2070(WW2), 2071(WW2), 2072(CP1)[c], 2073(IR2)[c], 2074(PO3)[c], 2075(ST6)[c], 2076(HY6)[c], 2077(SM3)[c], 2078(WW2)[c].

---

c. Discussion of several papers, grouped by divisions.

AMERICAN SOCIETY OF CIVIL ENGINEERS

OFFICERS FOR 1959

PRESIDENT

FRANCIS S. FRIEL

VICE-PRESIDENTS

Term expires October, 1959:
WALDO G. BOWMAN
SAMUEL B. MORRIS

Term expires October, 1960:
PAUL L. HOLLAND
LLOYD D. KNAPP

DIRECTORS

Term expires October, 1959:
CLINTON D. HANOVER, Jr.
E. LELAND DURKEE
HOWARD F. PECKWORTH
FINLEY B. LAVERTY
WILLIAM J. HEDLEY
RANDLE B. ALEXANDER

Term expires October, 1960:
PHILIP C. RUTLEDGE
WESTON S. EVANS
TILTON E. SHELBURNE
CRAIG P. HAZELET
DONALD H. MATTERN
JOHN E. RINNE

Term expires October, 1961:
THOMAS J. FRATAR
EARL F. O'BRIEN
DANIEL B. VENTRES
CHARLES W. BRITZIUS
WAYNE G. O'HARRA
FRED H. RHODES, JR.
N. T. VEATCH

PAST PRESIDENTS

Members of the Board

MASON G. LOCKWOOD

LOUIS R. HOWSON

EXECUTIVE SECRETARY

WILLIAM H. WISELY

ASSISTANT SECRETARY

E. LAWRENCE CHANDLER

ASSISTANT TREASURER

ENOCH R. NEEDLES

PROCEEDINGS OF THE SOCIETY

HAROLD T. LARSEN
Manager of Technical Publications

PAUL A. PARISI
Editor of Technical Publications

MARVIN SCHECHTER
Assistant Editor of Technical Publications

COMMITTEE ON PUBLICATIONS

HOWARD F. PECKWORTH, *Chairman*

PHILIP C. RUTLEDGE, *Vice-Chairman*

E. LELAND DURKEE
TILTON E. SHELBURNE
CHARLES W. BRITZIUS
FRED H. RHODES, JR.